



SINTEF

# excon

## Grønn forvaltning av konstruksjoner for infrastruktur

Kilde: Votna I, Jan Lindgård, SINTEF

# Report

## NDT methods and sensors for existing concrete structures

Literature review

### Author(s):

Cosmin Popescu, Tobias Danner, Roar Myrdal, Jan Lindgård, Andres Belda Revert, Björn Täljsten

### Report No:

2023:01487 - Unrestricted

### Client(s) (pos partner):

SINTEF AS

# Report

## NDT methods and sensors for existing concrete structures

Literature review

### KEYWORDS

Concrete, structure, inspection, monitoring, NDT, sensor, condition assessment

### VERSION

2

### DATE

2023-09-11

### MAIN AUTHOR(S)

Cosmin Popescu, Tobias Danner, Roar Myrdal, Jan Lindgård, Andres Belda Revert, Björn Täljsten

### CLIENT(S)

SINTEF AS

### CLIENT'S REFERENCE

Tor Arne Hammer

### PROJECT NO.

102028198

### NO. OF PAGES

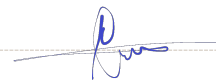
92

### SUMMARY

This report provides an overview over the most common used NDT methods and sensors for inspection and monitoring of existing concrete structures. The methods are briefly described with regard to their working principle and the parameters and properties of concrete structures that can be investigated. NDT methods are divided into three groups; a) optical b) mechanical and acoustic and c) electro-magnetic methods. The part on sensors is divided by the parameter to monitor, e.g. sensor for monitoring deformation, tilt, strain, cracks, vibrations, temperature, humidity, corrosion, pH, chloride, water pressure, etc. An own chapter deals with fibre optical sensors applicable for many different purposes.

### PREPARED BY

Cosmin Popescu, Tobias Danner



SIGNATURE

### CHECKED BY

Tor Arne Hammer



SIGNATURE

### APPROVED BY

Carine Lausset



SIGNATURE

### REPORT NO.

2023:01487

### ISBN

978-82-14-07184-9

### CLASSIFICATION

Unrestricted

### CLASSIFICATION THIS PAGE

Unrestricted

# Document history

VERSION	DATE	VERSION DESCRIPTION
1	2023-12-24	First draft. Finalized by authors for distribution to the project team
2	2024-09-11	Final version

## Preface

This report is part of a series of State-of-the reports (STAR) written for the R&D project EXCON – Sustainable management guidelines to extend the service life of concrete constructions and infrastructure. The current STAR report is a milestone within work package 3 (condition assessment), task 1 (further development of prioritized NDT-methods).

The first part on NDT-methods was written under the lead of Cosmin Popescu, while the second part on sensors was written under the lead of Tobias Danner, both with significant contributions from project partners in terms of content and proof reading. Jan Lindgård is acknowledged for gathering information and contributing to writing of the chapter on humidity sensors and dam inspections. Roar Myrdal, Karla Hornbostel and Andres Belda Revert are acknowledged for their contributions regarding sensors for corrosion, pH and chloride.

The project is financed by Green Platform agreement being a collaboration between the Norwegian Research Council, Innovation Norway, Siva and Enova. The following partners are involved in the research project.

**Infrastructure owners:** Equinor (representing offshore platforms), Glitre Energi, Hafslund Eco, Hydro, SFE (all representing dams), Nordland County Municipality and Norwegian Public Roads Administration (both representing bridges)

**Consulting agencies:** Multiconsult, Norconsult, OPAK

**Executing companies:** Aker Solutions, Protector

**Method suppliers:** Consolvo, Elop

**Material suppliers:** Mapei

**Digitalisation:** ProXpect drones

**R&D:** SINTEF, NTNU

# Table of contents

<b>1</b>	<b>Introduction</b> .....	<b>6</b>
1.1	Background and significance.....	6
1.2	Aim and objectives.....	7
<b>2</b>	<b>Inspection of concrete structures and common defects</b> .....	<b>8</b>
2.1	Concrete structures in general.....	8
2.2	Common defects in concrete structures.....	8
2.2.1	Concrete defects.....	9
2.2.2	Reinforcement and prestressing defects.....	11
<b>3</b>	<b>Condition assessment of concrete structures</b> .....	<b>16</b>
3.1	Level 1 - Basic Condition Analysis.....	17
3.2	Level 2 - Extended Condition Analysis.....	17
3.3	Level 3 - Comprehensive Condition Analysis.....	17
3.4	Condition assessment of prestressed concrete structures.....	20
<b>4</b>	<b>NDT&amp;E definitions and systems</b> .....	<b>23</b>
<b>5</b>	<b>NDT toolbox</b> .....	<b>26</b>
5.1	Visual inspection and simple methods.....	30
5.2	Optical methods.....	30
5.2.1	Active 3D imaging – active sensors.....	31
5.2.2	Passive 3D imaging.....	36
5.2.3	Infrared thermography.....	40
5.3	Mechanical and acoustic methods.....	41
5.3.1	Impact echo (IE).....	41
5.3.2	Ultrasonic Pulse velocity (UPV) and Ultrasonic Pulse Echo (UPE).....	43
5.3.3	Ultrasonic Tomography.....	45
5.3.4	Acoustic emission (AE).....	47
5.3.5	Impulse response (IR).....	49
5.4	Electro-magnetic methods.....	50
5.4.1	Covermeter.....	50
5.4.2	Ground-penetrating radar (GPR).....	51
5.4.3	Half-cell potential.....	52
5.4.4	Radiography.....	54
<b>6</b>	<b>Monitoring of Concrete Structures</b> .....	<b>55</b>
6.1	Structural monitoring.....	58



6.1.1	Deformations and displacements.....	58
6.1.2	Tilt and inclinations.....	60
6.1.3	Strain.....	63
6.1.4	Formation of Cracks.....	64
6.1.5	Vibrations and acceleration.....	66
6.1.6	Fibre optical sensors (FOSs).....	67
6.1.7	Non-contact optical sensing technologies.....	71
6.2	Structural health monitoring .....	73
6.2.1	Temperature.....	73
6.2.2	Relative humidity (RH).....	73
6.2.3	Corrosion sensors .....	76
6.2.4	Chloride and pH .....	78
6.2.5	Water pressure in dams .....	79
6.3	Norwegian case studies on existing infrastructure.....	81
6.3.1	Bridge monitoring.....	81
6.3.2	Dam monitoring.....	83
6.3.3	Field stations.....	85
<b>7</b>	<b>References .....</b>	<b>87</b>

APPENDICES

---

Klikk eller trykk her for å skrive inn tekst.

---

# 1 Introduction

## 1.1 Background and significance

Regular inspections of existing bridges, dams or offshore constructions are scheduled during their service life to evaluate their health and as part of proactive maintenance where future deterioration is anticipated. The time interval of minor and major detailed inspections varies for different types of constructions. Inspections are often categorized as either 1) Visual, 2) Main and 3) Special inspections. Typically, a routine (visual/minor) inspection consists of field measurements and visual observations made by an inspector. In main and special inspections advanced equipment like drones might be used. In case of concrete dams, the main purpose of general inspection is to gather information about concrete deterioration, potential steel rebar corrosion, water seepage, spalling, deflection/settlements and cracks (Alani et al., 2014; Phares Brent M. et al., 2004). The data is documented through field inspection notes, freehand sketches, and photographs. Often, the data is stored in different systems and data collection and visualization still relies on paper-based record keeping processes (Popescu et al., 2019b). In addition, the procedure is highly dependent on the inspector's experience (Phares Brent M. et al., 2004), and knowledge of the structural behaviour and material properties of the system being investigated. The method has its limitations in the sense that only accessible parts are investigated due to the difficult terrain in the location of the structure. This is especially true for large structures, such as dams, where investigating the whole area would be highly time-consuming and potentially unsafe. For a comprehensive evaluation and monitoring of both general reinforced concrete structures and specifically prestressed concrete structures, relying solely on visual inspections and concrete sampling is insufficient. Alternatively, opting for a more advanced assessment is expected to yield results that more closely mirror reality.

It is widely recognized that major structures require comprehensive health monitoring systems for the purpose of damage detection and condition assessment (Chang et al., 2003). The damage can be detected by observing a set of certain features such as structural vibration and static deformation. A large amount of research has dealt with maintenance and monitoring of civil structures addressing relevant areas such as loads, hazards, monitoring and inspection, management, etc. However, there are few initiatives to implement results obtained from NDT&E (Non-destructive testing and evaluation) to achieve a data-driven assessment. While a data-driven assessment has been approached in a few projects recently (Alonso Medina et al., 2022; Xia et al., 2022; Xu and Azhari, 2022), there are still important challenges and barriers to be resolved such as:

- **Technical barriers**
  - a) **Data Accuracy and Interpretation:** Ensuring accurate data collection and interpretation, especially for complex structures, can be technically challenging.
  - b) **Sensor Placement and Calibration:** Deciding where to place sensors and calibrating them properly to capture meaningful data.
  - c) **Validation of NDT Techniques:** Verifying the accuracy and reliability of NDT methods for large structures.
  - d) **Lack of standardization** of available NDT&E methods
  - e) **Lack of training** for NDT&E personnel
- **Logistical barriers**
  - a) **Access and Logistics:** The physical access to and logistics of inspecting and monitoring large structures.
  - b) **Environmental Factors:** Dealing with adverse weather conditions and environmental factors can be a logistical obstacle to consistent monitoring.
  - c) **Safety Concerns:** Ensuring the safety of personnel working on large structures, especially in hazardous environments, is a logistical consideration.

- **Liability barriers**
  - a) **Interpretation Responsibility:** Determining liability for data interpretation and making decisions based on the data can pose legal challenges.
- **Cost barriers**
  - a) **General:** Special funding might be needed on public structures and in case of special inspections. Public procurement sometimes needed to decide who is to perform the inspection.
  - b) **Initial Investment:** Potential substantial initial investment required for equipment, sensors, and personnel.
  - c) **Ongoing Maintenance:** Maintaining monitoring systems over the long term can incur significant costs.
  - d) **Data Management:** Establishing and maintaining effective data management systems can be costly.
  - e) **Sensor Replacement:** Replacing sensors and updating technology as needed can contribute to ongoing costs.
  - f) **Personal replacement:** Replacement of educated and trained personal for specialised NDT or sensor techniques and monitoring systems can be a challenge.
  - g) **Access:** Gaining access needs to be coordinated with traffic, public events and other arrangements

Among all barriers, the cost barriers can be identified and overcome through a cost-analysis, as evidenced by numerous studies delving into the quantification of the value of NDT&E (Mandić Ivanković et al., 2018). While the remaining obstacles could be overcome, achieving this requires a combination of state-of-the-art technology, sound methodology, and trained personnel.

A better understanding of NDT&E methods is required, especially concerning prestressed concrete structures, where their size, cable placement, and potential types of damage complicate inspections, making them time-consuming when conducted without partially destructive testing.

In this project, our goal is to provide an up-to-date review of the current NDT techniques, prioritizing them based on their effectiveness in assessing the most prevalent issues in concrete structures, with a particular emphasis on prestressed concrete. Furthermore, an overview of available sensors for continuous structural health monitoring is given in the second part of the report.

## 1.2 Aim and objectives

The current report is part of H3 work package of the EXCON project, where the overall aim is to provide guidelines for the use of NDT, with and without robots/drones, and the use of sensors for continuous monitoring. Specifically for the current report the aim is to provide a broad overview of existing NDT&E methods and sensors, and, based on the most common deterioration mechanisms found in the target structures (bridges, dams and offshore oil platforms), suggest a priority list of the most relevant methods for further development.

## 2 Inspection of concrete structures and common defects

### 2.1 Concrete structures in general

Concrete always consists of cement, water, sand, gravel, and stone as its core components. Additionally, concrete can incorporate various additives to achieve specific properties during both fresh and hardening stages. Cement may also contain supplementary cementitious materials (SCMs) like fly ash, silica fume, ground granulated blast-furnace slag, or many other pozzolanic or latent hydraulic materials which can partially replace a portion of the cement in the concrete mix.

Concrete has many advantages, such as formability, high compressive strength, high stiffness, durability, in general long life, wear resistance, fire resistance, good noise properties, resistance to moisture and water and its potential to be reused or recycled. On the other hand, it has some drawbacks, such as low tensile strength, notable shrinkage, and the significant CO<sub>2</sub> emissions mainly associated with current cement manufacturing processes.

To address the issue of low tensile strength, reinforcement materials like steel (and occasionally other materials like glass or carbon fibre bars/rods/tendons) are used. Furthermore, there is global focus on reduction of CO<sub>2</sub> emissions from cement and concrete manufacturing to net zero in 2050 by R&D on e.g. developing new binders with high amounts of SCMs, implementing carbon capture and storage (CCS) facilities at cement plants, increasing efficiency in concrete production and design and construction methods, as well as enforced carbonation of recycled concrete or other waste materials (<https://gccassociation.org>).

### 2.2 Common defects in concrete structures

Concrete structures typically have a long lifespan and high durability. However, over time, these structures are exposed to various influences. These can include external factors such as traffic, wind, temperature, and more. They can also involve wear and tear, chlorides from road salts and seawater, as well as carbonation of the concrete due to reaction with airborne CO<sub>2</sub>. Chlorides and carbonation

can, in turn, lead to corrosion of the reinforcement. Figure 1 summarizes typical damages that can occur in a concrete structure together with the associated causes of such defects.

The classification of damage is based on its underlying cause. It is implied that concrete structures may require regular inspections, which can be referred to as condition assessments. Understanding the types of damage that can occur in concrete is essential for conducting condition assessments, both visually and through non-destructive testing. Therefore, concrete and reinforcement damage is briefly described below.



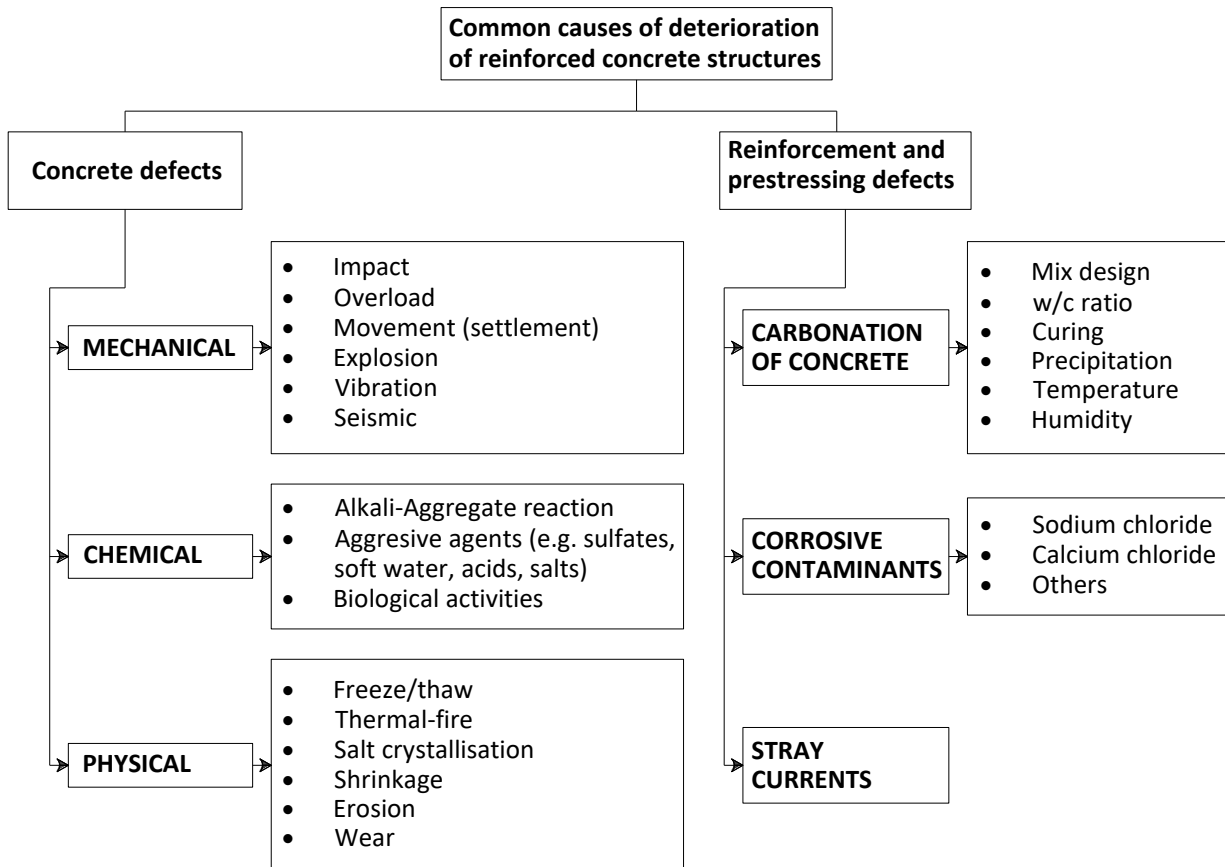


**Figure 1. Deterioration process (after Part 9 of EN 1504)**

## 2.2.1 Concrete defects

### 2.2.1.1 Mechanical

There are various types of damage that can have mechanical causes, such as abrasion, impacts, damage caused by fatigue, movements, overloading, and more. Sometimes, it can be challenging to immediately determine the cause of damage, and the damage itself may not be readily visible. For instance, fatigue in concrete is characterized by the onset of microcracks that are not visible to the naked eye and require assessment through techniques like thin-section analysis. Often, fatigue in concrete isn't a problem itself, but when discussing fatigue, it's typically related to the reinforcement. In this case, identifying the issue is simpler because it's mostly localized to tension cracks that open and close under load.

Damage from excessive loads (overloading) can occur during the construction phase, especially when concrete hasn't yet attained its intended strength. Premature removal of formwork, the placement of heavy materials, or the operation of machinery in proximity to the structure can lead to the overloading of specific concrete components. A frequent mistake arises when precast elements aren't adequately supported during transportation and installation. In post-tensioned construction, overload cracking can also result from errors like improperly timed or sequenced strand releases.

Wear and tear can be easily observed visually and may result from factors such as studded tires in parking garages or erosion due to flowing water and cavitation on ship hulls. Damage from overloading or impacts often manifests as crack patterns or delamination, rarely resembling the extensive damage shown in Figure 2.



**Figure 2. Damages due to vehicle impact: Vehicle impact to Sgt. Bluff bridge in Iowa, March 17, 2005 (Harries et al., 2012)**

### 2.2.1.2 Chemical

Chemical attacks are linked to damage caused by alkali-silica reactions (ASR), sulphates, soft water, biological influences, and acids. Reinforcement corrosion due to chloride or carbonation is treated in a separate sub-chapter below. The damages due to different chemical attacks exhibit somewhat different characteristics, with ASR being perhaps the most well-known and most common mechanism in Norwegian dams. These damages are characterized by so-called "map cracking," as seen in Figure 3, with cracks forming a grid-like pattern, but can also manifest as spalling and "pop-outs" on the concrete surface. The cause of ASR damage is the combination of reactive silica in the aggregates, alkalis from cement, and water, which serves as both a reactant and a transport medium. The most severe cases are primarily found in older structures from the 1960s and 1970s. Even if the crack pattern is recognized, a petrographic analysis may be required to map ASR for the individual structure.

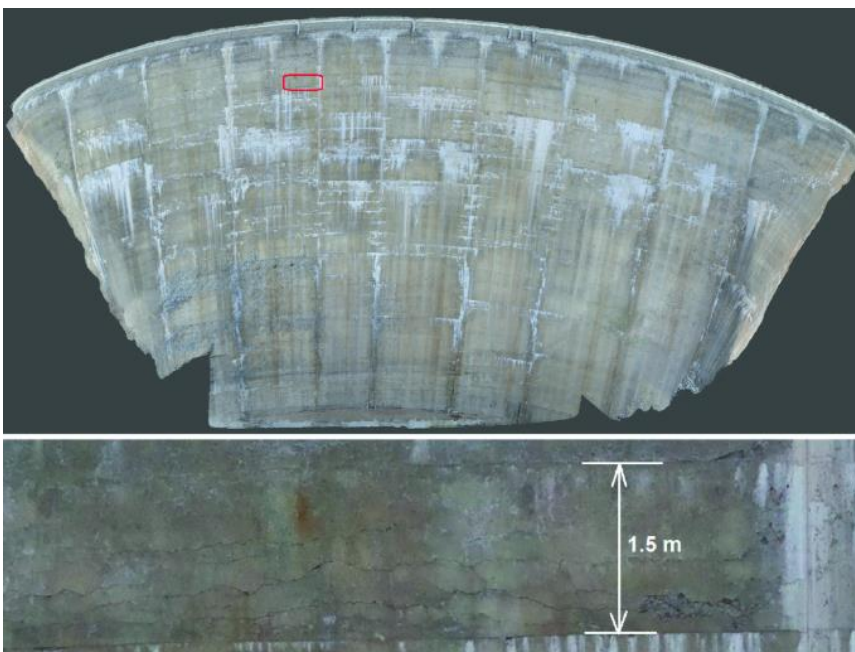


**Figure 3. Concrete dam suffering from ASR (Salamon et al., 2021).**

Chemical attacks, such as those from acids, typically manifest as spalling and are primarily localized to industries with chemical operations. Other, less common attacks involve damage from sulphates, which are

salts of sulfuric acid, often dissolved in water as sulphate ions ( $\text{SO}_4^{2-}$ ). Initially, these damages may appear similar to ASR damages but are caused by the reaction of calcium aluminate hydrates (AFm) and calcium hydroxide ( $\text{Ca}(\text{OH})_2$ ) with sulphates, resulting in expansive products. Sulphate attacks fall into the category of salt attacks since sulphates are salts of sulfuric acid.

### 2.2.1.3 Physical

Physical damages include frost damage, damages caused by temperature variations, such as those from curing and hydration heat, or from external heat sources. Physical damages can also result from erosion and various types of wear, similar to mechanical damages from abrasion. Shrinkage of concrete is also classified under this category. Concrete shrinks as it loses water, so proper curing, such as through watering or membrane protection, is important. It is also essential to design and dimension for the shrinkage forces that may occur. The moisture loss in hardened concrete, i.e., drying shrinkage, is one of the major causes of bridge deck cracking. Restrained shrinkage cracking of concrete bridge decks creates a significant durability problem.

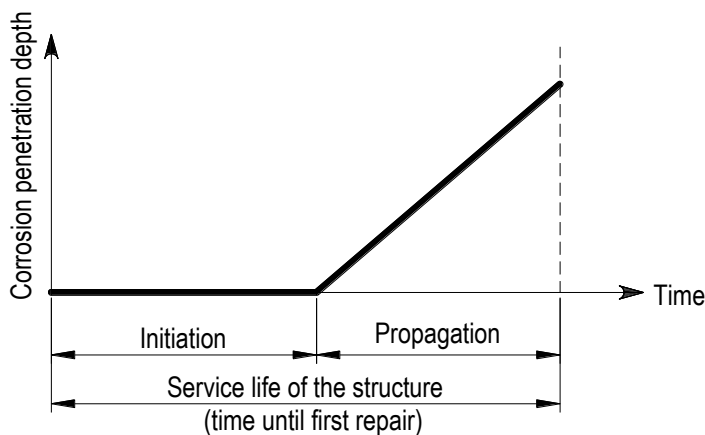
Frost damages typically manifest as spalling on the concrete surface and can, over time, deteriorate the entire structure. Figure 4 shows a typical frost damage example. The primary cause of frost damage is usually attributed to the expansion of water when it freezes, as well as osmotic processes and the formation of ice lenses. The risk of frost damage is high for non-air entrained concrete, and the minimum of air for frost-resistant concrete is approximately 4%. Furthermore, the extent of damage through scaling is typically increased in the presence of chlorides. Horizontal surfaces have the highest risk, hence to protect against frost damage, it is necessary to divert water away from the concrete.



**Figure 4. Example of frost damage in concrete that has caused delamination on the surface.**  
[www.fritzpak.com](http://www.fritzpak.com)

### 2.2.2 Reinforcement and prestressing defects

Reinforcement corrosion is one of the most common causes of compromised safety and reduced service life. Corrosion on reinforcement bars is typically divided into corrosion caused by carbonation and corrosion caused by chlorides. Many times, the damages that occur and are observed are a combination of both, but not always. The process of damage by reinforcement corrosion is typically divided into an initiation and propagation period to estimate the time until first repair (Figure 5). Corrosion is an electrochemical process in which electrons are transferred between the anode and cathode. Positively charged iron ions,  $\text{Fe}^{2+}$ , dissolve at the anode, releasing electrons through the rebar to the cathode. At the cathode, a chemical reaction occurs between electrons, water, and oxygen, forming hydroxyl ions ( $\text{OH}^-$ ). Iron ions  $\text{Fe}^{2+}$  and hydroxyl ions  $\text{OH}^-$  react to form  $\text{Fe}(\text{OH})_2$ , i.e., rust.



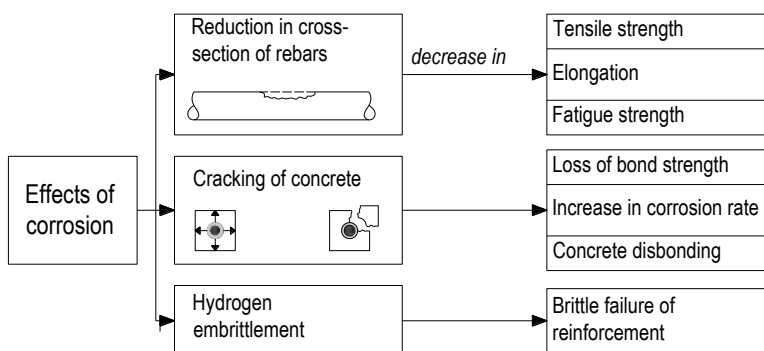
**Figure 5. Initiation and propagation periods for corrosion in a reinforced concrete structure (Tuutti, 1982)**

Figure 5 illustrates the division of the service life into two distinct phases:

- In the initial phase, referred to as initiation, the reinforcement remains passive. However, phenomena that can lead to the loss of passivity, such as carbonation or the penetration of chloride into the concrete cover, occur.
- The subsequent phase, known as the propagation of corrosion, begins when the steel becomes depassivated and continues until a critical state (e.g. rebar diameter reduction, concrete spalling) is reached. Beyond this point, the consequences of corrosion cannot be tolerated any further (Tuutti, 1982).

Corrosion of steel reinforcement does not solely impact the external condition or serviceability of a structure; it can also have implications for its structural performance and, consequently, its safety.

Main consequences of corrosive attack are shown in Figure 6.



**Figure 6. Structural consequences of corrosion in reinforced concrete structures (CEB, 1992)**

### 2.2.2.1 Carbonation-induced corrosion

In undamaged concrete, the reinforcement is protected by the high pH value present. Carbonation is a diffusion process that occurs when carbon dioxide in the air penetrates the pores of the concrete and neutralizes the alkaline, passivating layer of concrete that covers the reinforcement. Carbon dioxide reacts first with calcium hydroxide,  $\text{Ca}(\text{OH})_2$ , causing a reduction in the concrete's pH value from approximately 13-14 to around 10 which is enough to break down the passive film (initiation phase). This pH reduction can lead to the onset of reinforcement corrosion if moisture and oxygen are present (propagation phase). In very dry environments, the carbonation process is slow, while in very wet environments, it also slows down. Corrosion caused by carbonation is characterized by evenly distributed corrosion over the affected area, as seen in Figure 7. Corrosion induced by carbonation can take place on the whole surface of steel in contact with carbonated concrete – general corrosion (Bertolini et al., 2003). To determine the depth of carbonation,



a thymolphthalein (earlier also phenolphthalein) solution is often used, which is applied to a freshly exposed or drilled concrete surface. The area that does not change colour (pH < 10) has undergone carbonation. This method allows for a relatively straightforward assessment of the depth of carbonation, as shown in Figure 8.



Figure 7. Corrosion caused by carbonation (Täljsten et al., n.d.)



Figure 8. Application of phenolphthalein on a recently exposed concrete surface, an uncoloured area indicates carbonation (www.structuralguide.com)

In summary, the propagation rate is controlled by oxygen diffusion and the presence of moisture. The initiation and propagation of corrosion through carbonation are illustrated in principle in Figure 9. The rate of carbonation depends on both environmental factors (humidity, temperature, concentration of carbon dioxide) and factors related to the concrete (alkalinity and permeability) (Bertolini et al., 2003).

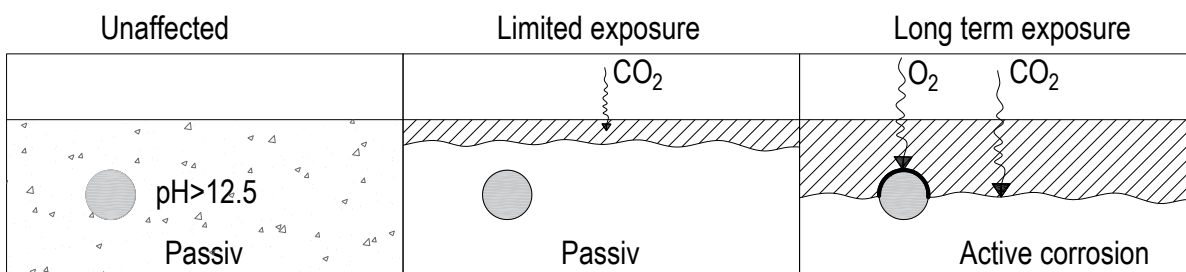


Figure 9. Schematic diagram of carbonation-induced corrosion (Fagerlund, 1992)

### 2.2.2.2 Chloride-induced corrosion

Chlorides in concrete can originate from sources such as de-icing salt, seawater, groundwater, or chemical additives. In accordance with the European standard EN 206, the permissible chloride levels are between 0.2% and 0.4% of chloride ions by the mass of binder for reinforced concrete, and between 0.1% and 0.2% for prestressed concrete.

In certain structures constructed in the past, chlorides were inadvertently or intentionally introduced into the concrete mix through contaminated mixing water, aggregates, or additives (with calcium chloride being the most common accelerating admixture used in the past, now being prohibited) (Bertolini et al., 2013). Chloride contents resulting from accelerating additives, ranging from 0.5% to significantly exceeding 2% by the mass of cement, have led to extensive corrosion damage following carbonation (Polder, 1999)

Chlorides typically infiltrate from the surface of the structure and generally increase over time at constant exposure. When the chloride concentration reaches a critical level at the reinforcement cover depth, known as the threshold value, corrosion can be initiated. Chloride ingress and its impact on propagation depend on several factors, and some of the factors mentioned by Fagerlund (1992) are presented below:

- Exposure chloride concentration
- Chloride transport rate
- Chloride binding capacity
- Critical chloride level/chloride threshold value

The general quality of the concrete (w/b ratio, strength, porosity), relative humidity etc. also plays a crucial role.

Chlorides can be absorbed or chemically bound in hydration phases of the cement paste. The main factor affecting the ability to bind chlorides is the chemical composition of the cement ( $C_3A$ -,  $C_4AF$ -, alkali content) and the amount of cations ( $OH^-$ ,  $SO_4^{2-}$ ,  $CO_3^{2-}$ ) competing for the sites where chloride ions can bind. Increased  $C_3A$  content and reduced alkali content both increase chloride binding. The addition of mineral admixtures, especially admixtures containing reactive alumina like fly ash or calcined clays enhances chloride binding. The chloride ions that are not bound to the cement paste are the free chlorides, which are the ones that affect the corrosion process. A schematic diagram of chloride-initiated corrosion is shown in Figure 10.

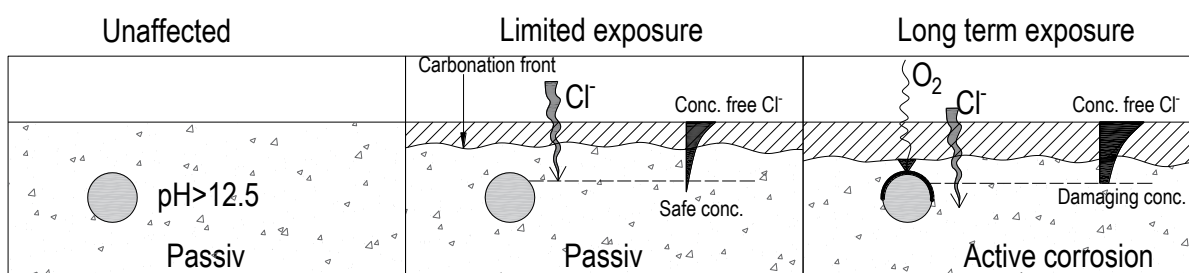


**Figure 10. Schematic diagram of chloride-initiated corrosion (Fagerlund, 1992)**

Chloride-initiated corrosion does not always spread uniformly across the reinforcement steel. It's often concentrated in specific areas, appearing as pitting in the steel reinforcement. In some sections, the reinforcement may be entirely corroded, while in others, it may be unaffected. Figure 11 shows the common pit shapes and a typical illustration of a reinforcement bar damaged by pitting corrosion.

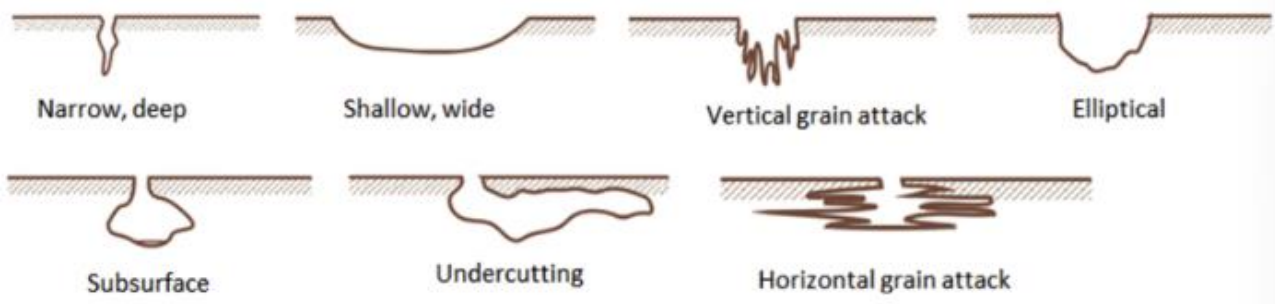


Figure 11. Sketch of common pit shapes (Bhandari et al., 2015)



Figure 12. Pitting corrosion in reinforcement caused by chlorides. Reinforcement extracted from a quay in northern Norway.

To measure the chloride content in concrete, one can either drill out concrete cores, and divide these into sections of interest by cutting or powder milling, or one can directly extract concrete powder from the areas of the structure to be investigated, preferably around the reinforcement. There are several standards for this, such as SE-EN 14620:2007, ASTM C1218, and ASTM C1152.

A common factor of all these damage types mentioned above is moisture ( $H_2O$ ), i.e., water. If constructions can be protected from moisture or relieved from its presence, the degradation process will cease or be delayed. In summary, the following conclusion can be drawn:

- Without moisture, there are no frost damages.
- Without moisture, there are no salt frost damages.
- Without moisture, there is no reinforcement corrosion.
- Without moisture, there is no ASR (Alkali-Silica Reaction).
- Without moisture, there is no calcium leaching.
- Without moisture, there is no increase in microcracks.
- Treated concrete is resistant to acid attacks.

Considering this, it can be concluded that it is not enough to merely repair existing damage; a protective treatment is also necessary to achieve a functional and long-lasting renovation.

### 3 Condition assessment of concrete structures

The condition assessment aims to map the status, repair needs, and ensure that sufficient safety exists regarding continued operation and the structural load-bearing capacity. In Figure 13, a schematic representation of a structural change over time is shown, assuming that materials degrade or that loads change over time. Figure 13 depicts the construction's function/performance on the y-axis and time on the x-axis. We assume that the construction has an approved function/performance according to design when it was built and that after a certain time, it reaches the minimum acceptable requirements. These requirements can vary, but they usually refer to safety and a level that should not be undercut. The solid line represents an assumed scenario where we have the estimated lifespan from the beginning. A condition assessment is conducted, and it indicates that the estimated lifespan was significantly shorter, as shown by the black dashed line.

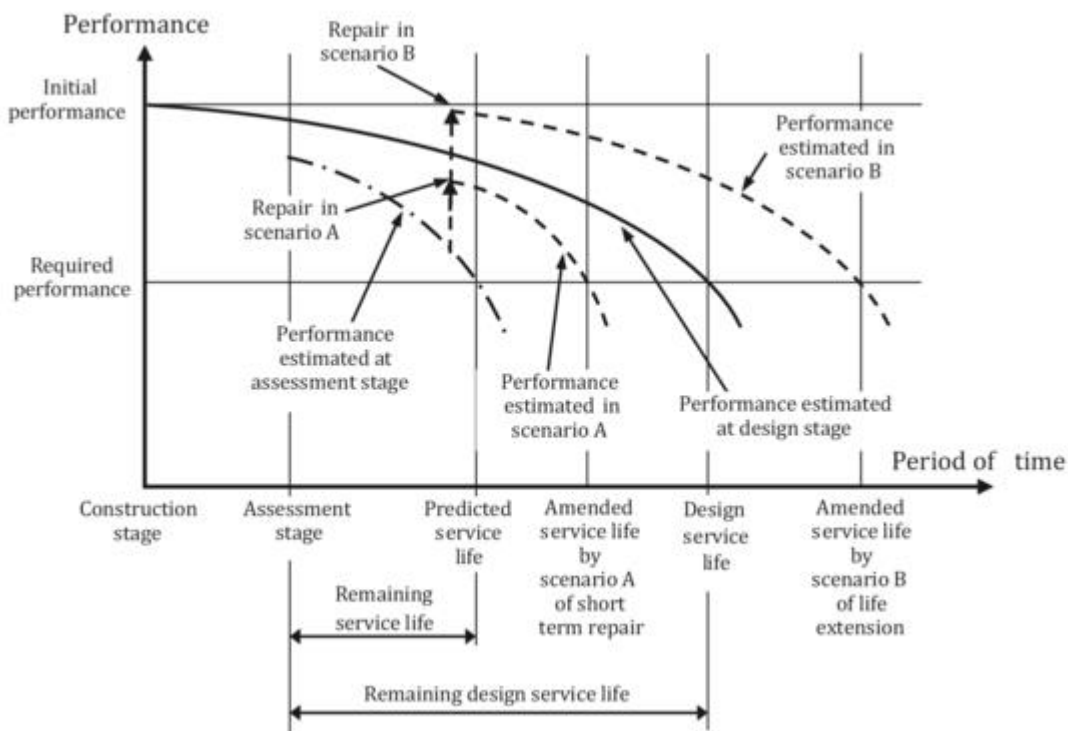


**Figure 13. Process for the degradation of concrete structures and definitions of service life (ISO 16311-1)**

When a decision is made to act, various strategies can be chosen. Scenario A involves smaller but more frequent actions over time to achieve the intended service life. The second dashed line, Scenario B, represents a larger intervention that extends the service life beyond the originally assumed one, while maintaining the same performance (e.g., load-bearing capacity). Another scenario may also be added where we upgrade the structure, resulting in both higher performance and a longer service life. Therefore, condition assessment is crucial in determining the most accurate course of action. It's advantageous to divide the assessment into three levels as follows:

- Level 1 - Simple condition assessment
- Level 2 - Expanded condition assessment
- Level 3 - Comprehensive condition assessment



### 3.1 Level 1 - Basic Condition Analysis

At this level, an evaluation of the condition is performed based on visual observations, potentially combined with cover layer measurements and registration of carbonation depth. Typically, the inspection is conducted without scaffolding or extensive access equipment. The primary tools for this analysis include photography/videography, and a general assessment is made of factors such as cracks, the condition of the cover layer, settlements, displacements, rust deposits, etc. A comparison is made with previous analyses, and plans are made for higher-level assessments. This level can also assess the need for preventive measures.

### 3.2 Level 2 - Extended Condition Analysis

An extended condition analysis involves a visual inspection of the entire structure, typically using scaffolding or a lift for access. The key objectives here are to identify the causes of damage, assess the extent of damage, and determine if the damage is expected to worsen. A level-2 inspection typically includes measurements of carbonation depth, cover layer measurements, chloride content, crack width measurements, assessment of corrosion, adhesion to concrete, uncovering parts of the reinforcement, and in some cases, potential measurements, reinforcement continuity measurements, and even measurements of deformations and settlements. This information is used to compile data for engineering projects and maintenance planning.

### 3.3 Level 3 - Comprehensive Condition Analysis

In addition to all the activities conducted at Level 2, a comprehensive condition analysis includes a deeper investigation into the deterioration mechanisms identified during Level 2, as well as strength testing. Typically, a structural assessment is performed, either for specific parts or the entire structure, based on the condition analyses conducted. In some cases, monitoring equipment may be installed on the structure to track changes over time, providing further information for the condition analysis. Furthermore, various non-destructive testing methods are often employed to assess the condition of the structure comprehensively.

The different levels should be seen as guidelines, and there is often no strict differentiation between them. The choice of which level to apply depends primarily on the specific object under investigation. Therefore, investigations of various parameters and their analysis are often combined.

In Figure 14, a flowchart is presented schematically, outlining the general steps for the condition assessment of structural elements, based on international standards (ISO 16311-2, ISO 13822). This flowchart is applicable to concrete structures in general. However, for prestressed structures, more specificity may be required, as described in the following sections.

In the planning stage, recommendations are provided regarding what should be done, the recommended equipment, and how reporting should be conducted. There is also an option for verifying the findings in the field, with the decision to do so depending on factors such as the surrounding environment, as exposing prestressed reinforcement may not always be practical. The assessment is summarized in a partial report, which is typically subject to approval by the responsible authority.

After evaluating the results, further investigations may be necessary, such as assessing chloride content. Finally, the work is summarized in a final report, with some cases skipping the intermediate partial report. An essential aspect of a condition assessment, as highlighted, is the use of non-destructive testing methods. Returning to concrete bridges, a focus in EXCON project, the main inspection is the most comprehensive inspection conducted and requires more planning compared to the others to ensure smooth execution. This

inspection is carried out at least once every six years on all of the Swedish Transport Administration's bridges. The first main inspection is conducted before the structure is put into operation (Trafikverket, 2015).

The purpose of the main inspection is to investigate if there are any deficiencies that, within a ten-year period, could have a negative impact on the bridge's functionality or safety. The inspection also aims to assess whether any unrepaired damage could lead to increased maintenance costs over time. All accessible structural elements and adjacent/connecting parts are visually inspected at close range. Some examples of adjacent parts include slopes, embankments, and road banks.

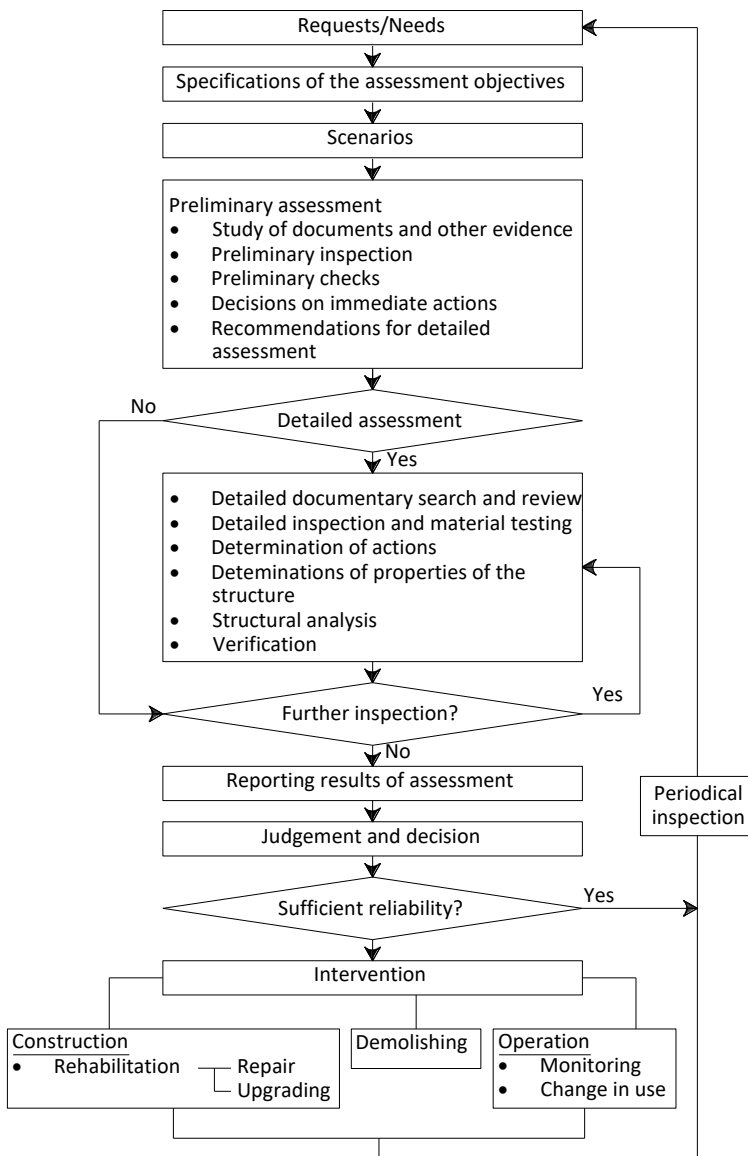


**Figure 14. General flowchart for assessment of existing structures (adapted from ISO 13822, Annex B)**

**Main inspections.** The inspector conducting the main inspection should assess whether a special inspection should be carried out to ensure the bridge's safety and load-bearing capacity and to avoid increased maintenance costs within a ten-year period. Such an inspection aims to monitor the progression of relevant deterioration processes and wear on the environment, rock, reinforcement, concrete, welds, rivets/screws, sealants, and bottom profiles. The inspector also assesses whether additional special underwater

inspections should be conducted for the same reasons. The basic knowledge and experience requirements for the inspector include:

- Academic education; the individual should have an engineering degree.
- Authority's inspection methodology: the inspector should have either applied this in practice for several years or received theoretical training.
- Utilization of current measurement methods.
- Experience in measurement and assessment of bridges' physical and functional conditions.
- Forecasting bridge durability through the analysis of damage progression and deterioration processes.
- Damage mitigation measures.

General inspections are primarily conducted as a follow-up to the assessments made during the most recent main inspection for damages that have not yet been addressed. During the inspection, an overall check is also carried out to detect and assess any newly emerged damages. Damages that could potentially lead to increased maintenance costs, reduced load-bearing capacity, or compromised traffic safety if left undetected before the next main inspection are documented. For minor damages that are not deemed to have such consequences, an assessment is made at the next main inspection.

Special inspections are conducted when there is deemed to be a need for more information to assess the condition of a structural element. These inspections require specific measurements that necessitate equipment and expertise not expected to be available during the main inspection. Two examples of such measurements are ultrasonic testing for inspecting welds on steel structures and detailed investigations of bedrock conditions. Special inspections are carried out by personnel who meet the basic requirements for main inspections and possess the specialized competence and experience necessary to conduct the examination (Trafikverket, 2015). Prestressed concrete structures are often in need of special inspections to due its complex nature. One challenge with prestressed concrete bridges is the ability to inspect the quality and functionality of existing prestressing systems without causing physical damage. Therefore, non-destructive testing methods are needed that not only map the placement of tendons and prestressing reinforcement but also detect voids, breaks, and potential corrosion in cables. Prestressed concrete bridges under the administration of Swedish Transport Administration, are shown in Table 1 and Table 2. The age distribution is crucial because standards and equipment had their early issues; for example, chlorides were allowed in grouting materials before 1968, and the earlier thin sheathing pipes were replaced with thicker ones around 1978. This means that well-executed condition assessments should ideally be carried out for prestressed bridges built before 1980. However, how this should be conducted is not covered by current regulations. The majority of these bridges, around 400, are managed by the Swedish Transport Administration and many of them serve as crucial transportation links. Nevertheless, there are also prestressed concrete bridges under the management of other entities, so the total number of prestressed bridges is likely to exceed 2000 in total in Sweden.

**Table 1. Prestressed concrete bridges administered by Trafikverket, Sweden**

	<b>Total</b>	<b>Average length, [m]</b>	<b>Total length, [km]</b>
Road bridges	1364	96	131
Railway bridges	<b>308</b>	<b>111</b>	<b>34</b>
Pedestrian bridges	<b>14</b>	<b>50</b>	<b>0.7</b>

**Table 2. Age distribution for prestressed concrete bridges managed by the Swedish Transport Administration (Trafikverket, n.d.)**

Opening year	-1929	30-39	40-49	50-59	60-69	70-79	80-89	90-99	2000-
Road bridges	4	3	3	23	131	173	143	279	605
Railway bridges	28	7	1	5	26	39	331	93	78
Pedestrian bridges					1	2		5	6
Total	32	10	4	28	158	214	174	377	696

### 3.4 Condition assessment of prestressed concrete structures

For the previously mentioned prestressed concrete bridges, defects are not always visible, and it's important to have a systematic investigation of hidden defects, with priorities ideally based on how critical the bridge is in the infrastructure system. A thorough desk study and planning are crucial. It is impractical and uneconomical to expose all hidden structural elements for inspection, and many competing factors must be considered before any investigation is carried out. The questions that need to be asked are:

- Is the building component critical for the safety of the structure?  
Assess whether the specific component plays a crucial role in the structural integrity and safety of the entire structure.
- What are the consequences of defects in the building component?  
Understand the potential outcomes and risks associated with defects in the component, including safety hazards and structural integrity concerns.
- Can the building component be safely exposed?  
Evaluate whether it is feasible to expose the building component for inspection without compromising safety or causing damage to the structure.
- Will exposing the building component lead to damage to the structure?  
Consider the potential impact of the exposure process itself on the structural integrity of the entire building.
- Will the building component be damaged if exposed?  
Assess the risks of exposing the component, including potential damage during the inspection process.
- Will exposing the building component lead to long-term sustainability issues with the structure?  
Examine whether exposing the component could result in long-term sustainability or maintenance problems for the structure.
- Is it cost-effective to expose the building component?
- Weigh the costs of the investigation against the potential benefits and risks, considering both short-term and long-term financial implications.
- What impact would the investigation have on the operation of the facility?  
Consider how the investigation might affect the normal operation and functionality of the facility, including potential disruptions.

These questions help guide the decision-making process and prioritize inspections based on criticality, safety, and economic considerations, ensuring that the investigation is both effective and efficient.

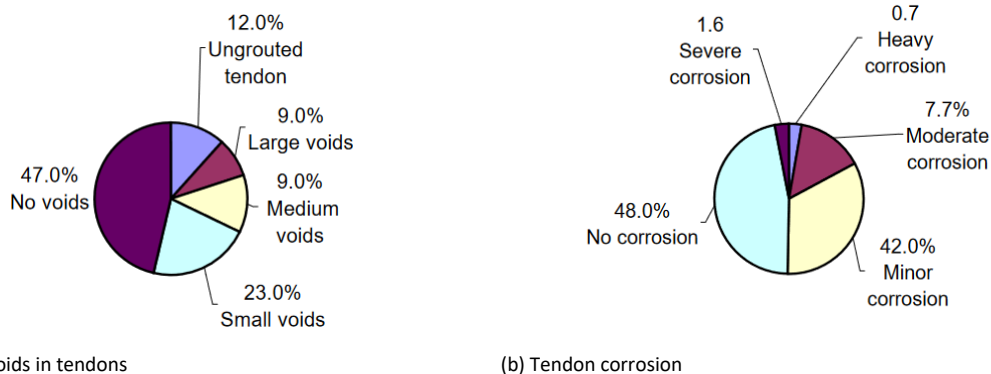
Additionally, a bridge owner may have specific limitations not mentioned here that must be considered in the assessment. The investigation of hidden defects can be conducted either as a special inspection or integrated into normal inspection routines. The former should be considered when there is a risk of defects in a hidden building component with significant consequences likely to occur before the next regular

inspection. If it is not possible to inspect all hidden building components within the required cycle or normal inspections, prioritize those with the highest risk.

In any structural condition evaluation, there are two primary categories of potential performance issues within an existing structure: defects and deterioration. A defect refers to a deviation from a standard or specified performance of a structural component in an existing structure. These defects are typically introduced during the design and/or construction phases before the structure enters its service life. Deterioration, on the other hand, represents a gradual decline in performance, such as a loss of material properties, over time. Defects can influence the rate of deterioration or even trigger premature deterioration in materials; thus, there is often a cause-and-effect relationship between the two.

For post-tensioned concrete bridges, one example of a defect could be incomplete grouting of the tendons, which, over time, might result in the deterioration of prestressed tendons, specifically corrosion leading to a loss of prestress force. The identification of such defects is crucial for extending the service life of existing prestressed concrete bridges. Without detection through condition assessments and subsequent repairs, these defects and the deterioration of prestressed tendons could potentially lead to structural failure.

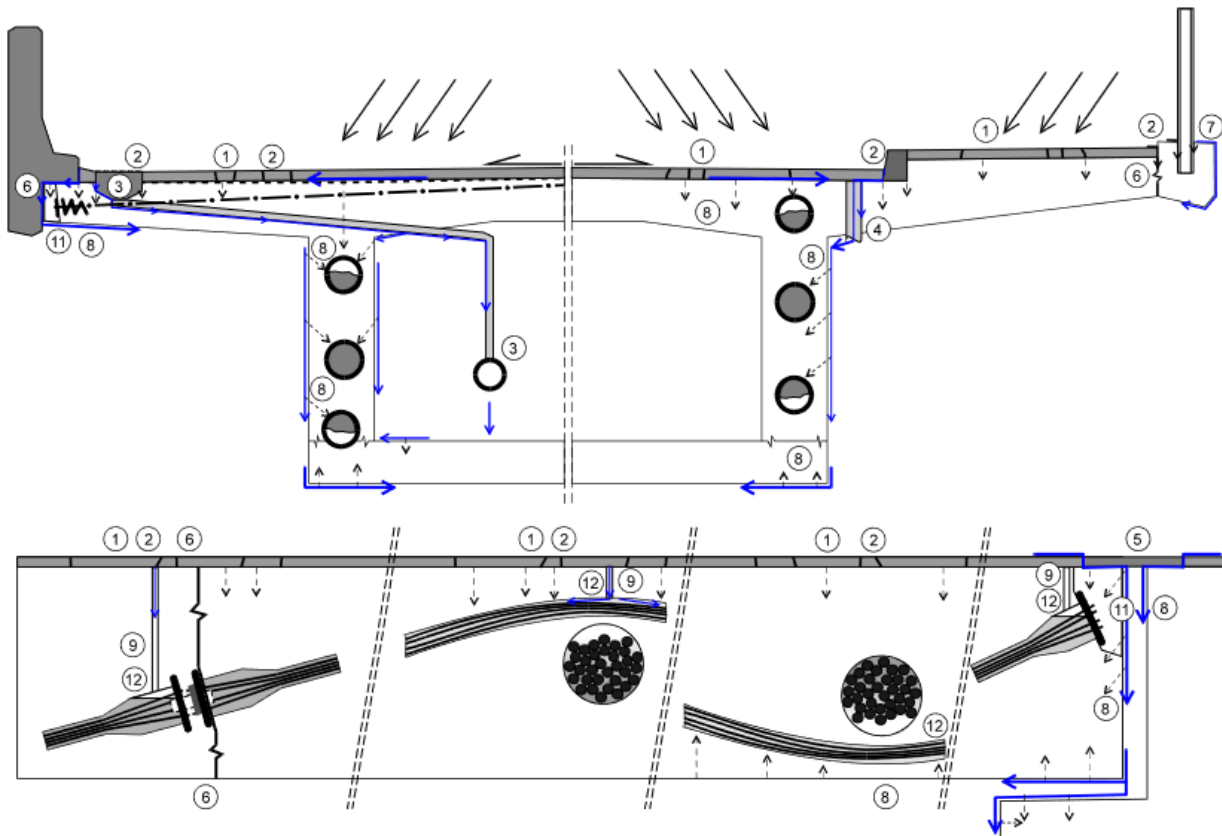
Previous research has demonstrated that prestressed concrete technology generally exhibits excellent durability. However, some studies (Woodward, 2001) have identified corrosion of post-tensioning tendons as one of the deficiencies in certain cases.



**Figure 15. Results of post-tensioning tendon inspection of 447 bridges in the UK (Woodward, 2001)**

Figure 15 presents the findings of a total of 447 post-tensioned bridges inspected in the UK showing that 47% of the tendon ducts had no voids while the remaining 53% had voids ranging from small voids (23%) to completely non-grouted (12%). Furthermore, in these bridges about 10% of the post-tensioning tendons showed moderate to severe corrosion.

Figure 16 shows hazard scenarios for prestressing steel in a typical box girder bridge together with weak points where water (possibly contaminated with chlorides) can gain access to the tendons, thus causing corrosion.


**Non-structural elements:**

- 1 Defective wearing course (e.g. cracks)
- 2 Missing or defective waterproofing membrane incl. edge areas
- 3 Defective drainage intakes and pipes
- 4 Wrongly placed outlets for the drainage of wearing course and waterproofing
- 5 Leaking expansion joints
- 6 Cracked and leaking construction or element joints
- 7 Inserts (e.g. for electricity)

**Corrosion protection system:**

- 8 Defective concrete cover
- 9 Partly or fully open grouting in- and incl. edge areas outlets (vents)
- 10 Leaking, damaged metallic ducts mechanically or by corrosion
- 11 Cracked and porous pocket concrete
- 12 Grout voids at tendon high points

**Figure 16. Hazard scenarios for prestressing steel in a typical box girder bridge indicating possible weak points (Matt, 2000)**

Detecting defects and deterioration of the prestressed tendons is a complex task due to inaccessibility. Exploratory openings (e.g. coring) would offer limited results to localized areas. Non-destructive methods should be preferred for minimum disturbance to the structure – i.e. coring done for validation only.

In non-destructive testing, the planning of the inspection is an important part for a successful end result. During the planning, a testing procedure is established where the overall problems of the construction are first mapped and then suitable NDT (non-destructive testing(s)) methods are selected, in which order they should be carried out and which construction areas should be prioritized in the investigation. When establishing the testing procedure, drawings, previous inspection reports and photos are reviewed – process known as desk study. With this as a basis, the inspection can be placed on the construction parts that are most relevant and where the greatest risk of serious damage exists.



## 4 NDT&E definitions and systems

According to (Chang et al., 2003), the process of tracking and monitoring the structural integrity and evaluating the extent of damage in a structure is often referred to as structural health monitoring. Non-destructive evaluation (NDE) constitutes an important aspect of structural health monitoring. In this context, continuous monitoring—such as tracking strains in material components, deflections, accelerations, etc. and alterations in structural properties—serves to determine the presence of damage in the structure. Non-destructive testing (NDT) encompasses all activities aimed at collecting data concerning the precise location, severity, as well as material and/or structure characteristics.

Considering the rapid growth of technologies available, these definitions are continuously changing. However, some essential features include: (1) real (or near-real)-time monitoring of in-service structures using a wide range of sensors to collect data. The data is transmitted remotely and wirelessly to a data engineer for post-processing using available algorithms. Data processing should provide damage localization and severity (usually also involving NDT methods), and in combination with advanced numerical simulations, the remaining life-time prediction.

Health monitoring of structures can be divided into several categories based on the time frame of monitoring (from few months to years) and the scale of monitoring (specific member part of the structural system to the whole structure) (Gastineau et al., 2009).

Structural health monitoring (SHM) metrics are measurements and parameters used to assess the condition, performance, and safety of civil engineering structures. These metrics help engineers track the structural integrity and detect potential issues or damage. Here are some common structural health monitoring metrics:

### **Loads: critical loads acting on a particular structure (e.g. bridge, dam, etc.)**

- **Self-weight** – important for large structures that are sensitive to its own weight. Can be evaluated by determining the specific weight of the construction material and the as-built geometry.
- **Traffic loads** – relevant for road bridges to accurately monitor the traffic loads in a particular area.
- **Hydrostatic pressure** – applied by the fluid on the dam body acting perpendicular to the contact surface.
- **Ice loads** – due to ice's action on the dam surface acting linearly along the length of the dam and depends on the temperature variations, restraint, etc. May be of interest for offshore structures.
- **Other dynamic loads** – wave, wind and seismic.

**Strain:** Strain gauges are used to measure the deformation or elongation of structural components under load. High strains may indicate stress concentrations or potential failures.

**Displacement:** Measuring the displacement or movement of specific points on a structure can help assess its overall stability and response to external forces.

**Tilt:** monitoring metric that quantifies the angular displacement or inclination of a structure.

**Acceleration:** Accelerometers are used to monitor the acceleration of a structure due to vibrations or dynamic forces.

**Frequency:** The natural frequencies of a structure can indicate its dynamic behaviour and susceptibility to resonance, which can lead to damage.

**Temperature:** Monitoring temperature variations can help identify thermal stress and expansion/-contraction effects that may affect the structure's integrity.



**Load/weight:** Load cells or load sensors measure the forces applied to a structure, helping assess if it operates within its design limits. Weight distribution on the structure may also affect its behaviour and can be determined based on optical methods.

**Crack Width, crack depth and crack pattern:** For concrete structures, measuring crack width/depth can indicate the severity of cracking and potential durability issues.

**Corrosion Rate:** Monitoring the rate of corrosion can help predict when maintenance or repairs are needed to prevent structural degradation.

**Vibration:** Vibration sensors help assess the dynamic behaviour and stability of a structure, particularly under external forces like wind or traffic.

**Deformation:** Laser-based sensors or inclinometers can measure small deformations or tilts in structures as well as differential settlements.

**Humidity/Moisture Content:** For some structures, monitoring moisture levels is essential to prevent degradation and ensure long-term durability.

**Resistivity:** Concrete resistivity is an important metric used to assess the corrosion risk of reinforcing steel within the concrete.

**Carbonation depth:** Measure the depth of carbonation in concrete, which can indicate corrosion risk.

**Chloride Content:** Determine chloride ion concentration to assess the potential for reinforcement corrosion.

**Alkali-Silica Reactivity (ASR):** Assess the risk of ASR-induced cracking and expansion in concrete.

The metrics mentioned above pertain to parameters applicable to any structure. However, when it comes to specific concrete structures and their unique monitoring objectives under NDT&E, certain parameters gain particular significance. Consequently, Figure 17 (originally designed for concrete dams, but suitable for use with other concrete structures too) provides a concise summary of the methods and equipment available for measuring and monitoring these specific parameters, depending on the initial motivations for NDT&E implementation.

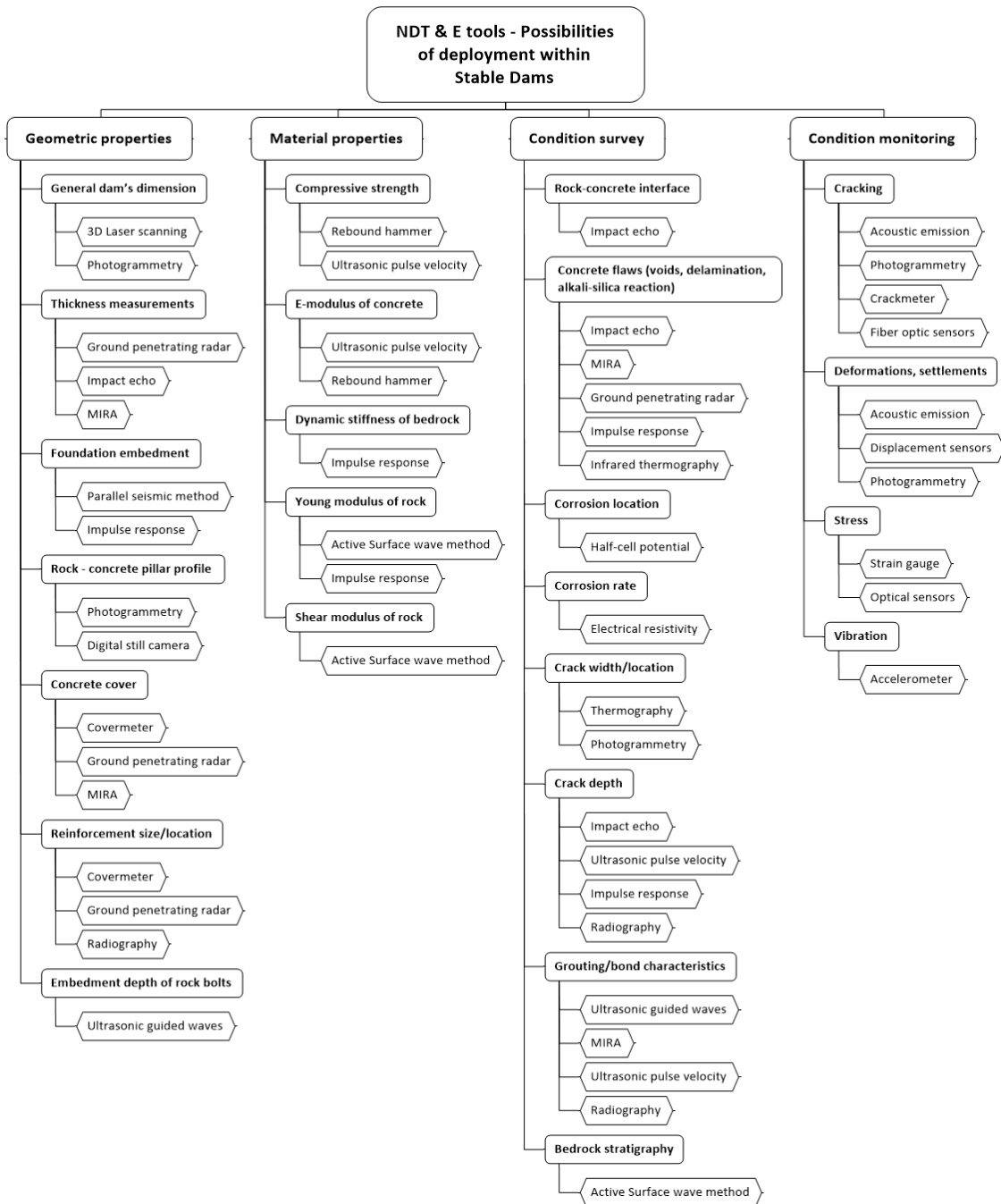


**Figure 17. Potential NDT & E (NDT + NDE) tools for condition assessment and monitoring of concrete dams (StableDams research project)**

## 5 NDT toolbox

Classification of non-destructive testing methods can be approached in several ways, as seen in references like (Blanksvärd, 2017; Kashif Ur Rehman et al., 2016). In this context, we have chosen to categorize non-destructive methods into visual, mechanical, acoustic, electromagnetic, and chemical methods. Additionally, there are partially destructive testing methods. It's worth noting that there are numerous other methods not covered in this report. Our selection is based on the most common and practical methods for assessing prestressed concrete structures, drawing from our experience in the field.

### Visual and simple methods

- Chain drag/chain sounding
- Optical methods
- Videoscope
- Crack microscope (not presented in detail)

### Mechanical and acoustic methods comprise:

- Acoustic emission (AE)
- Impact Echo (IE)
- Ultrasonic Pulse-Echo (UPE)
- Ultrasonic tomography (MIRA, Elop Insight)
- Ultrasonic Pulse Velocity (UPV)
- Impulse Response (IR)
- Rebound hammer

### Electromagnetic methods encompass:

- Ground Penetrating Radar (GPR)
- Cover meter
- Thermography (IR)
- Electrical resistivity

### Chemical and potential measurement include:

- Half-cell potential measurement (EKP)

### Partially destructive methods involve:

- Carbonation test
- Chloride test
- Thin-section analysis
- Adhesion test

### Other methods include:

- Radiography (X-ray)
- Acoustic inspection
- Synthetic Aperture Radar Imaging

To comprehensively assess structural constructions, it is often necessary to combine various NDT methods, and partially destructive testing may also be required. Table 3 provides an overview of the usability of NDT methods as a function of concrete damage.

For effectively evaluating issues related to prestressing cables in ducts, the following methods are primarily suitable:

- Cover meter
- Ground Penetrating Radar (GPR)

- Ultrasonic Tomography (MIRA, Elop Insight)
- Impact Echo
- Radiography (requires strict safety precautions)
- Acoustic Emission (possibly for cable breakage)

Furthermore, methods for assessing material properties, cracks, and other degradation effects should be considered when conducting condition assessments of prestressed concrete structures. This also applies to methods for investigating corrosion in post-tensioned reinforcement. It should also be possible to examine potential ongoing corrosion in prestressing strands, but this would require the opening of the duct.

Below, various NDT methods and their suitability for prestressed concrete structures are discussed, with a particular focus on the ability to detect ducts and voids within them.



**Table 3. Use of NDT for defect investigation of concrete structures**

Identified defects/parameters that affect concrete structures	Likely caused by design or production							Likely caused by degradation mechanisms/loading												
	Thickness measurement	Concrete cover	Honeycomb	Voids in tendon ducts	Localization of reinforcement and/or ducts	Insufficient grouting	Concrete properties (strength, E-modulus, etc.)	Concrete surface - quality/status (carbonation/chlorides)	Delamination/spalling	Moisture content	Surface cracks	Mechanical degradation (Fatigue, overloading, settlements)	Chemical degradation (ASR, acids, etc.)	Physical degradation (Frost damage, abrasion)	Crack depth	Tendon rupture	Active cracks	Remaining thickness	Remaining diameter	Reinforcement corrosion
<b>Visual</b>																				
Visual inspection	•						•	•		•	(•)	(•)	•			(•)	(•)	(•)	(•)	
Impact (hammer sounding, chain-drag)							•	•		•			•							
Optical (3D-scanning/LIDAR)	•						(•)			•	(•)									
Videoscope			(•)	(•)																
<b>Mechanical and acoustic NDT methods</b>																				
Acoustic emission (AE)								•			(•)				(•)	•			(•)	
Impact Echo (IE)	•		•	(•)	(•)	(•)		•		(•)										
Ultrasonic pulse Velocity (UPV)	•		•				•			•				•						
Ultrasonic tomography (shear wave - MIRA)	•	(•)	•	•	•	•				•	•							•		
Ultrasonic tomography (pressure wave – Elop Insight)	•	(•)	•	•	(•)	•		•		•				(•)		(•)				
Impulse Response (IR)								•												
Rebound hammer							•	(•)	(•)											
<b>Electrical and electromagnetic methods</b>																				
GPR (Geo-radar)	•	•	(•)		•			(•)										•		
Cover meter		•			•															
Thermography								(•)	(•)	(•)			(•)							

Electrical resistivity																					(•)	•
<b>Chemical and potential methods</b>																						
Electrochemical potential measurement (EKP)																						•
Minimally invasive methods																						
Carbonation test/Chloride test								•														
Thin section petrography												•	•	•								
<b>Others</b>																						
X-ray (High demands on safety)	•	•	•	•					•												•	
Test load/Concrete cores/Adhesion test	•						•	•		•												

## 5.1 Visual inspection and simple methods

The visual inspection is one of the most versatile NDT tools in which the inspector evaluates the visible, usually on the surface, defects. It is highly dependent on the inspector’s experience and knowledge about the structural behaviour and material properties of the system being investigated. It is usually the first step towards a more advanced investigation (McCann and Forde, 2001). The main purpose of this method is to gather basic information about the structural member’s condition including the existence of defects such as concrete deterioration, possible rebar corrosion, water seepage, concrete cover delamination, spalling and cracks (Alani et al., 2014). The severity of these defects should be quantified by use of more advanced NDT tools.

The visual survey aims to determine the straightness/verticality and dimensions of the structural member. Usually, no special equipment is needed other than e.g. handheld magnifier, hammer, crack width meter, laser distance meter, light and a still camera (Figure 18). Digital microscopes are available for crack width measurements. Accuracy depends on several factors including magnification, screen resolution, and proper calibration. Videoscopes are ideal for use for remote visual inspection. Several lengths and tip diameters are commercially available.



Figure 18: Examples of simple methods to supplement visual inspection.

## 5.2 Optical methods

Advanced techniques for documenting as-is condition are part of optical methods. Their main advantage is that they allow us to create an as-built 3D model of a given element that in many instances was built differently than it was designed.

Emerging technologies are now becoming more and more common in the civil engineering field. One such example is the use of optical methods – arguably a more advanced visual inspection – where the imaging characteristics of an object are recorded using high precision, high sensitivity cameras. According to (Fathi and Brilakis, 2011), optical-based sensors are classified as active or passive sensors. Active sensors obtain depth information by emitting energy and recording the reflected signals. Passive sensors make use of ambient light to capture the surrounding environment, and with the use of post-processing techniques, range data are obtained. A more detailed structuring of the imaging techniques are shown in Table 4.

**Table 4: Differentiation between active and passive 3D imaging techniques**

3D IMAGING TECHNIQUES	
ACTIVE	PASSIVE
<ul style="list-style-type: none"> <li>• Structured light</li> <li>• Laser scanning</li> <li>• Spectral imaging</li> </ul>	<ul style="list-style-type: none"> <li>• Stereo-vision</li> <li>• Fixed-view approach</li> <li>• Multiple-view approach</li> </ul>

Two methods are widely recognized, i.e. photogrammetry (both ground-based and airborne) and terrestrial-laser scanning. The methods are used to digitally recreate the as-built condition, documentation that is needed for assessment, reverse engineering, and design with reused elements. The advanced methods are described in detail under optical methods.

### 5.2.1 Active 3D imaging – active sensors

#### 5.2.1.1 Structured light

Structured light is an active 3D imaging technique as it employs structured light without depending on external light source. The cameras project a modulated pattern to the surface of a scene and calculate the disparity between the original projected pattern and the observed pattern deformed by the surface of the scene. The light source can be chosen between visible light, laser or infrared. Structured light 3D scanning devices use projected light and a camera system to shoot light onto the surface of an object. The cameras are mostly used indoor because of sunlight interference with projected light pattern. With the increase of AR/VR (augmented reality/virtual reality) there has been a growing demand in this type of technology due to their ability to capture depth information with high accuracy in short to medium range. Notable commercial products are: GOM GmbH ATOS Core, Afinia EinScan-Pro, Matterport Pro2, Intel® RealSense™ Depth Camera D455. The working distance is about 4-5 m although the Intel D455 solution can collect data from up to 20 m.

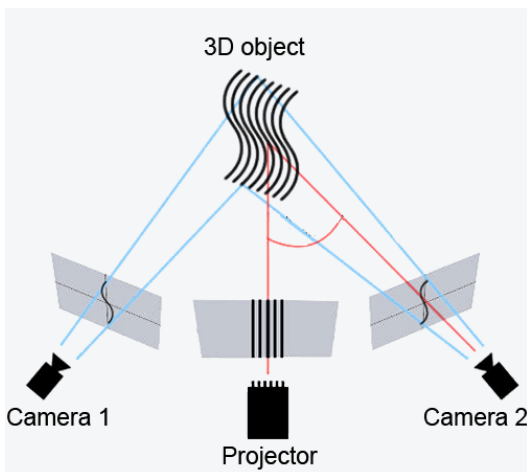


**Figure 19: Principle of structured light imaging application (<https://www.instructables.com/DIY-3D-scanner-based-on-structured-light-and-stere/>)**



**Figure 20: Different types of commercially available cameras for structured light imaging**

Technical reports have been published highlighting the use cases of the technique. For example, (Popescu et al., 2019b) used Matterport Pro2 camera to evaluate its performance in reconstruction of three-dimensional (3D) geometric modelling of existing concrete bridges. Matterport's scanning solution uses RGB-D cameras in combination with an infrared camera and an infrared projector to augment the still image with depth information. The sensors project a structured infrared light pattern onto the scene, and the reflected light is captured by the infrared camera and used to calculate depths. The camera used in the study was a Matterport Pro2 3D Camera (Figure 20c) that has three infrared sensors for capturing depth data together with visual data (RGB) at 360 (left – right) and 300 (vertical). The images are captured at a resolution of 8092x4552 pixels. The camera is wirelessly connected to a tablet from which the scanning is performed. The capture time for each scan is about 40 secs, including the transfer time from camera to tablet and the time needed for alignment. The camera's range is about 4.5m in indoor environments. Although not supported by the developer, if scanning is performed outdoors, more scan positions are required. To avoid alignment issues, the scanning must be performed during civil twilight (30 minutes before sunrise or 30 minutes after sunset), or on a cloudy day to avoid infrared light from the sun. When completed, the scans are uploaded to Matterport's cloud service for 3D data registration and the point cloud is obtained. In addition, the scan positions around the bridge can be visualised, as shown in Figure 21.



**Figure 21: Infrared scanning using Matterport Pro2 camera for Juvajokk Bridge (Popescu et al., 2019b)**

In another study, (Sayyar-Roudsari et al., 2020) proposed an alternative solution to visual inspection using Intel RealSense D435 depth cameras to detect external defects of RC members. The cameras were mounted on a robot, allowing for inspection of inaccessible areas such as crawl spaces or other spaces difficult for a person to access safely. The MATLAB toolbox is used to convert the matrix data into image processing technique and the Mesh Plot is exploited to capture the images (Sayyar-Roudsari et al., 2020). Intel RealSense D435 depth cameras have also been mounted on a drone (Figure 22), thus, being able to reach what would otherwise be difficult as stand-alone or mounted on robots.

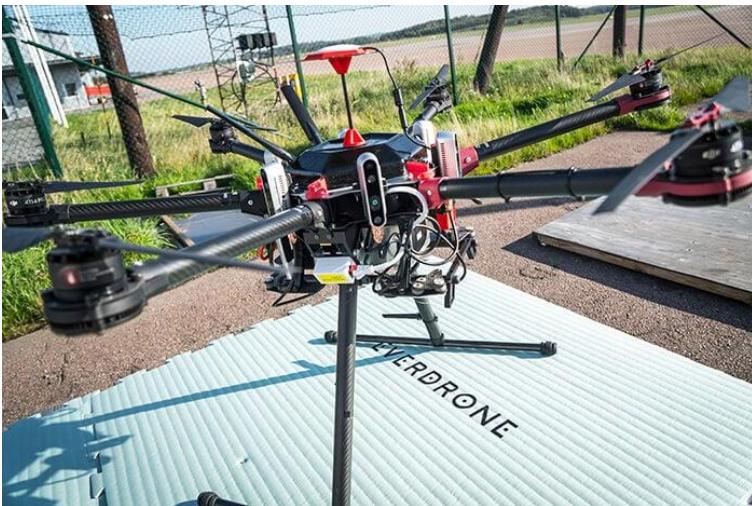


**Figure 22: Intel RealSense D435 depth cameras mounted on a drone (<https://www.intelrealsense.com/everdrone/> on 2023-08-11)**

#### 5.2.1.2 Laser scanning

The method, also known as LiDAR (light detection and ranging), is a technique to acquire three-dimensional digital data, containing (XYZ) coordinate information from the entire details of an object. It is used to digitally recreate the as-built condition, documentation usually needed for assessment, reverse engineering and forensic engineering. There are different types of laser scanners:

- based on triangulation principle



- phase shift-based laser scanner
- time of flight-based laser scanner

Scanners based on triangulation principle are less known to be used in inspection of large structures. The scanners are mainly handheld and similar to structured light sensors. The difference is the density of points clouds and accuracy of the scans. Commercial scanners are for example FARO Freestyle3D X, Creaform HandyScan BLACK, etc.

Phase-based scanning emits a constant laser beam into multiple phases and by using phase-shift algorithms is able to determine the distance to the imaged object. However, the approach that is used most commonly in civil engineering applications are based on time-of-flight (Riveiro and Solla, 2006). The time-of-flight scanners works by emitting light and detecting its reflection to determine the distance to the reflected object.

According to (Feng, 2012) there are three different scanning systems depending on the range of scales (from few millimetres to several tens of hundreds of metres): airborne laser scanning, terrestrial laser scanning and micro-laser scanning. The former is mostly used to scan very large areas such as dense urban areas, industrial plants, etc. while the latter is more used for scanning small objects. For civil infrastructure the best suitable system is the terrestrial laser scanning and drone-mounted lidar sensors. The advantage of laser scanning when compared with photogrammetry lies in its ability to reach structures of any size, being weather and natural light-independent, automated data collection and higher ranges. This aspect makes the techniques ideally for large structures. Besides geometric reconstruction, the laser scanning is also used in structural health monitoring for shape changes and displacements.

Commercial 3D laser scan systems can be seen in Figure 23 and Figure 24.



**Figure 23: Examples of time-of-flight laser scanners**



**Figure 24: Examples of phase-based laser scanners**

The terrestrial laser scan has shown good results in capturing with high accuracy the geometrical characteristics of a concrete bridge (Figure 25). The equipment used in this study was a long-range, RIEGL VZ-400, 3D terrestrial laser scanner (Figure 23). This 3D scanner operates on the time-of-flight principle and can make measurements ranging from 1.5m to 600m with a nominal accuracy of 5mm at 100m range. It uses near infrared laser wavelengths with a laser beam divergence of 0.3 mrad, corresponding to an increase of 30mm of beam diameter per 100m distance. The instrument's maximum vertical and horizontal scan angle ranges are 100° and 360°, respectively. The raw TLS data, i.e. point clouds captured from multiple

scans, were post-processed (registered and geo-referenced) using the Leica Cyclone software package, which automatically aligns the scans and exports the point cloud in various formats for further processing.

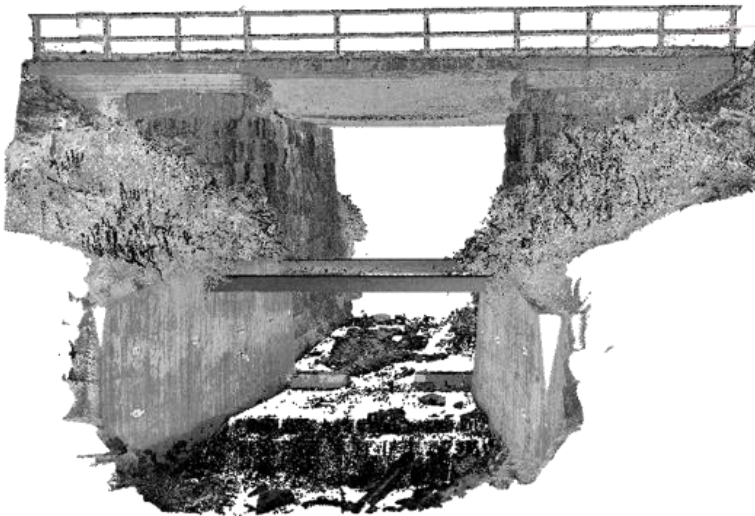


**Figure 25: 3D model of Juovajokk bridge obtained by terrestrial-laser scanning**

### 5.2.1.3 Spectral imaging

Spectral imaging is a non-destructive method that provides data of reflectance information over a certain wavelength range in the electromagnetic spectrum that cannot be seen by the human eye (Ptacek et al., 2021). Depending on the number of frequency bands and its width, spectral imaging can be divided in multi- or hyperspectral imaging method (Figure 26). The main difference between multispectral and hyperspectral imaging is the number of bands and how narrow the bands are. Multispectral imaging considers 3 to 10 wide bands between infrared and visible electromagnetic spectrum. Hyperspectral imaging utilizes narrower bands (10 to 20 nm) and higher number of bands are considered (order of hundreds or thousands). The typical core or common components of any spectral system are a light source, detector, wavelength dispersion device, and a computer supported with image acquisition software.

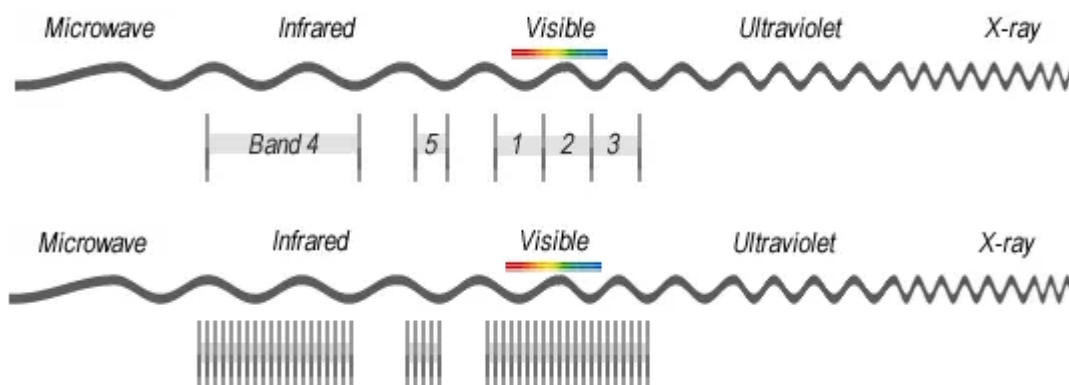


**Figure 26: Principle of multi- and hyperspectral imaging (gisgeography.com)**

(J. Valença et al., 2013) have tested multi-spectral image analysis of concrete surfaces, in order to classify surface images of exposed concrete buildings where biological colonization, exposed aggregates, repairing mortars and cracks were previously detected on a visual inspection. The method automatically produced Concrete Damages Maps with an overall accuracy of 94% (J. Valença et al., 2013).

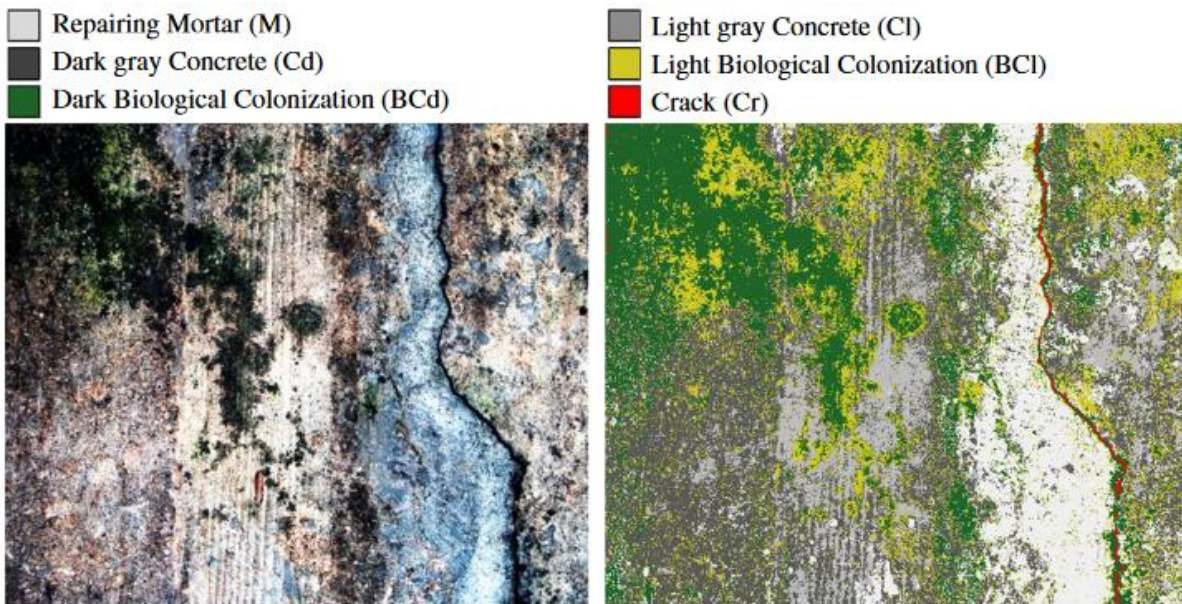


**Figure 27: Concrete surface analysed with multi-spectral image analysis: RGB image vs concrete damage map (Jónatas Valença et al., 2013)**

Sensors for drone deployment are already available and currently used in multispectral imaging for the recording of the vegetation index in farming. According to (Kerdoncuff et al., 2017) these would only have to be adapted for the required wavelengths to detect corrosion.

Hyperspectral Imaging can be paired with LIDAR in order to obtain a 3D model to highlight the spectral properties of the concrete surface inspected. Headwall company published an application note highlighting opportunities in infrastructure inspection and corrosion detection using hyperspectral data and imagery either from the air using a custom-made drone or on the ground for remote detection of material degradation (headwallphotonics.com). Their sensors come with different spectral sensitivity ranging from 250 nm to 2500 nm.



**Figure 28: Headwall's hyperspectral sensor integrated with lidar-enabled drones (headwallphotonics.com, 2021)**

## 5.2.2 Passive 3D imaging

### 5.2.2.1 Stereo vision

The technique simulates human visual depth perception. The cameras have two lenses spaced at 60 mm apart (similar to humans' eyes) which enables them to capture slightly different images. These images are then post-processed in order to generate the depth map. The cameras require no external light other than ambient light. Suitable for outdoor applications in good light conditions. The stereo cameras work in short



range, about 2 m, which makes it feasible only when is mounted on a drone. A commercial example is the ZED 2K Stereo Camera from Sterolabs (Figure 29).



**Figure 29: ZED 2K Stereo Camera from Sterolabs (<https://thenextweb.com> on 2023-10-01)**

#### 5.2.2.2 Fixed-view approach

The approach uses single or multiple cameras optical non-destructive and contactless measurement technique used to acquire information on the state of the structure without interrupting its normal service. This information relates to geometry, displacement and deformation data using three main components: an image acquisition tool (digital camera), image processing tools and enablers (lighting, robots, etc.). A series of images are recorded using digital cameras, and coordinates of points (targets), patterns, and features in the images are subsequently identified using image processing techniques (Baqersad et al., 2016). A single camera is used when in-plane (2D) measurements are needed while two synchronised cameras gather data when both in- and out-of-plane (3D) measurements are likely to be important. Depending on the type of optical targets the photogrammetry can be categorized into point-tracking (PT), digital image correlation (DIC) and target-less approaches (Baqersad et al., 2016)). A series of optical targets, e.g. retro-reflecting circular points, are mounted at discrete points on the object under investigation. Their displacements are determined by tracking their movement in different time stages and comparing it with the reference stage (Baqersad et al., 2016)). In contrast to PT, where displacement are recorded at only a handful of points, the DIC technique is a full-field measurement technique. To enable DIC measurements, the monitored surface needs to be prepared beforehand. These preparations require a high contrast speckle pattern, ideally stochastic, on the structure (usually black and white). The measurements start by imaging the specimen's surface in initial undeformed and later deformed stages to obtain deformation (strain) data. Subsequently, a software divides the image into multiple facets for analysis in the reference stage (undeformed state), which are tracked in all subsequent images (deformed). In the target-less approaches, no optical targets or speckle patterns are created in order to find the deformation (Baqersad et al., 2016); a less accurate method, however, with its own advantages when there is no possibility to create a pattern or to add optical targets. Several techniques in computer vision are used for damage detection in this case. According to (Baqersad et al., 2016) the most used ones are the edge detection and pattern matching algorithms. Several DIC systems are now commercially available. One such example (Figure 30) is the ARAMIS system (GOM mbH) which has the ability to acquire full-field as well as point-based measurements, both in 2D and 3D. Its field of view ranges from few millimetres to several meters in size (GOM mbH).

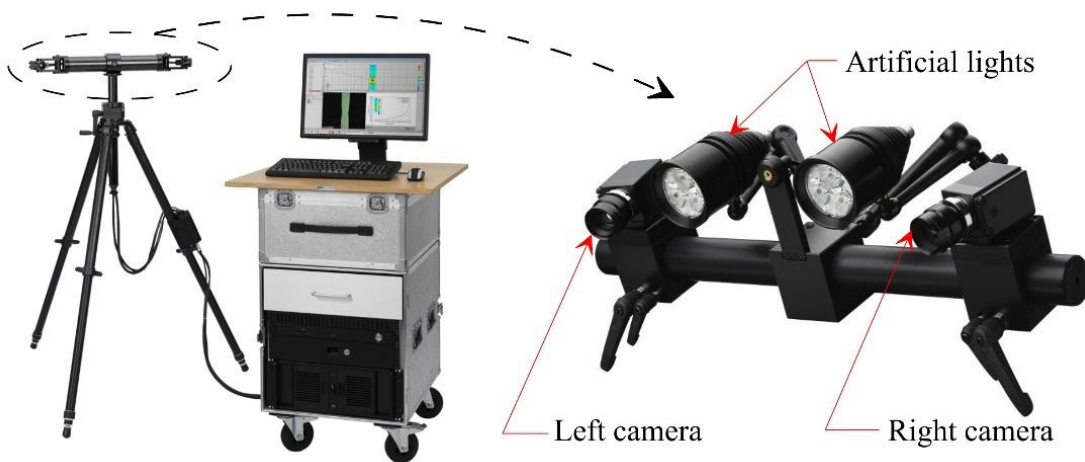


**Figure 30. 3D-DIC system and ARAMIS system (GOM mbH)**

In practice, the method is more suitable for long-term changes occurring in the field-of-view of the camera(s). For large structures where long-range measurement is expected, telephoto lenses are required together with retro-reflective targets. The retro-reflective targets help in monitoring changes in harsh environments where light and dust are of concern. Real-world applications need a displacement-free location for the camera. The technique has been successfully implemented in applications for displacement monitoring on bridges (Barros et al., 2022; Lavezzi et al., 2024) or crack development over time in dams (Popescu et al., 2019a). DIC has been tested at R.E. Ginna nuclear power plant in the US, (Hohmann et al., 2012) on selected containment concrete surfaces (Figure 31). The objective of the testing was to quantitatively measure the behaviour of the concrete while being pressurized. The information, such as increased magnitudes of local strains or increased crack opening displacements, was recorded and compared with future results for change detection.

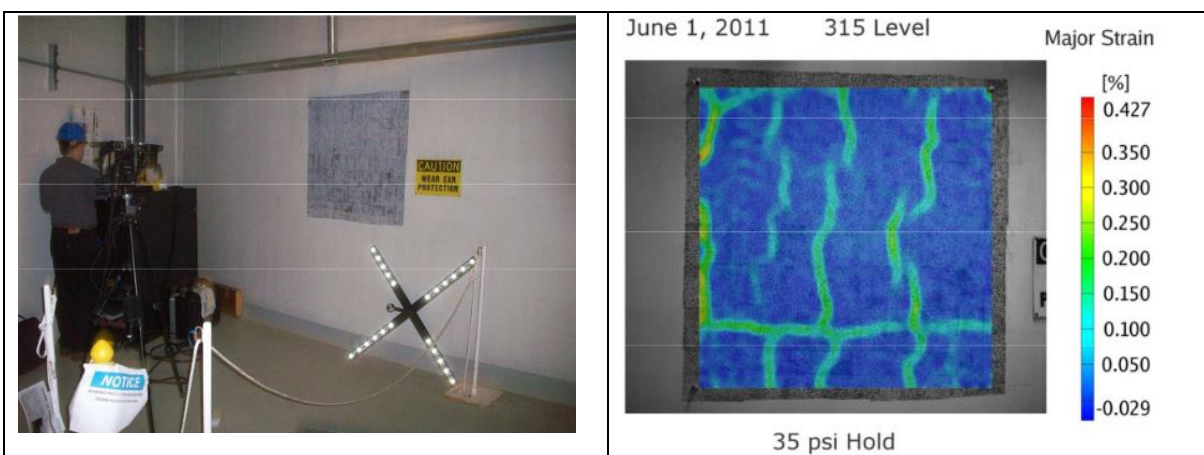


**Figure 31: DIC application during a containment pressure test: (a) DIC cameras and inspection location; and (b) principal strain at 0.24 MPa showing strain concentrations – a sign of hairline cracks on the concrete surface (Hohmann et al., 2012)**

### 5.2.2.3 Multiple-view approach

Passive multiple view 3D imaging is also called photogrammetry. In photogrammetry, a series of images is recorded using digital cameras, and coordinates of points (targets), patterns, and features in the images are subsequently identified using image processing techniques (Baqersad et al., 2016). When the measurement is done by two or more cameras simultaneously - a process named stereophotogrammetry – triangulation is used to calculate distance of a point from two or more images taken from different viewpoints. The

measurement can be performed by a single camera taking multiple images around the object. The process of estimating the 3D structure of a scene from a set of 2D images is known as structure from motion (SfM). The approach relies on pixel correspondence between images and, in contrast to older photogrammetry algorithms, no pre-calibration of the camera is necessary. To make the process easier, the surfaces of the imaging object must have distinct features, either natural (sharp edges, discoloration, bolts, rails etc.) or artificial (targets). A minimum of 60% overlap between images is necessary, in both the longitudinal and transversal directions. The equipment consists of either a digital single-lens reflex camera (DSLR) camera (for ground-based photogrammetry) or a digital camera mounted on a drone (airborne photogrammetry). According to the rules of best practice (“Cultural heritage imaging,” n.d.), the following camera settings are recommended: (1) the aperture should remain fixed during the capture sequence (preferably not smaller than  $f/11$  on a 35mm camera to avoid diffraction effects); (2) the lowest possible ISO setting should be used; (3) image stabilization and auto-rotate camera functions should be disabled and (4) in variable light conditions, the camera should be set to aperture priority mode (with the  $f$ -stop ranging from 5.6 to 11) which locks the aperture and evens out exposure by varying the shutter speed. These recommendations should be followed as closely as possible; however, given the particularities of each structure, some deviations might occur.

There are different types of remote sensing platform. The platform provides support for the sensor, i.e. camera, and can be divided into two types: ground-based (using hand-held cameras and/or high poles) and airborne (drones). Commercial equipment is shown in Figure 32.

	
DSLR camera	DJI Mavic Pro
	
3DR SiteScan	Intel Falcon 8+ Octacopter

**Figure 32: Ground-based and air borne camera devices for multiple view 3D imaging**

Practical application of the technique has been demonstrated on numerous applications. One example is the reconstruction of Juvajokk Bridge (Figure 33). The equipment consisted of a digital single-lens reflex camera (DSLR) camera, a Canon EOS 5D. This is equipped with a full-frame ( $35.8 \times 23.9$  mm) complementary metal–oxide–semiconductor (CMOS) optical sensor giving 12.8 megapixels ( $4368 \times 2912$  pixels) resolution. The camera was equipped with a Canon EF 35mm wide-angle prime (fixed zoom) lens. On a full-frame camera body, this lens gives a large field of view angle ( $54^\circ$  horizontal viewing angle), thus covering a broad area, meaning that fewer images are needed to capture the entire structure. Although the size of the bridge is relatively small (6 m span length) certain areas were difficult to scan using regular cameras.





**Figure 33. Ground-based photogrammetry camera for Juvajokk Bridge (left), artificial targets used in the alignment process and for scaling: (a) coded targets and (b) calibration scale bars (Popescu et al., 2019b)**

### 5.2.3 Infrared thermography

The infrared thermography is an inspection method used to locate near surface defects in concrete. Common applications include delamination in bridge decks, delamination in members strengthened by fibre-reinforced polymers, defective cladding on buildings and energy loss in buildings. To be able to take measurements a heat source must exist. The natural source, the sun, fulfil the requirements in most of the cases. However, in difficult to reach areas an artificial heat must be produced by other methods such as laser for surface heating, lamps, etc. Infrared thermography can be divided in two approaches: the passive approach and the active approach (Figure 34a). External stimulations are not needed for passive approach while active thermography needs thermal excitation. A comprehensive review on active thermography has been published recently by (Milovanović and Banjad Pečur, 2016). The method creates surface temperature patterns by detecting thermodynamic properties of the object under investigation. A sound concrete would reveal uniform temperature over the whole surface monitored due to its high thermal conductivity. A poor-quality concrete has low thermal conductivity, and this will be highlighted by differences in the temperature patterns (Figure 34b). This means that delaminated areas, heat up faster (and cool down rapidly, respectively) than a good-quality concrete. It is a very useful method for inspection of large surface areas (in the range of kilometres if proper lenses are available, (Kashif et al. 2016). However, the depth of the anomalies cannot be detected. In such cases where the depth is important, it is advisable to use the method in combination with ground penetrating radar (Kashif et al. 2016). Infrared thermographic equipment is commercially available (see for example, FLIR T630sc camera shown in Figure 34c). No standards are available for this method.

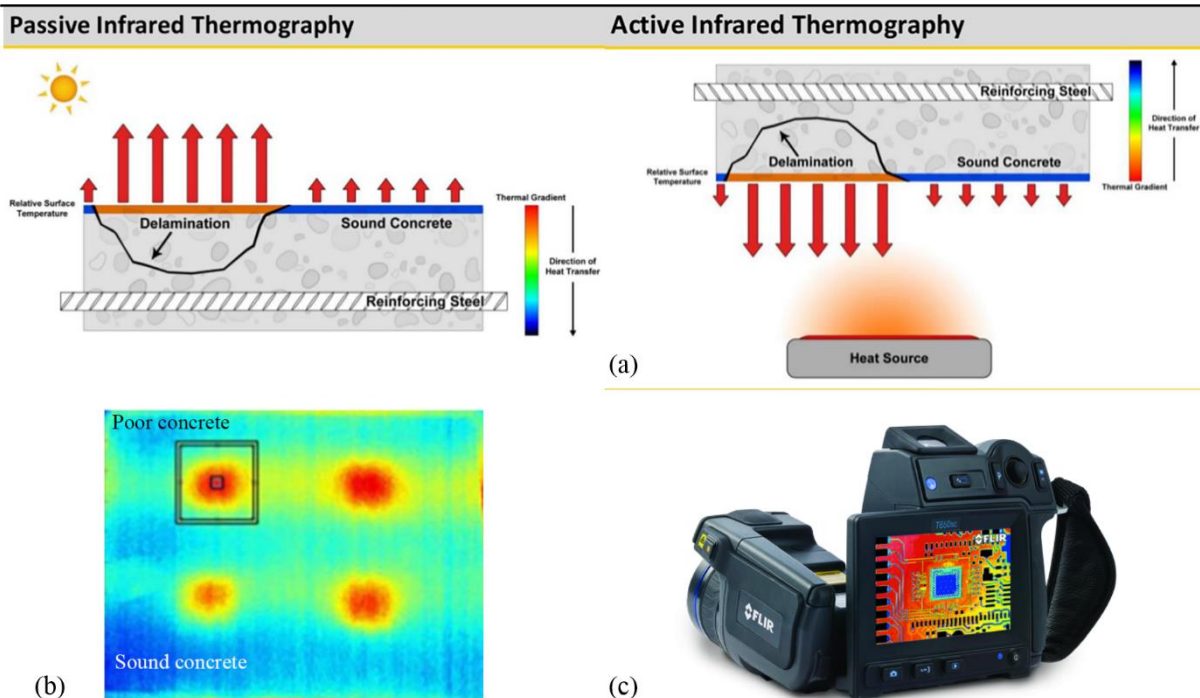


Figure 34. Infrared thermography: (a) the principle of passive and active thermography (Ahlborn et al., 2015); (b) typical results indicating concrete quality, and (c) a commercially available camera T630sc (flir.com, 2017)

## 5.3 Mechanical and acoustic methods

### 5.3.1 Impact echo (IE)

IE-method," which involves striking the surface of the area to be examined with a small impact or impulse hammer and detecting the reflected wave energy using a displacement or accelerometer receiver mounted on the surface near the impact point. Reflections of stress waves from internal defects, material interfaces, or other anomalies are picked up by sensors on the test surface. Since the impact generates a high-energy pulse and can penetrate deep into concrete, the IE-method is particularly promising for identifying defects in concrete structures. It produces a better signal-to-noise ratio than other ultrasound techniques due to its low attenuation in composite materials like concrete (Krüger and Grosse, 2007)

In Figure 35, a sensor records surface displacements caused by multiple wave reflections over time. These displacement signals are then transformed into the frequency domain using FFT (Fast Fourier Transform). The depth of any internal defects or interfaces can be determined by analyzing the incoming signal and its characteristic frequency spectrum (FFT) using the following simple equation:

$$d = \frac{v_p}{2f_R}$$

where  $v_p$  is the P-wave velocity and  $f_R$  is the measured frequency. The depth to a defect can be illustrated using the example in Figure 36 with the measured velocity of 4350 m/s in the concrete:

$$d = \frac{v_p}{2f_R} = \frac{4350}{2 \cdot 10} = 0.22m$$

resulting in a depth of 0.22 m to the defect.

The minimum detectable defect size varies depending on the depth of the defect. It is a highly effective testing method for depths ranging from 0.1 m up to approximately 1.2 m (Helmerich et al., 2007). This method is commonly used for thickness determination, locating delaminations, voids, inhomogeneities, as

well as voids in lining pipes. There are commercially available instruments on the market, and one such instrument is known as the DOCTer Impact-Echo. Figure 37 illustrates the equipment and its operational principles. One of the most recognized standards for Impact-Echo testing is ASTM C1383 - Standard Test Method for Measuring the P-Wave Speed and the Thickness of Concrete Plates Using the Impact-Echo Method.

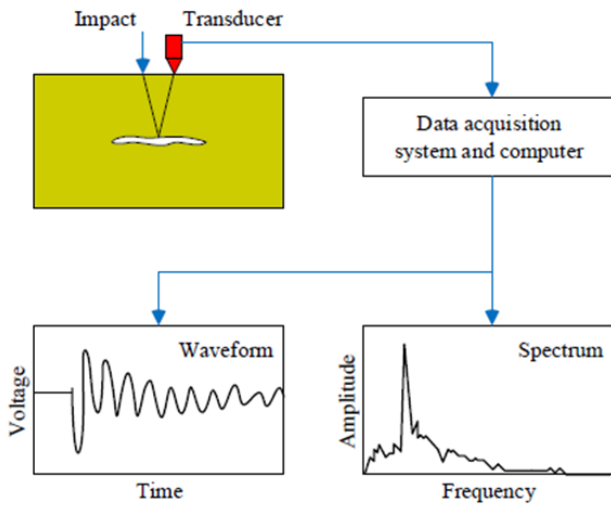


Figure 35: A simplified diagram of the IE method (from [www.ndt.net](http://www.ndt.net))

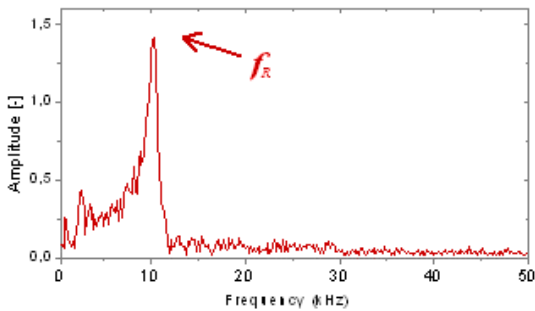
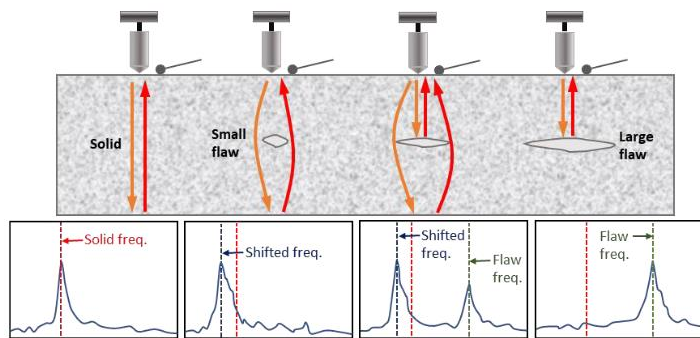


Figure 36: Example of IE analysis



(a)



(b)

Figure 37. DOCTer impact echo: (a) equipment; and (b) working principle (Germann Instruments, n.d.)

In summary, the advantages and limitations of the IE technique are outlined below:

**Table 5: Advantages and limitations of the IE technique**

<b>Defects</b>	The Impact-Echo (IE) method cannot locate defects in tensioned wires in internal or external lining pipes. IE can provide a reasonable level of accuracy in locating voids and water infiltration in ducts. It can also provide a reasonable level of accuracy in locating inadequate grout injection, voids, and water infiltration in external High-Density Polyethylene (HDPE) ducts.
<b>Placement of tendon ducts</b>	Used to locate placement of ducts in concrete. Has been used to locate cavities in external ducts.
<b>Type of ducts</b>	Applicable to ducts made of both metal and non-metal materials.
<b>Effect of cover layer</b>	The results are affected by the cover layer of concrete. A very thick cover layer, greater than 70-80 mm, can have a negative impact on the measurement.
<b>Impact of multiple layers of ducts</b>	Ducts in 'shadow' areas can be challenging to obtain results from
<b>Impact of dense reinforcement</b>	Dense reinforcement adversely affects the measurement
<b>Corrosion</b>	No possibility to detect corrosion
<b>Accessibility requirements</b>	The required area is typically 0.5 x 0.5 meters with close spacing. Depending on the size of the damage, it may be necessary to go down to a grid of around 5 x 5 cm. Larger defects are easier to locate.

### 5.3.2 Ultrasonic Pulse velocity (UPV) and Ultrasonic Pulse Echo (UPE)

The Ultrasonic Pulse Velocity method (UPV) is a non-destructive technique used to evaluate the condition of concrete. Among the parameters that can characterize the condition of concrete are compressive strength, internal defects, cracks, and more. The principle of the method involves measuring the time it takes for an ultrasonic pulse to travel through a known distance, such as through the concrete being tested in Figure 38.

By applying ultrasonic pulse velocity measurement, the pulse frequency is controlled by longitudinal vibrations through the concrete. The main areas of application include:

- Homogeneities in concrete elements
- Presence of cracks, voids, or other defects
- Crack depth
- Changes in the concrete structure that may occur over its lifespan
- Concrete quality in relation to standard requirements
- Indicative values for concrete compressive strength and elastic modulus

The method requires access from both sides of the element, which can be a disadvantage in certain situations. New technology has been developed, namely, Ultrasonic Pulse-Echo (UPE), based on the original method. With ultrasonic pulse-echo, it is now possible to examine objects where access is limited to only one side. UPE involves the transmission (T) of ultrasonic pulses into concrete that are reflected by material defects or at the interfaces between areas with different densities and/or elastic moduli. A receiver (R) connected to the surface receives the reflected waves. Point measurements are combined to visualize the reflections. It is worth noting that the propagation of ultrasonic waves is limited by layers containing air, such as concrete with a high volume of air voids and densely packed reinforcement bars. This method is used

for inspecting the internal structure of reinforced and/or prestressed concrete, as well as for locating reinforcement and tendons, voids, and poor compaction. See a schematic diagram in Figure 39 for an illustration of the principle.

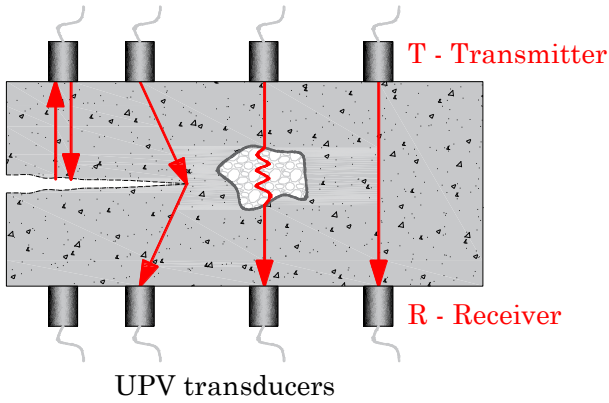


**Figure 38: Ultrasonic Pulse Velocity Testing in Concrete Elements (adapted from [www.ndt.net](http://www.ndt.net))**

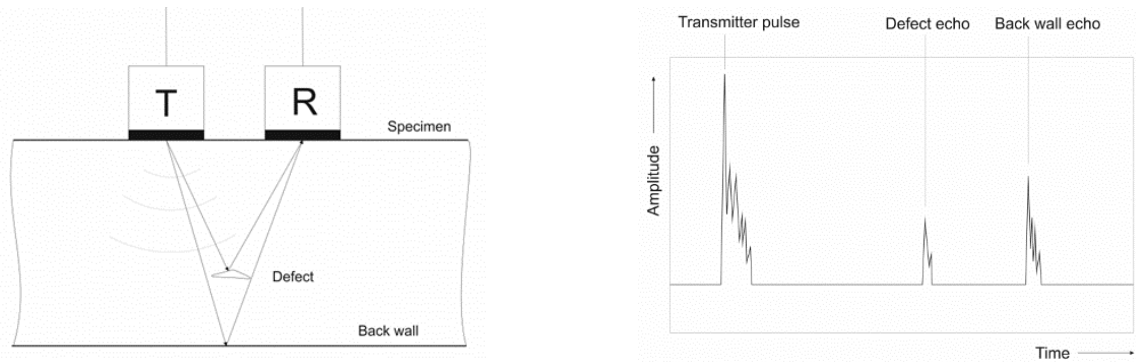


**Figure 39: A simplified diagram of the UPE method (source: [www.ndt.net](http://www.ndt.net))**

When using the UPE method, it is not advisable to rely on a single measurement value to draw conclusions about damage, crack depth, or reinforcement location. Multiple measurements are often required for credible results. In the case of measuring crack depth, typically 5 measurements are taken, and the mean value and standard deviation are reported. Table 6 summarizes the possibilities and limitations of UPV and UPE techniques.



**Table 6: Advantages and limitations of UPV and UPE**

<b>Defects</b>	UPV and UPE methods cannot precisely locate defects in tensioned wires in internal or external lining pipes. UPV and UPE can provide a moderate level of accuracy in locating voids and water infiltration in ducts. They can also offer a moderate level of accuracy in locating inadequate grout injection, voids, and water infiltration in external High-Density Polyethylene (HDPE) ducts.
<b>Placement of ducts</b>	Locating ducts in concrete can be time-consuming. It's essential to have a reasonably high degree of confidence in the duct's placement
<b>Type of duct</b>	Applicable to ducts made of both metal and non-metal materials
<b>Effect of cover layer</b>	The results are influenced by the concrete cover layer. A very thick cover layer, exceeding 70-80 mm, can adversely affect the measurement
<b>Impact of multiple layers of ducts</b>	Ducts in 'shadow' areas can be challenging to obtain results from
<b>Impact of dense reinforcement</b>	Dense reinforcement adversely affects the measurement
<b>Corrosion</b>	No possibility to detect corrosion
<b>Accessibility requirements</b>	The required area is typically 0.5 x 0.5 meters with close spacing. Depending on the size of the damage, it may be necessary to go down to a grid of around 5 x 5 cm. Larger defects are easier to locate.

### 5.3.3 Ultrasonic Tomography

The specific type of wave used in ultrasonic testing can vary depending on the application and the equipment being used. Ultrasonic testing can employ both shear waves (also known as transverse waves) and pressure waves (also known as longitudinal waves).

- **Shear Waves (Transverse Waves):** Shear waves involve particle motion perpendicular to the direction of the wave. They are commonly used when the detection of flaws or the characterization of materials requires the analysis of shear wave reflections. Shear waves are especially useful for detecting flaws in concrete and examining the integrity of materials.
- **Pressure Waves (Longitudinal Waves):** Pressure waves involve particle motion parallel to the direction of the wave. They are often used for general ultrasonic thickness measurements and to detect flaws, voids, and other anomalies in a wide range of materials. Pressure waves are typically easier to generate and are widely used in industrial applications.

The choice between shear waves and pressure waves depends on the specific testing requirements and the nature of the material being examined. Each type of wave has its advantages and limitations, and the selection is made to optimize the inspection process for a given application.

An advanced ultrasound method is one often referred to as MIRA. However, MIRA is a trademark, and there is similar equipment that functions in a similar way, see, for example, ([www.screeningeagle.com](http://www.screeningeagle.com)). The method is based on ultrasonic shear wave tomography. It relies on a low-frequency ultrasound system capable of detecting internal defects in reinforced concrete, such as voids and delamination. MIRA is based on the ultrasonic pitch-catch method and employs an antenna consisting of an array of dry point-contact transducers that emit shear waves into the concrete. An advantage of using MIRA is its scanning depth, which penetrates up to 1 m in heavily reinforced concrete structures and up to 2 m in lightly reinforced



concrete structures. The control unit inside the antenna excites a row of transducers, and the other rows of transducers act as receivers.

Phase I in Figure 40b shows the first row of transducers functioning as transmitters, and the remaining rows of transducers functioning as receivers. Transition to the second row, where the receivers now act as transmitters, is depicted in Phase II. Here, the next row of transducers is excited, and the other rows to the right function as receivers. This process is repeated until each of the 10 rows of transducers has served as a transmitter, as seen in Figure 40 a) - c).

If there is a sufficiently large interface between concrete and air (a defect) inside the element, a portion of the emitted wave will be reflected by the defect, as illustrated in Figure 40c). MIRA equipment system consists of a phase-controlled antenna system, a portable computer with MIRA software (the software is based on SAFT - Synthetic Aperture Focusing Technique), and a power unit. To perform a scan, the user lays out a series of parallel scan lines on the surface to be examined. The signals captured by the antenna are automatically transferred to the computer, where the SAFT algorithm is used to reconstruct a 3D model of the concrete's internal structure.

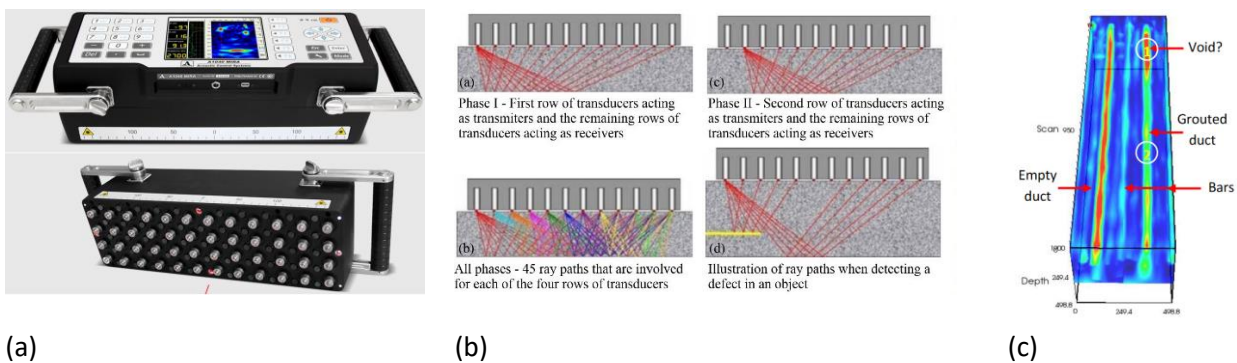


**Figure 40: Shear wave tomography: (a) MIRA equipment; (b) working principle; and (c) MIRA 3D image grouted vs un-grouted tendon ducts (<https://www.germanninstruments.com>)**

An alternative approach to concrete imaging involves utilizing the Elop Insight Ultrasonic Scanner (Figure 41), which provides a dry coupling solution for detecting damage within concrete structures. The Elop Insight (EI) is a rolling ultrasonic scanner that employs all eight transmitters and eight receivers, offering up to 64 combinations akin to Full Matrix Capture (FMC) for cross-track synthetic aperture.

In the process of image reconstruction, Full Matrix Capture (FMC) is achieved when A-scans from all sensor element combinations within an array are utilized. Additionally, Total Focusing Method (TFM) is implemented by focusing these A-scans into each grid position within the imaged volume. To further enhance data acquisition, the scanner incorporates a built-in rotational encoder during movement, extending the captured matrix in the scan direction to acquire a significantly higher number of data points. Both the along-track and cross-track data are subsequently focused into each image grid point, or voxel (the 3D equivalent of a pixel), following the TFM approach, ensuring that imaged features are sharp and focused from all orientations. For the EI scanner, approximately 10,000 A-scans are typically employed to generate amplitude data for each voxel in the 3D image, particularly in what we refer to as "high accuracy mode." This mode employs a 2 mm along-track sampling distance, meaning a complete set of up to 64 A-scans is acquired for every 2 mm of rolling with the scanner. This considerably surpasses the capabilities of non-rolling devices.

It is important to note that the primary distinction between high accuracy and high-speed modes lies in the along-track sampling distance and, consequently, the number of A-scans combined within each voxel. In high-speed mode, the scanner can be moved at speeds of up to approximately 1 m/s, equivalent to a normal walking pace.

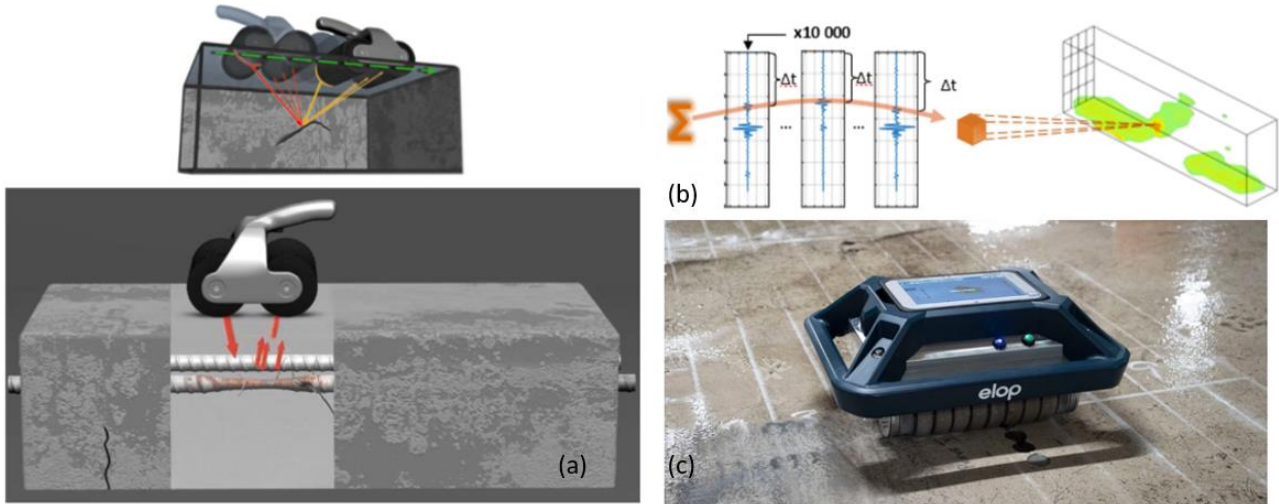


Figure 41: Elop Insight: (a) Ultrasonic signals sent and echoes received as the scanner moves; (b) SAFT delay-and-sum process; and (c) Elop Insight instrument (source: [SAFT \(Synthetic Aperture Focusing Technique\) for 3D image reconstruction and noise reduction in Elop Insight Ultrasonic Scanner - Elop](#))

Table 7 presents the capabilities and limitations of UPE Tomography technology, outlining the possibilities and constraints of the system described above.

Table 7: Advantages and limitations of ultrasonic imaging

<b>Defects</b>	Ultrasonic imaging can accurately locate voids, inadequate grouting, and water infiltration in ducts.
<b>Placement of ducts</b>	Ducts are located using Ground Penetrating Radar (GPR). The process of scanning over the duct is then relatively quick
<b>Type of duct</b>	Applicable to ducts made of both metal and non-metal materials
<b>Effect of cover layer</b>	The cover layer does not notably affect it
<b>Impact of multiple layers of ducts</b>	Ducts in 'shadow' areas can be challenging to obtain results from
<b>Impact of dense reinforcement</b>	Dense reinforcement adversely affects the measurement
<b>Corrosion</b>	No possibility to detect corrosion
<b>Accessibility requirements</b>	The required area depends on the equipment's size, and the surface should be flat. Work is then conducted in 10 cm segments along the duct

### 5.3.4 Acoustic emission (AE)

Acoustic emission (AE) refers to the generation of transient elastic waves produced by a sudden redistribution of stress within a material, such as the propagation of cracks in concrete. When a structure is subjected to an external impact (changes in pressure, load, or temperature), local sources trigger the release of energy in the form of stress waves. These waves propagate to the surface and are detected by sensors, as shown in Figure 42.

An acoustic testing method involves a series of individual sensors (at least 4) or a row of sensors attached to the surface of a structure (Kaiser and Karbhari, 2004). Ultrasonic signals released through crack formation are recorded. Information such as noise amplitude, energy, duration, and crack type (formation, delamination, cracking) can be captured. Active cracks can be identified and located before the crack can be measured. As the damage pattern in the concrete increases, the reflection time changes. No signals occur when the crack is not active, i.e., when it does not propagate under load. Filtering out noise from traffic, existing cracks, etc., is necessary.

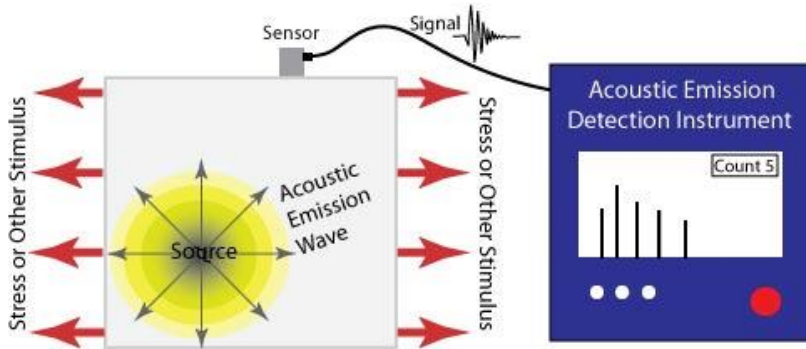


**Figure 42: Working principle of the AE method (from [www.nde-ed.org](http://www.nde-ed.org))**

Acoustic emission differs from most other non-destructive testing methods (NDT) in two respects. The first difference is related to the source of the signal. Instead of applying energy to the object being examined, AE simply listens for the energy released by the object. AE tests are often conducted on structures in operation because this provides sufficient stress to propagate defects and trigger the acoustic emissions. The second difference is that AE deals with dynamic processes or changes in a material. This is particularly meaningful because it only affects active properties (e.g., crack growth). The ability to distinguish between propagating and arresting defects is significant. However, it is possible that crack propagation is not entirely detected if the load is not high enough to cause an acoustic event. Additionally, AE testing typically provides an immediate indication of the load-carrying capacity or the risk of failure of a structural component. Other advantages of AE include rapid and comprehensive volumetric inspection using multiple sensors, permanent sensor installation for process control, and no need to disassemble and clean a sample. Unfortunately, AE systems can only qualitatively measure the extent of damage in a structure. To obtain quantitative results about part size, depth, and overall acceptability, other NDT methods (often ultrasonic testing) are necessary.

**Table 8: Possibilities and Limitations of AE Technology**

<b>Defects</b>	AE cannot distinguish static defects but can be used under load to detect ongoing defects, such as possible fractures in tensioned cables
<b>Placement of ducts</b>	Not applicable
<b>Type of duct</b>	Not applicable
<b>Effect of cover layer</b>	Not applicable
<b>Impact of multiple layers of ducts</b>	Not applicable
<b>Impact of dense reinforcement</b>	Not applicable
<b>Corrosion</b>	Cannot detect corrosion but should be able to detect cable fractures due to corrosion over time
<b>Accessibility requirements</b>	Requires accessibility for the sensors, and many sensors may be needed for large structures.

### 5.3.5 Impulse response (IR)

Impulse response uses an impact to generate relatively low stress, which is achieved by an instrumented hammer with a rubber tip, to send stress waves through the element or structural component under investigation. The impact causes the element to vibrate in a bending mode, and a geophone placed near the impact point measures the velocity and amplitude of the reflecting wave. The resulting velocity spectrum is divided by the impact force spectrum to obtain mobility as a function of frequency. By Fourier transformation, information is analysed and then derived into 4 parameters (average mobility, mobility slope, dynamic stiffness, and void index) used for the integrity assessment of the examined area represented visually with contour plots. Figure 43 displays 3 of the 4 parameters graphically (Sajid and Chouinard, 2019). The average mobility is clearly evident, calculated as the average within the frequency range of 100 – 800 Hz. Dynamic stiffness is calculated from the slope of the curve between 0 – 40 Hz, and the so-called mobility slope is the best possible curve fit. Void index is calculated as the ratio between the peak of the curve, usually below 100 Hz, and the average mobility. IR is not directly applicable for finding voids in ducts but is a powerful method for mapping delaminations, for example.

Table 9 outlines the possibilities and limitations of the technique with respect to post-tensioned structures. The standard method of using the impulse response method is described in [ASTM D5882-16 \(2016\)](#).

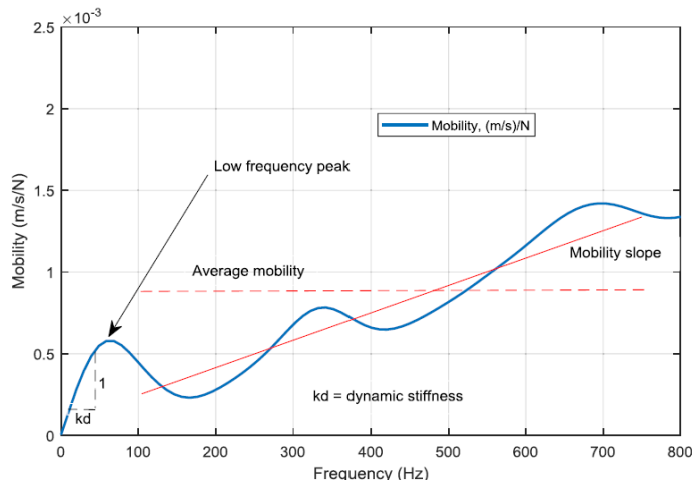


Figure 43: Typical mobility as a function of frequency diagram (Sajid and Chouinard, 2019)

Table 9: Possibilities and Limitations of AE Technology

<b>Defects</b>	IR is primarily used to detect delaminations and voids in concrete
<b>Placement of ducts</b>	Not applicable
<b>Type of duct</b>	Not applicable
<b>Effect of cover layer</b>	Not applicable
<b>Impact of multiple layers of ducts</b>	Not applicable
<b>Impact of dense reinforcement</b>	Not applicable
<b>Corrosion</b>	Not applicable
<b>Accessibility requirements</b>	Requires access for hammer impacts and geophone, typically examines areas larger than 1 m <sup>2</sup>

## 5.4 Electro-magnetic methods

### 5.4.1 Covermeter

Cover meters employ electromagnetic pulse induction technology to detect reinforcement bars. This method also serves to determine various parameters, including the concrete cover thickness, rebar diameter, and spacing between metallic reinforcements. The probe contains coils that cyclically receive current pulses, generating a magnetic field in the process. When this magnetic field interacts with any electrically conductive material on its surface, it induces eddy currents in the opposite direction, resulting in a change in voltage. This change in voltage is harnessed for measurement purposes. Importantly, this method remains unaffected by non-conductive materials like concrete, wood, plastics, and bricks. Nevertheless, any conductive materials within the magnetic field, typically within a radius of approximately 200 mm, can influence the measurement.

The measurement principle of the Profometer 650 AI cover meter is depicted in Figure 44 (a). Other available cover meters on the market include the Proceq Profoscope, Elcometer 331 Cover Meter, Hilti Ferroskan PS 200, ZBL-R660 Concrete Rebar Locator, Mitech MT200 Rebar Locator, and James Instruments Profoscope+. The measurement range is contingent on the size of the reinforcement bars. Figure 44b illustrates the expected accuracy of the cover measurement. The instrument offers three distinct measuring ranges: standard, spot probe, and large. Arguably, the most precise mode is the standard range, wherein, for the smallest bar diameter (6 mm), the bar can be detected if it lies within a 70 mm thick concrete cover. For reinforcement bars with sparser distribution (greater than 200 mm apart) and larger diameters (exceeding 20 mm, such as anchor bolts), the instrument can locate them provided the concrete cover is no more than 150 mm thick. Additionally, the Profometer 650 AI cover meter can be upgraded to assess the likelihood of corrosion using the half-cell potential technique.

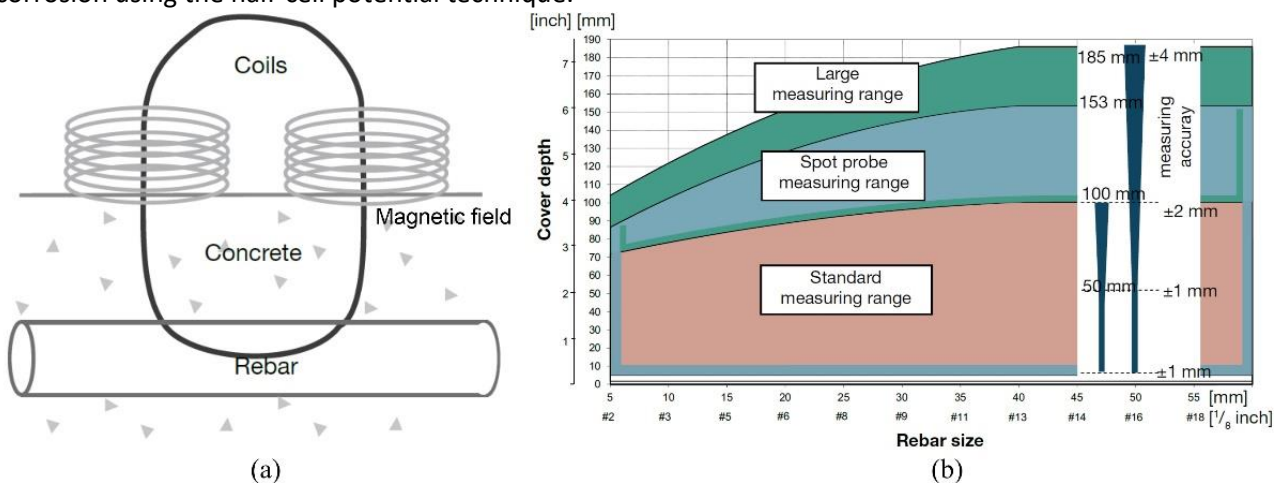


Figure 44: Profometer PM 650 AI: (a) measurement principle; and (b) measuring ranges and accuracy



Figure 45: Covermeter instrument (<https://www.screeningeagle.com>)



### 5.4.2 Ground-penetrating radar (GPR)

This method applies electromagnetic waves by moving one or two antennas over the concrete surface. It's important to note that if the variation in the dielectric properties of different materials is low, only a small amount of energy will be reflected. For example, electromagnetic waves cannot penetrate any metal layers. The shape of construction elements (e.g., rebar diameter) or material inhomogeneities is difficult or impossible to estimate. This method is often used to inspect the internal structure of building elements made of reinforced or prestressed concrete and masonry to detect and locate inhomogeneities (voids, metal or wood inclusions), thickness of structures that are only accessible from one side, the internal structure of complex elements, and in some cases, to determine moisture content and its distribution. GPR data are collected in either a 2D (distance and time) or 3D (x, y, and time) fashion, depending on the application.

Figure 46 provides an example of GPR usage. The evaluation of results heavily relies on existing algorithms and user interfaces. The possibilities and limitations of GPR inspection technology are discussed in Table 10, outlining GPR's capabilities and constraints.

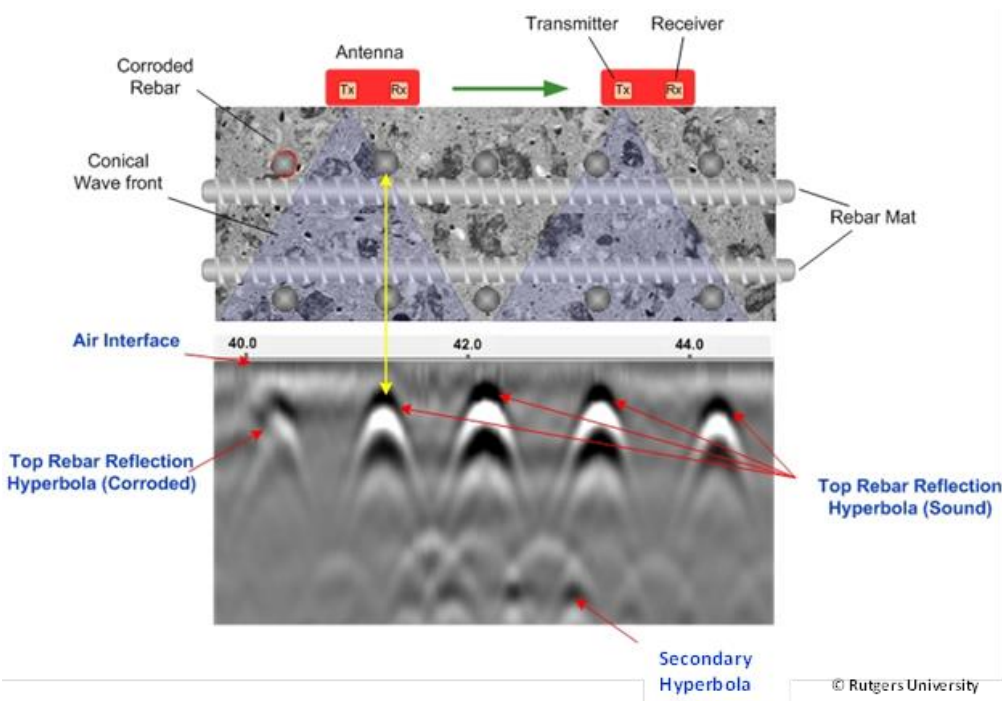


Figure 46: Ground-penetrating radar (GPR) (<https://fhwaapps.fhwa.dot.gov>)



Table 10: Possibilities and Limitations of AE Technology

<b>Defects</b>	GPR (Ground Penetrating Radar) can detect defects in concrete. It can also detect voids in external HDPE ducts with moderate accuracy, but it cannot quantify the volume of these voids. GPR can identify damaged grout and water infiltration defects in external HDPE channels, but its accuracy is low. However, GPR cannot detect defects in tensioned wires in external HDPE or metal ducts. It also cannot detect voids or defects in tensioned wires in internal ducts. GPR can be used to locate internal ducts.
<b>Placement of ducts</b>	Used to locate the placement of ducts in concrete. Has been used to locate voids in external ducts.
<b>Type of duct</b>	Applicable to ducts made of both metal and non-metal materials.
<b>Effect of cover layer</b>	The effect of the cover layer depends on the scanning frequency. For high frequencies (~500-3000 MHz), the penetration depth can typically exceed 600 mm. However, the signal is disrupted by dense reinforcement.
<b>Impact of multiple layers of ducts</b>	GPR can have difficulty locating ducts in shadow zones due to the significant reflections from reinforcement and ducts closest to the surface.
<b>Impact of dense reinforcement</b>	The presence of steel strongly reflects the electromagnetic waves, significantly affecting GPR's ability to locate ducts, especially in the anchoring areas.
<b>Corrosion</b>	It may potentially detect corrosion but requires larger areas to do so, and the results may be uncertain. It's challenging to evaluate.
<b>Accessibility requirements</b>	The area required for a GPR scan depends on the type of GPR equipment used. For ground-coupled GPR inspection, the device's wheels need to be in physical contact with the structure to ensure wheel rotation, which also functions as a distance measurement. Creating a 3D image typically requires either a manually accessible test surface of 0.5 x 0.5 meters or 0.5 x 1.2 meters. Testing within the anchorage areas usually doesn't provide useful information due to the large volume of strongly reflective reinforcement present in these areas. Scanning can be done using both line scans and area scans for many equipment setups.

### 5.4.3 Half-cell potential

Corrosion activity of steel reinforcement can be monitored using half-cell potential technique. It is an electrical technique which consists of a copper-copper sulphate half-cell, connecting wires, and a high-impedance voltmeter (ACI 228.2R-98 1998). If the reinforcement is corroding, the electrons would tend to flow from the bar to the half-cell. The method only indicates the probability of corrosion activity at time of testing and not the rate of corrosion. The method requires direct access to the reinforcement, as shown in Figure 47. Figure 48a shows a typical result (the condition maps) of a concrete bridge deck obtained using half-cell potential method. Areas where there is a high likelihood of corrosion activity are delineated through the colour palette. A lightweight, portable equipment, is commercially available by upgrading the Profometer 650 AI (see Figure 45: Covermeter instrument (<https://www.screeningeagle.com>)) to Profometer Corrosion (PROCEQ 2017). The standard test method is given by ASTM C 876-15 (2015) and presented in Figure 47.

If the corrosion rate is needed, one can use the electrical resistivity test method or the linear polarization resistance method. None of these methods are simple and for reliable results it is advisable that both methods be used in conjunction with half-cell potential method. (Dinh et al., 2016) showed that deteriorated areas found with electrical resistivity test method as well as the half-cell potential method correlate very well as can be seen in Figure 48. Limitations of these test methods include: cover depth should be less than 100 mm, the reinforcing steel should not be epoxy coated or cathodically protected and all methods requires a connection to the embedded reinforcement (ACI 228.2R-98 1998). No standard procedures exists for interpreting corrosion-rate measurements, however, some guidance is given in ACI 228.2R-98 (1998) for using the linear polarization resistance method.

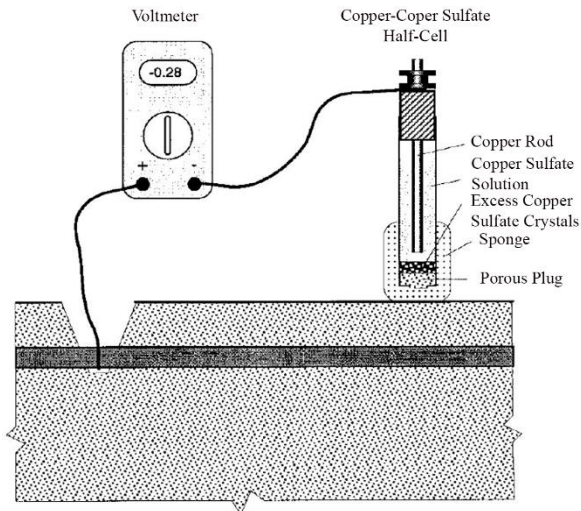


Figure 47: Apparatus for half-cell potential method (ACI 228.2R-98 1998)

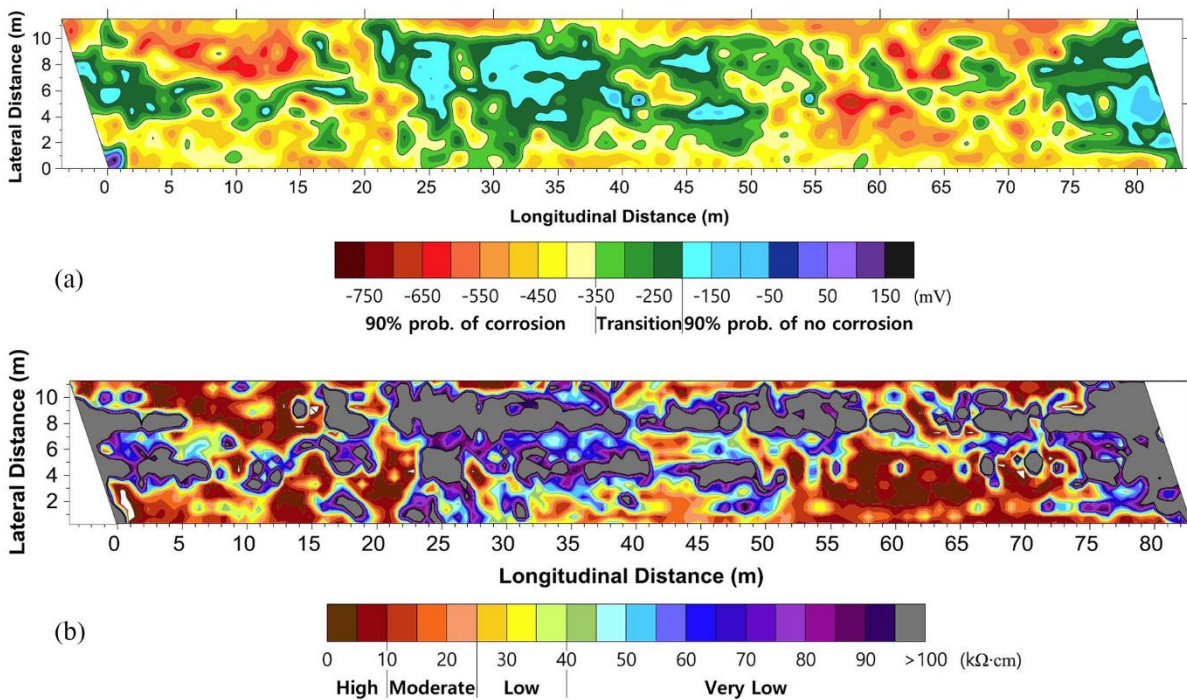


Figure 48: Condition map of a concrete bridge deck showing: (a) probability of corrosion activity using half-cell potential method and (b) rates of corrosion as measured by the electrical resistivity method (Dinh et al., 2016)

#### 5.4.4 Radiography

The radiography testing is a nuclear method using high-energy electromagnetic radiation to view the internal structure of an object (Kashif Ur Rehman et al., 2016). It is possible to detect reinforcement location, cracks, material heterogeneity and internal flaws. The principle of radiography is to transmit radiation through a material and then measure its attenuation, where attenuation depends on the density and object thickness (Yang et al., 2016). The radiation can be produced by X-ray or Gamma-ray. Although the method provides accurate results, it requires specialized training due to safety concerns (Pla-Rucki and Eberhard, 1995). It is generally believed that ground penetrating radar provides important advantages over the X-ray such as lower costs, access from one side only, fast data collection, real-time inspection results and possess no safety hazards (cnilocates.com, 2017). However, radiography can provide valuable information for post-tensioned bridges.

The method necessitates access from both sides of the wall or slab under examination. A radiation source is positioned at a certain distance on one side, and an X-ray film sheet is affixed on the other side. The choice of radiation source, either iridium-192 or Cobalt-60, depends on the thickness of the concrete (Kakade and Limaye, 2019). The absorption of radiation varies depending on the concrete type, necessitating extensive experimentation to determine the optimal exposure time and source-to-object distance for achieving high-quality images. Additionally, a significant area around the test site must be evacuated to minimize radiation exposure (Kakade and Limaye, 2019). Figure 49 displays a radiograph of ducts, revealing the interior tendons.



**Figure 49: Radiograph of ducts showing the interior tendons (Kakade and Limaye, 2019)**

## 6 Monitoring of Concrete Structures

Structural (health) monitoring (SHM) means to continuously collect data from a structure to identify any changes in its performance or signs of deterioration before they become critical.

Monitoring can be divided into three main categories (fib, 2023):

- 1) Monitoring of structure performance under identified loads based on the effects of interaction between the tested structure and loads acting on the structure. These load-dependent tests (static or dynamic) measure the structural response to various loads including traffic or environmental influences. This category usually monitors the global condition of a structure.
- 2) Monitoring of structure performance in random operating conditions. This load-independent testing provides results independent of loads acting on the structure and is also used to assess local conditions.
- 3) Monitoring of material deterioration processes due to environmental loads, e.g. corrosion or ASR can refer to global condition and local conditions of a structure.

NDT methods as described in the previous chapters are part of inspection-based monitoring while sensors fall in the category of device-based monitoring carried out by means of installed technical equipment. The monitoring system provides continuously and autonomously data and real-time information about the whole structure or its components.

Sensor based monitoring has the advantage of the recognition of condition changes at all times and in areas difficult to access, without the need for personal in place. Data can be checked and evaluated remotely. Therefore, sensors can be of great support during and in between inspections. Sensors can either be embedded in the concrete or installed on the surface of structures. At the moment, many sensors are still connected by cables and data transport is guaranteed by wires. However, development of wireless sensors and data transmission is moving fast.

The recognition of structural response to physical or environmental loads can be monitored by physical-electrical and optical technologies (e.g. displacements, strain/stress, vibrations), chemical technologies (e.g. corrosion, chloride ingress, carbonation) or biological technologies where relevant (e.g. activity of microbes or plants).

The structural behaviour is typically monitored during load tests (static or dynamic). Load tests are carried out to quantify the load bearing capacity of a structure and rule out any uncertainties. Ongoing corrosion or ASR can impact the load bearing capacity which is difficult to accurately evaluate by calculations and models. Hence proof load tests can reveal the effective structural performance and actual level of safety.

There is a various number of different sensors available on the market and even more is in the development stage. This makes it challenging to categorize all types of SHM sensors, which can be made by measuring principle (mechanical, electrical, optical), measuring parameter, contact or non-contact sensor, global or local monitoring, surface vs bulk detection, etc. Today's sensing systems are mainly based on contact or embedded sensors collecting data on global conditions or local conditions of critical parts. The next generation of SHM systems is working towards non-contact by cameras, unmanned aerial vehicles - UAV (e.g. drones) and other mobile sensors (see also NDT methods).



An example of a complete SHM monitoring system measuring different parameters (inc. deformations, corrosion etc.) on a cable supported bridge is in Figure 50. An illustration of typical sensors that could be installed to monitor concrete dams is given in Figure 51.



Figure 50: Example of structural health monitoring of a cable-stayed bridge (Al-Khateeb et al., 2019)

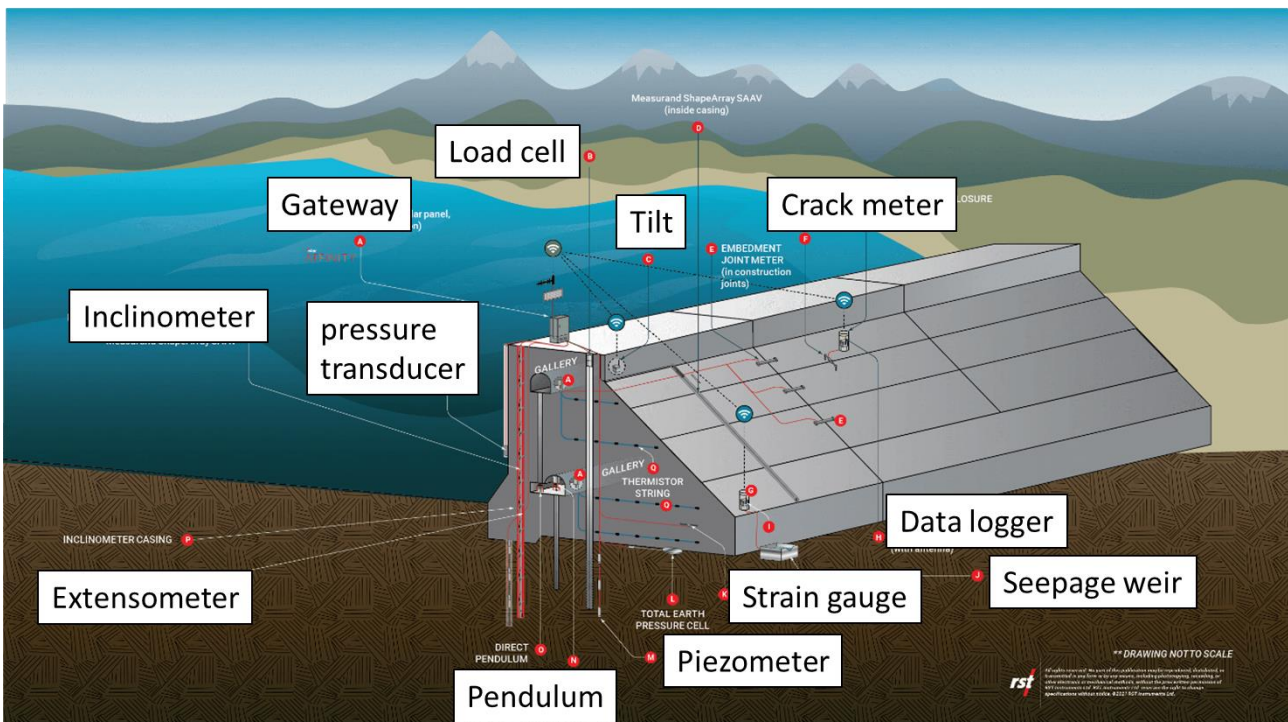


Figure 51: Illustration of monitoring sensor potentially to be applied at concrete dams, based on <https://rstinstruments.com/applications/dams/concrete-dams/>



(Myrland Jensen, 2012) gave an overview over the market potential for monitoring systems in Norway. In the report an overview over existing bridges was given where sensors were installed after some years. Typical parameters that were measured were displacement, strain (e.g. vibrating wire dynamometers) and accelerations in addition to weather data like wind and temperature. There is also a large number of dams that are monitored mainly with regard to deformations and changes in cracks due to ASR (e.g. with sliding micrometres).

In the following sub-chapters a short overview over the most common sensor types and their application is given. The text is based on two main reports and the references herein (Bergmeister et al., 2003; Schumacher et al., 2021).

For detailed descriptions on the working principle, required equipment, installation, and deployment it is referred to the mentioned reports. Most of the sensors described for monitoring structural response, have all achieved a rather high level of maturity and proofed their quality in field conditions. However, not all types of sensors are yet tested in large scale in Norway (e.g. fibre optic sensors). Sensors measuring the corrosion potential and currents of steel reinforcement have also high maturity level and proven their suitability. However, reliable sensors measuring critical material properties in concrete directly linked to the probability of corrosion like free chloride ions and pH in the pore solution, are still under development.

## 6.1 Structural monitoring

### 6.1.1 Deformations and displacements

Deformation may be defined as the change in size or shape of an object while displacements are absolute changes in position of a point on the object. Hence, measurements can refer to geometrical changes or positional changes of the whole structure or parts of the structure to be monitored. These sensors are used for either measuring local displacement against a measuring base (fixed point outside the investigated structure) or relative displacement between two points on the structure.

#### 6.1.1.1 Mechanical sensors

##### Wire and tape extensometers

Extensometers are stretched tapes or wires, used to measure changes in the distance between two reference points permanently installed at measurement stations along the structure.

Different type of tape and band materials are available and proper calibration and installation are crucial for the results. An accuracy of 0.05 mm is possible measuring changes in distances stretching from 1 to 20 m. For the accuracy temperature corrections are necessary.

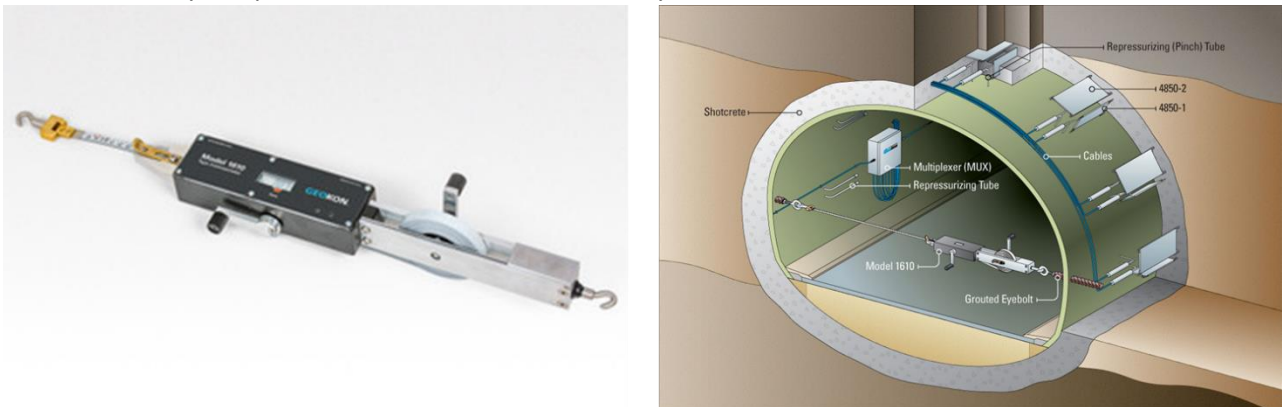


Figure 52: Tape extensometer and application example in tunnels (<https://www.geokon.com/1610>)

*Sliding micrometers* fall under the group of extensometers and are commonly used in Norway to measure expansion in dams. These are usually installed in boreholes in the concrete structure. Accuracies of 0.002mm/m are reported.

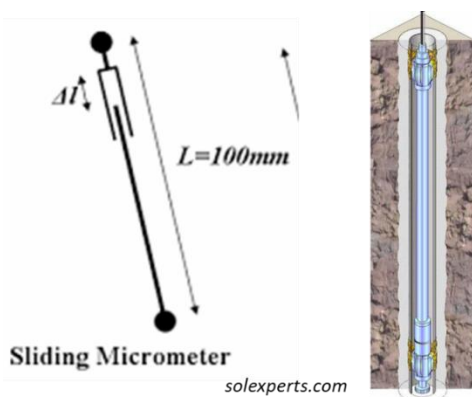


Figure 53: Typical and simplified working principle of sliding micrometers that can be installed in boreholes (solexperts.com)

### 6.1.1.2 Electrical sensors

A large number of electrical sensors is available, transforming various physical effects due to physical changes in the structure into electrical signals.

#### Inductive sensors (LVDT)

The working principle of inductive sensors is the change of the electromagnetic field of a coil in the sensor as result of the displacement of a ferromagnetic core. The most common type of inductive sensor is the *linear variable differential transformer (LVDT)*. LVDT consists of a primary and two secondary windings and a moveable core. An alternating magnetic field is created at the primary winding, resulting in an alternating voltage at the secondary windings. When the core is moved from its zero-position due to displacements, the voltage in the secondary windings will change giving an electrical output signal.

The advantages of LVDT are that the technique is very robust, operating in extreme conditions (incl. high and low temperatures) and that it has an infinite resolution. LVDT can be made in many different sizes ranging from thousands of centimetres to several centimetres. The main disadvantage is that they are only suitable for measuring local small displacements.

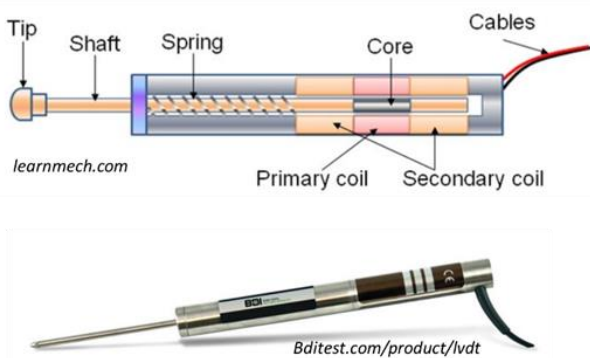


**Figure 54: Left: Working principle of LVDT sensor (learnmech.com) and an example of a commercial sensor (bditest.com). Right: Example of LVDT installation to measure displacement between two structural parts (sisgeo.com)**

#### Potentiometer sensors

This type of displacement sensor is called resistive sensor in other places. A potentiometer utilizes the physical principle that the resistance of an electrical conductor is proportional to its length. Linear displacements are detected by moving a variable contact through a known distance proportional to the displacement, resulting in a change in resistance. The physical appearance of the sensors is similar to LVDT. Potentiometers might be somewhat cheaper than LVDT however their lifetime is limited due to friction and consequent wear of the sliding contact.

Furthermore, with a similar set-up to the above mentioned potentiometric and LVDT sensors, also capacitive sensors are available measuring displacement based on changes in dielectric properties of a material.

**Table 11: Strengths and limitations of selected displacement sensors techniques (Schumacher et al., 2021)**

	<b>Strengths</b>	<b>Limitations</b>
Mechanical (Tape)	Can measure over large distance >50 m Accuracy 0.1 mm	Lower accuracy compared to electrical sensors
Potentiometers	Easy to use Inexpensive Large measurement range High accuracy	Not suitable for dynamic measurements Limited durability
LVDT	Good durability Infinite resolution & high accuracy (<0.01 mm) Fast dynamic response Insensitive to radial movement	Sensitive to temperature changes Limited measurement range Local measurements

### 6.1.2 Tilt and inclinations

Deflection of concrete structures might be the result of external loads, temperature, or movements in the foundation. Tilt is usually understood as deflections from the horizontal plane while the term inclination is used for deviation from the vertical plane. Tiltmeters or inclinometers might therefore be regarded as an own category within displacement sensors. The sensors measure the angle of an object with respect to gravity. Typical applications are deflection of bridge piers and abutments or embankment and dam stability.

#### 6.1.2.1 Vibrating wire sensors

A tensioned wire in contact with a pendulous mass is forced to vibrate at constant frequency induced by an electromagnetic coil. When the structure (part) is tilted with the sensor embedded, the mass moves which will change the vibrating frequency of the wire. The frequency output in the wire is proportional the angle of measurement.

Vibrating wire sensors come with high sensitivity and the output signals can be transmitted over long distances without accuracy loss. The sensors have excellent long-term stability and near-zero temperature dependency. However, they may be of high cost and limited to static measurements due to poor dynamic response. Vibrating wire sensors are also described within strain sensors together with an illustration of the measuring principle.

#### 6.1.2.2 Electrolytic tilt sensor

A set of positive and negative charged electrodes of equal length is submerged in an electrolytic solution. When the embedded sensor is tilted with the structure the degree of immersion between the different electrodes will vary resulting in a potential difference between the electrodes. The measurement range of tilt angles is limited by the geometry (volume of fluid, electrode spacing and height).

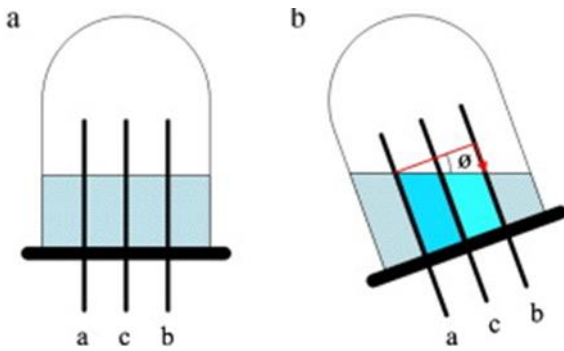


**Figure 55: Working principle of electrolytic tilt sensor: (a) before tilt, (b) in the state of tilt (Lee and Lee, 2011)**

Electrolytic sensors provide high accuracy and stability. They are relatively cheap, small and easy to install. The sensors are usable in extreme conditions in terms of temperature variations, humidity and shock. Disadvantages are that they are limited to use with alternating current to prevent electrolysis. As the fluid might take time to settle after a sudden event, the dynamic response is poor.

### 6.1.2.3 Microelectromechanical systems (MEMS)

This is a type of capacitive sensor. Electrode pairs, where one electrode is fixed while the other one is allowed to move. The movable electrodes are connected to a proof mass. When tilt occurs, the proof mass will move due to gravity and induce a change in capacitance between the fixed electrodes.

MEMS do often have lower precision than the sensors mentioned above and are also more sensitive to temperature variations (thermal drift). However, the dynamic response is better compared to vibrating wire and electrolytic sensors.

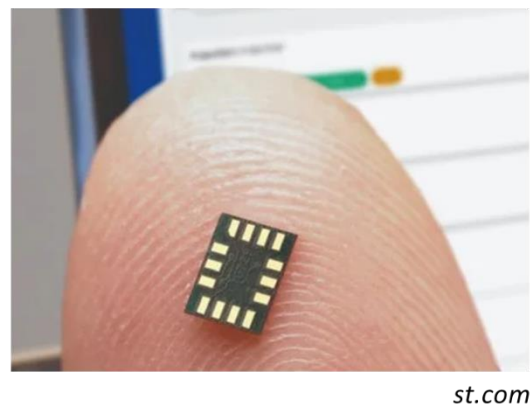
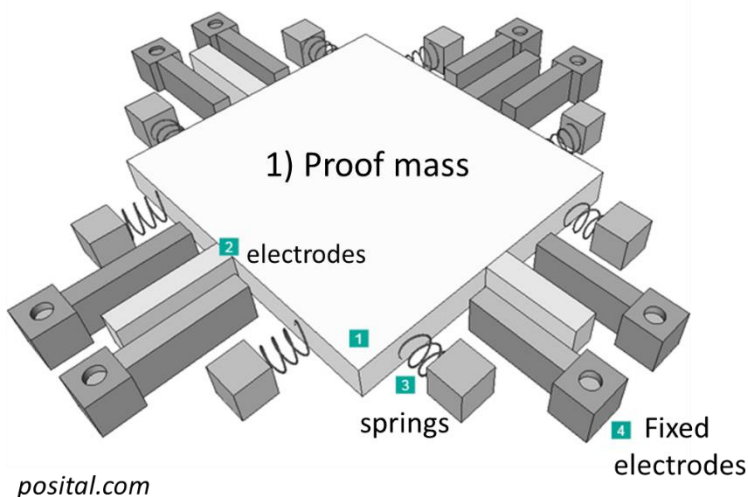


**Figure 56: Working principle of MEMS tilt sensors (posital.com, left) and commercial example (st.com, right)**

### 6.1.2.4 Pendulum

Pendulums are mechanical sensors based on the principle of plumb line with a weight at its end. Optical sensors, or others, measure the position of a wire of straight or inverted pendulums to determine the position or cartesian coordinate displacement and/or rotations.



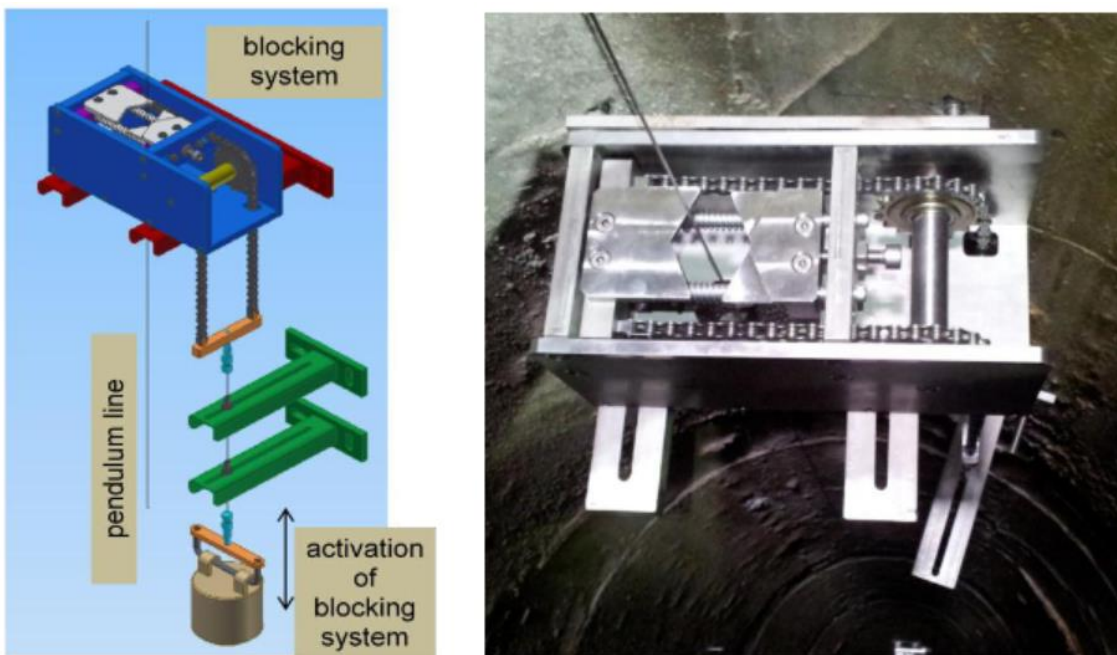


Figure 57: Example of pendulum sensor measuring displacements in an ASR affected dam in Switzerland (Droz et al., 2013)

Table 12: Strengths and limitations of selected tilt sensors techniques (Schumacher et al., 2021)

	Strengths	Limitations
Vibrating wire	<ul style="list-style-type: none"> <li>Wide measurement range</li> <li>High sensitivity</li> <li>Long-term stability</li> <li>Little sensitivity to temperature changes</li> <li>Output signal transported over long distances without loss of accuracy</li> </ul>	<ul style="list-style-type: none"> <li>Expensive</li> <li>Poor dynamic response</li> </ul>
Electrolytic	<ul style="list-style-type: none"> <li>Inexpensive</li> <li>Small size and easy to install</li> <li>Usable in extreme environments</li> <li>Shock resistant</li> <li>High stability, repeatability, accuracy</li> </ul>	<ul style="list-style-type: none"> <li>Poor dynamic response</li> <li>Only usable with alternating currents</li> <li>Sensor set up (fluid volume, electrode spacing etc.) limits the angle range</li> </ul>
MEMS	<ul style="list-style-type: none"> <li>Better suited for dynamic measurements</li> <li>Low costs, portable</li> <li>Low power requirements</li> </ul>	<ul style="list-style-type: none"> <li>Lower precision</li> <li>Sensitive to temperature changes</li> </ul>
Pendulum	<ul style="list-style-type: none"> <li>Simple</li> <li>Reliable long-term measurements</li> <li>Several measurements can be taken at different locations/depth of the plump line</li> <li>Manual or automatic monitoring</li> </ul>	<ul style="list-style-type: none"> <li>Size; generally limited to vertical changes</li> <li>Temperature dependency of damping fluid</li> </ul>

### 6.1.3 Strain

The measurement of strain can be regarded as measuring deformation from a material point of view over a short-length base. Concrete structures are designed to tolerate a certain stress (referred to its strength) before it fails. The stress defined is directly correlated to the strain which can result from loads (mechanical), temperature variations (thermal), creep or shrinkage (rheological), or expansion due to alkali silica reactions in mature concrete. Strain sensors are installed at critical points on the surface of reinforcement or concrete, and best suited to monitor local behaviour in contrast to global behaviour of the deformation sensors mentioned above. All sensors are designed to transform a mechanical motion into an electrical signal.

Strain gauges are amongst the most used sensors and a wide variation is commercially available. The technique is very mature, has a low cost, high precision and is rather easy to use and operate. A general limitation is the interference with other electromagnetic fields from e.g. lightning, radio waves, that might affect the measurements.

#### 6.1.3.1 Resistive strain gauge

A resistor wire is applied on a substrate which can be applied on the surface of the structure or reinforcement. A length change of the wire will change the resistance of the wire resulting in a changed output voltage as electrical signal.

Strain gauges are generally limited to short term strain measurements. Other limitations are potential drift of circuit, sensitivity to temperature change and problems related to ageing in humid climate conditions.

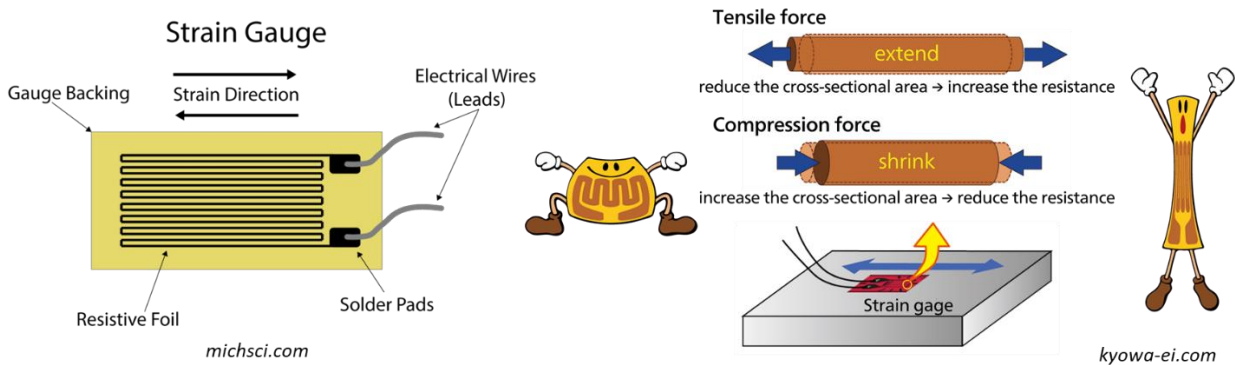


**Figure 58: Working principle of strain gauges (michsci.com & kyowa-ei.com)**

#### 6.1.3.2 Vibrating wire strain sensor

A metallic wire is tensioned between two fixed points in the sensor. Through a magnetic field, the wire is put into vibration of constant frequency which is measured and converted into an electrical signal. The vibrational frequency of the wire will depend on the strain in the measured location.

Vibrating wire sensors are stated to have better long-term stability than strain gauges.

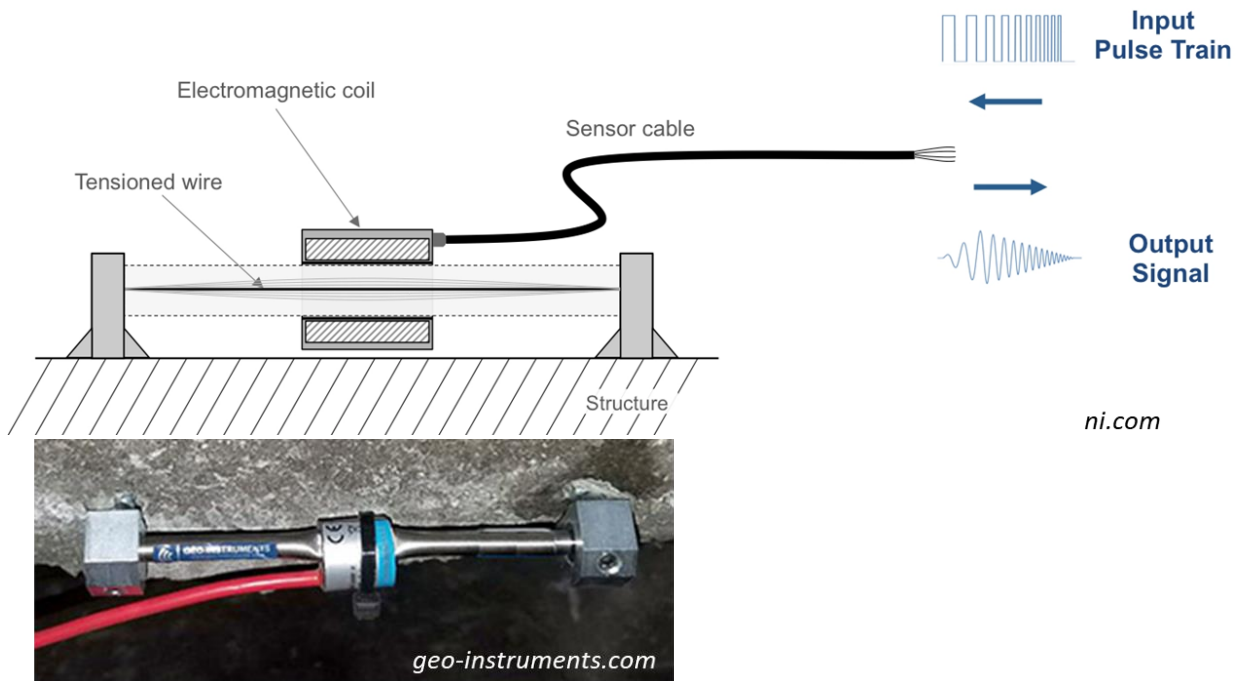


Figure 59: Working principle of vibrating wire sensors (ni.com) and commercial application example (geo-instruments.com)

Table 13: Strengths and limitations of selected strain sensors techniques (Schumacher et al., 2021)

	Strengths	Limitations
Vibrating wire	<ul style="list-style-type: none"> <li>High precision and resolution</li> <li>Long-term stability</li> <li>Can be Surface mounted or embedded</li> <li>Easy handling and operation</li> </ul>	<ul style="list-style-type: none"> <li>Limited size and gauge length</li> <li>Physical size and stiffness could be critical in certain application</li> </ul>
Strain gauge	<ul style="list-style-type: none"> <li>Small size, low weight</li> <li>High precision and resolution</li> <li>Low cost</li> <li>Dynamic measurements</li> </ul>	<ul style="list-style-type: none"> <li>Not embeddable</li> <li>Temperature sensitive</li> <li>Short gauge length</li> <li>Complicated handling and demanding installation</li> <li>Difficult to re-use</li> <li>Effects of lead wires on stability and accuracy</li> </ul>

Piezoelectric sensors are also able to detect strain signals, but the principle is here described under accelerometers and acoustic emissions below. Furthermore, fibre-optic sensors can be used for strain detection. However, as this type of sensors comprises a larger group of different working principles and are very versatile for different applications they are treated as an own group later.

## 6.1.4 Formation of Cracks

### 6.1.4.1 Acoustic emission sensor (AE)

A sudden release of energy as result of e.g. formation of cracks in concrete, wires, strands etc, will generate a stress wave moving through the solid that can be detected as acoustic emission signal. Typical sensors of this type work on the principle of piezoelectricity. Piezoelectricity stands for electricity resulting from pressure (here stress wave) and the piezoelectric effect is hence based on transforming mechanical energy into electrical energy. When the sensor is subjected to external pressure, electrical polarization of the crystal

domains in the piezoelectric material occurs, creating an electrical field that can be measured as voltage. Sensors can be mounted on the concrete surface directly with glue or epoxy.

The interpretation of the measured signals is still a challenge and therefore only qualitative approaches are applied so far. The main role of AE sensors is to capture ongoing fracture and warn from potential overloading. The strength of the method is that it is relatively simple in application and of low cost. A large area can be covered with a few sensors. The main application is in structural load testing.

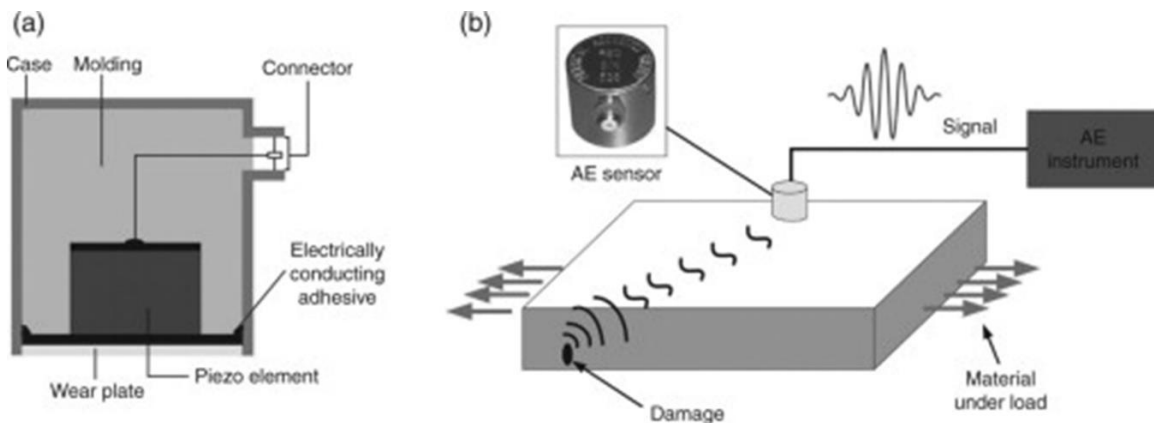


**Figure 60: Principle of piezoelectric measuring of stress induced acoustic waves (An et al., 2014)**

#### 6.1.4.2 Conductive surface sensor (CSS)

CCS are electrically- conductive materials applied to the surface of concrete. When the concrete moves (strain) or cracks, the CSS will be stretched or ruptured resulting in a change of the electrical resistance. The resistance is measured at externally applied electrodes. The sensors can come in a variety of materials, e.g. colloidal copper foil, colloidal paint etc. Metal based foils are more robust and recommended for application in harsh climate. CSS is in general very sensitive to small changes and can detect microdamage at an early age. Another advantage is the potential monitoring over a wider distributed area. The sensors are inexpensive, easy to apply, and the signals are easy to read and interpret. The main disadvantage is that the sensors only detect surface defects. CSS is still under development and there are no commercial sensors available yet. Performance under real world conditions has not been fully demonstrated yet.



**Figure 61: working principle of conductive surface sensors (left, tml.jp) and example of crack detection by installation of conductive paint (Raoufi et al., 2011).**

Further development/enlargement of already existing cracks can also be monitored with e.g. LVDT type or vibrating wire type sensors (see chapter 4.1.1.2 and 4.1.3.2)



### 6.1.5 Vibrations and acceleration

Vibrations are often measured as acceleration and velocity in terms of dynamic motion of a structure. Motion can be caused by e.g., live loading, seismic activity or construction works. Vibration measurements help identifying structural damage as signals can be converted to receive information on e.g. change in stiffness or elasticity properties of the structure. The change in modal properties can also be used to evaluate the cracking potential of structural parts.

#### 6.1.5.1 Laser Doppler vibrometer (LDV)

This technique measures surface vibrations contactless based on laser interferometry with an external laser source focused on a structural part and measuring the reflecting light. The detection principle is based on the Doppler shift of reflected laser light based on the vibration velocity. A vibrating object moving away or towards the laser source will reflect light with a changed frequency compared to the light emitted from the source, with the frequency change being proportional to the velocity of the vibrating object. The LDV system is placed nearby the structure, often on the ground and needs to be installed and standing in a way to not experience any vibrations itself during the measurement. The systems give direct measurements of displacement and velocities but are hence only used for short term monitoring.

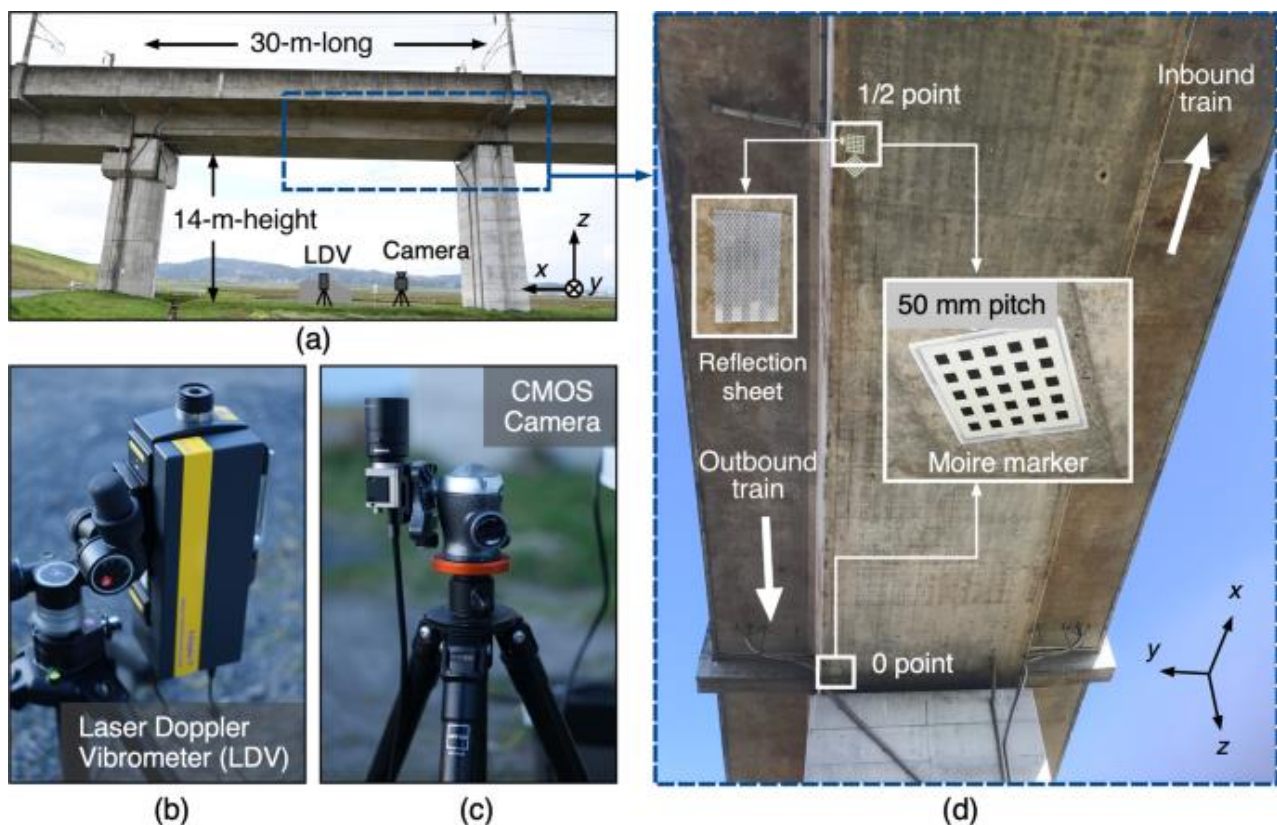
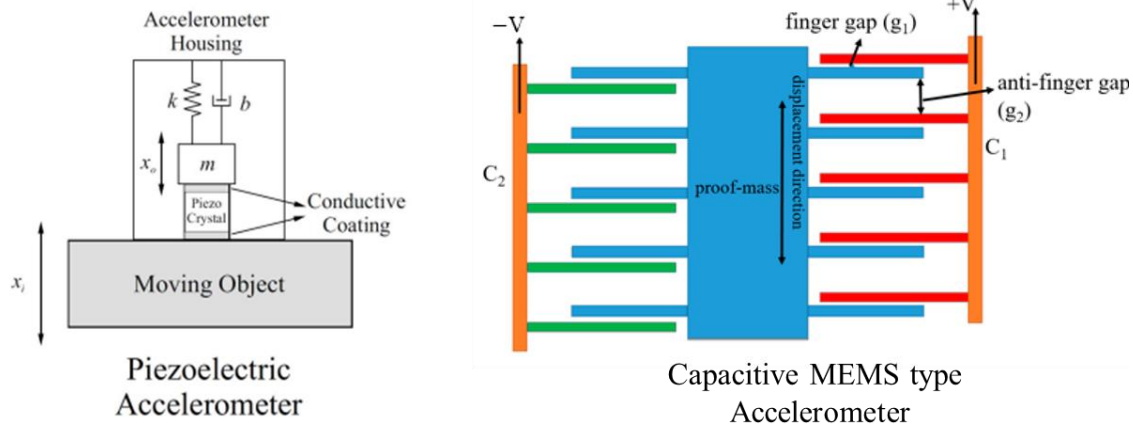


Figure 62: Photographs of the target bridge and the experimental setup: (a) Target bridge, (b) Laser Doppler vibrometer (LDV) measured under the bridge, (c) CMOS camera recorded under the bridge, (d) moiré marker (grid-pattern) attached on the bottom side of the bridge (Ri et al., 2023)



### 6.1.5.2 Accelerometers

Accelerometers can be attached directly to the object of interest (e.g. reinforcement, concrete surface) and provide data on static or dynamic accelerations as well as uniaxial or triaxial measurements. Accelerometers typically work based on piezoelectric or capacitive principles.



Candy 2021, Accelerometer Modeling in the State-Space, osti.gov

**Figure 63: left: Principle of piezoelectric accelerometer, Right: capacitive MEMS accelerometer (right) (Candy, 2021)**

In the piezoelectric versions a seismic mass puts pressure on a piezoelectric material to generate a voltage proportional to the acceleration. In capacitive accelerometers a seismic mass will induce movement between two capacitive plate electrodes generating a change in output voltage. Capacitive sensors are more frequently used in civil infrastructure monitoring due to their higher sensitivity to low frequencies. These are often also based on MEMS sensor principle described earlier. Accelerometers are easy to install but post processing of data to convert the measured signals to displacement and velocity can be complicated.

### 6.1.6 Fibre optical sensors (FOSs)

FOSs are commonly designed for transmitting information via light over long distances. The glass fibre technology is very similar to data transmission cables. In general, FOSs can be divided into 4 different types of sensory systems.

#### 1) Point sensors (Fabry Perrot):

Point sensors are cables with a small air cavity at a certain point (Fabry Perrot cavity) and with a mirror plate at each end of the cavity. Light is sent through the cable where part of the light is reflected from the first mirror and part of the light is reflected from the second mirror. The total reflected light results in a defined interference pattern that is registered. If the distance between the two mirrors changes e.g. due to elongation, strain of the cable, thermal expansion, the reflected beam interference will be changed and registered as an event. For each new point sensor, a new cable with new light source and detector needs to be installed.

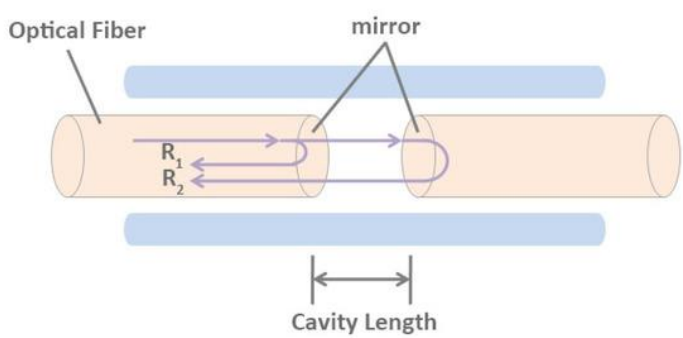


Figure 64: Schematic diagram of Fabry-Perot interference cavity (Wu et al., 2020)

2) Quasi distributed fibre bragg grating sensors (FBG)

This type of fibres has special gratings included. The gratings work on the principle of a light filter. Based on the grating spacing, all but one wavelength of the incident beam will pass the filter. One wavelength will be reflected to the detector. If the length of the cable changes due to strain, temperature or other effects the spacing of the grating will change as well. Hence, the reflected beam wavelength will change and an event is registered. This system allows for several gratings, filtering out different wavelengths along one fibre at specific points of interest.

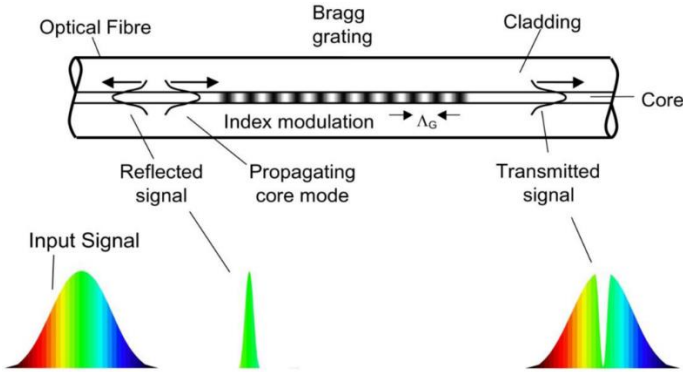


Figure 65: Schematic diagram of an FBG having an index modulation of spacing  $\Lambda_B$  inside a single-mode optical fibre (Mihailov, 2012)

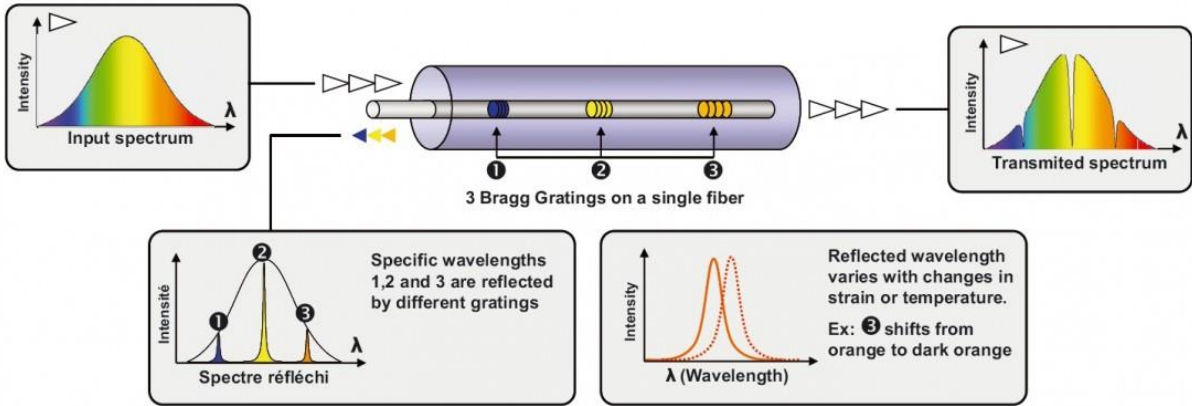
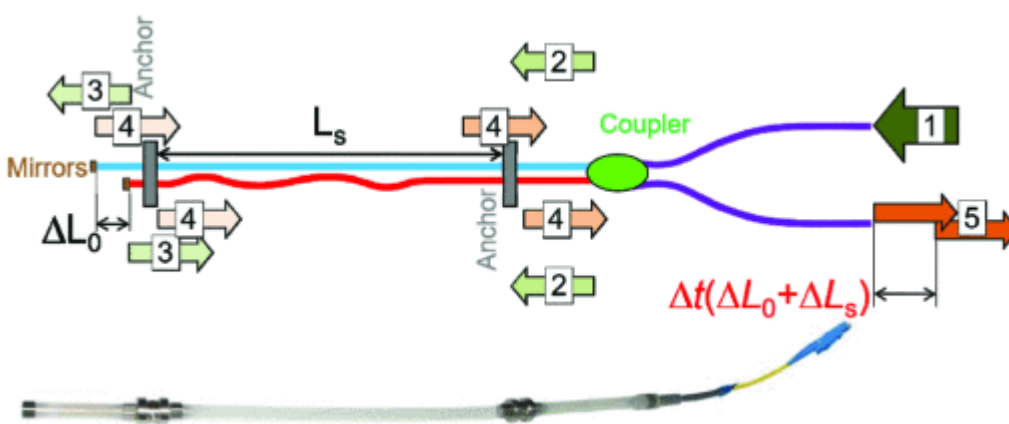


Figure 66: principle of fibre grating technology filtering out different wavelengths at different locations along the same fibre (<https://scaime.com/fibre-bragg-grating-technology>)

### 3) Long base interferometric (SOFO) sensor:

Here the fibre itself is the sensor and measurements are made between two points that can be some cm or several metres apart. This type of sensor is well suited for measuring global deformations of concrete structures in contrast to more local events for the point sensors described above. The sensor set up consists of two cables between two anchor points. The reference cable is loose while the measuring cable is tensioned to about 0.5% of the sensor lengths. Light is emitted and equally distributed between the reference and measuring cable. At the end of the cables light is reflected and again combined in the coupler to an interference wavelength. As the measuring cable is slightly tensioned both deformation by elongation and shortening can be detected. Any change in length of the cable will change the travelled distance of light. This will result in a shift of interferent wavelengths of the light from the reference and measuring cable. Any shift will correspond to a certain deformation of the structure.



**Figure 67: Schematic representation of an interferometric SOFO sensor (based on Michelson interferometry). Measurement steps: (1) light is injected into sensor; (2) coupler splits light into two optical fibres; (3) light in reference fibre reflects off the mirror and travels back; (4) light in measurement fibre reflects off the mirror, travels back, and combines in coupler with the light from reference fibre; and (5) combined light signals are decoded to find shift in phase and infer change in strain in sensor (Glisic, 2019).**

### 4) Fully distributed sensors:

Fully distributed sensors refer to several measuring points within one cable, e.g. every meter. Fully distributed fibre optic sensor cables can be several kilometres long. The strength of this technique is global monitoring with only one cable and at the same time being very sensitive to local events like formation of cracks. This is very powerful for monitoring where it is not known beforehand where a certain event will appear.

When light of a certain wavelength is sent, most of the light will just travel through the fibre. However, at every point of the fibre, there are always small amounts of light that are scattered by the atoms in the glass fibre. Parts of that scattered light will travel back to the source together with the reflected original light. There are different scattering events that can be detected. Raman scattering is just related to temperature, in specific the movement of atoms in the glass fibre. If the temperature is increased in one point the intensity of the scattered light will increase. Brillouin scattering is related to the distance of atoms in the glass fibre. If a crack appears or the structure is deformed, the cable length will change resulting in increased atom distance and change of the scattered wavelength. To localize events, a pulse of light is sent through the cable (in contrast to constant light source for point measurements). The time from the light pulse to the

backscattering event (time of light travel from event back to the detector) is recorded. The longer it takes, the further away is the event.

FOSs are fully mature techniques and have proven their suitability in many case studies and projects world-wide. The sensors can be embedded in concrete, applied at the reinforcement surface, or simply be mounted on the concrete surface in forms of tapes etc. The sensors are of high precision and durability and have excellent long-term stability. In contrast to other electricity-based sensors FOSs are not affected by lightning or other electromagnetic interferences. The systems have high resolution even over long distances.

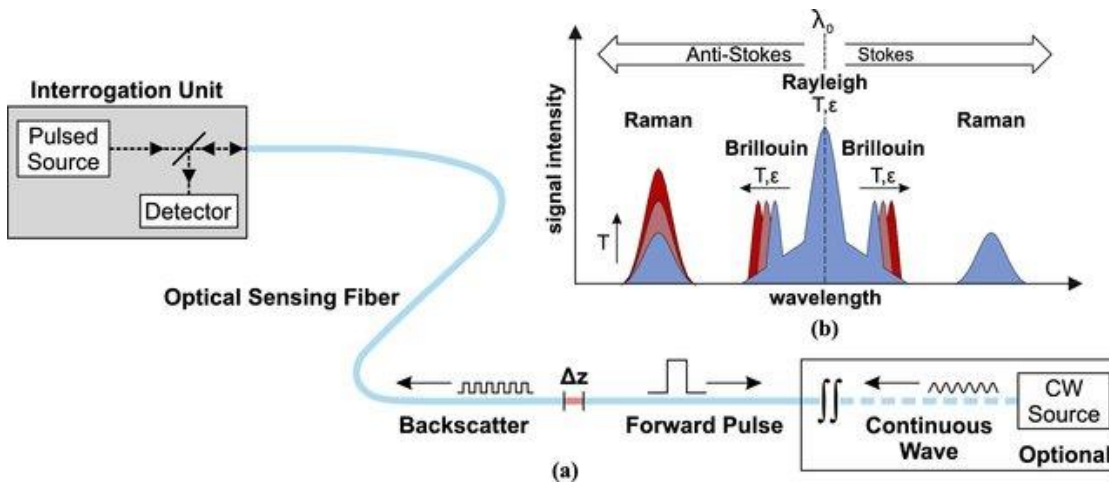


Figure 68: Distributed fibre optic sensing techniques (Monsberger et al., 2020): a) basic scheme of sensing setup (López-Higuera, 2002) and b) different scattering components in optical glass fibres (Glisic and Inaudi, 2007, p. 200)

Table 14: Strengths and limitations of different fibre optic sensor principles (Schumacher et al., 2021)

	Strengths	Limitations
General	High precision Excellent long term stability and durability Not affected by electromagnetic interference	High upfront cost Specialized personnel required Challenging and costly repair if necessary
Point	High stability Insensitive to temperature	Limited channels Sensing length: 50-70 mm
SOFO	Thermal self compensation Unlimited channels Resolution static measurements: 2 $\mu\text{m}$ Resolution dynamic measurements: 10 nm sensing length: 250 mm – 20 m	difficult to combine static and dynamic measurements – different reading units required number of channels for dynamic measurements is limited
FGB	Possible to combine static and dynamic measurements at one reading unit Quais distributed sensing	Need for thermal compensation Limited measurement range due to optical losses Sensing length: 10 mm – 2 m
Distributed (Rayleigh)	Measurement speed: 10 – 250 Hz High resolution strain measurements High spatial resolution: 1 mm Sampling interval: 0.4 mm	Maximum sensing length: 70 m
Distributed (Brillouin)	Sensing length: 250 m – 5 km	Low spatial resolution: 0.5-5 m Measurement speed: 10 s to 25 min Lower resolution for strain Sampling interval: 50-100 mm

### 6.1.7 Non-contact optical sensing technologies

These types of techniques are at the border between NDT and sensors. Parts of sensing equipment (cameras) are not directly installed on the structure but next to it. Often these techniques are not used yet for permanent monitoring but rather short-term monitoring.

#### 6.1.7.1 Digital Image correlation (DIC)

DIC is an optical technique to measure 2D in-plane or 3D out-of-plane displacements and deformations during loads. The resolution is dependent on the camera equipment used and proper calibration is needed for e.g. light effects, especially in field conditions. Usually, a special dotted pattern is applied on the surface to be investigated and pictures are taken from a camera at a fixed location. The exact location of the dotted pattern will be followed over time. The measured deformations during loads acting on the structure can be transformed to strain. The main strength of the technique is that it can provide results over a large area, compared to other techniques (e.g. strain gauges) that are more local. The set-up is often fast and cheap and has a high accuracy under ideal light conditions. Of course, the technique requires direct line of sight from the camera source to the structure and is limited to surface measurements. The method is readily available and can be customized for each case. There are many case studies available on large area deformation measurements and following up crack development on concrete structures.

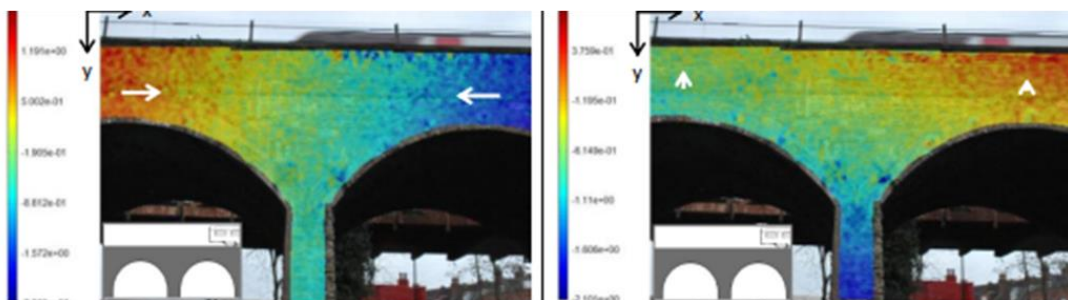
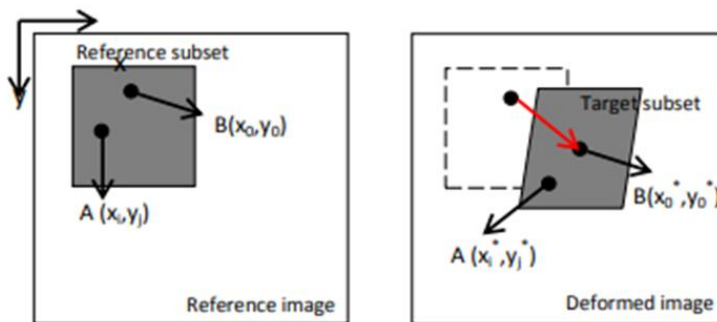


**Figure 69: Measuring principle with reference square subset before and after deformation and measured horizontal and vertical displacements during train traffic (Koltsida et al., 2013)**

#### 6.1.7.2 Light detection and Ranging (LIDAR)

LIDAR systems emit laser light and detect the reflected light from an object to the detector. There are two main principles. The first is that light pulses are sent to an object and the detector registers the time it takes for the reflected light to move back (TOF – time of flight pulse-based method). The other is based on transmission of continuous beam of laser radiation. A range value is derived by comparing the transmitted and received versions of the wave pattern of the beam and comparing their phase difference (phase-based method). The systems can be used by stationary ground-based platforms or mobile by airplanes, cars etc. to



create precise 3-D representations of structures. This can then be used to detect 3-D displacement of any specific point in a structure. Terrestrial measurements can also be effective in detecting cracking of concrete. Damaged sections with cracking, spalling or staining can be distinguished from undamaged parts of concrete structures. LIDAR is often used in geotechnical engineering but has also been successfully used for collecting data from buildings, bridges or tunnels. The accuracy and resolution is best for stationary systems compromising a slower data collection time. Mobile LIDAR systems are dependent on maintaining a GPS signal.

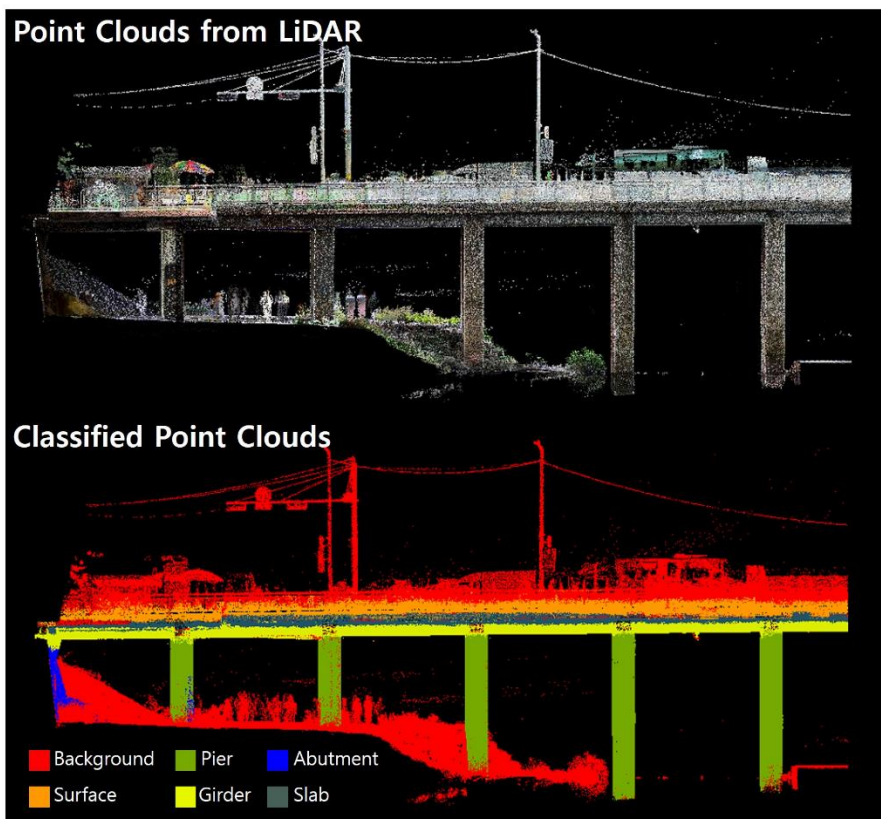


**Figure 70: 3D created overview image of bridge based on LIDAR technology (Kim and Kim, 2020)**

### 6.1.7.3 Radio detection and ranging (RADAR)

RADAR is a technique to detect objects from which directed radio waves may be reflected in terms of range, displacement, and velocity. In structural health monitoring of concrete structures, the range to targets can be used to detect displacements, structural movements, settlements, vibrations etc. over time. As LIDAR, RADAR can be utilized from mobile or static terrestrial sources. In recent years different types of wave detection and data processing have been developed.

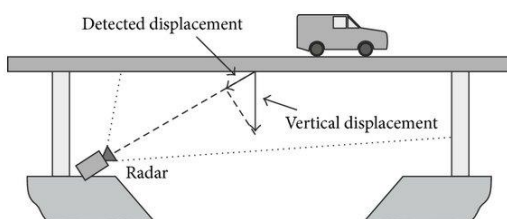


**Figure 71: Principle of interferometric radar camera (also applicable for LIDAR), installed at a fixed point under a bridge to monitor displacements due to traffic load (Pieraccini, 2013)**

## 6.2 Structural health monitoring

A recent publication from the Norwegian Federation of Concrete rehabilitation gathers important information on instrumentation and monitoring of structures with special focus on the risk of reinforcement corrosion (Eri et al., 2022). The report covers sensors for measuring crucial parameters of the reinforcement steel (electrochemical potential, currents, etc.) as well concrete properties (temperature, relative humidity, etc.) influencing the interpretation of the results. Besides reporting the basic principles, the report also serves as a guideline for correct planning and implementation of the sensors.

### 6.2.1 Temperature

Several producers offer equipment for measuring the internal concrete temperature. The temperature sensors can either be cast in during production of the concrete structures, or alternatively, for existing structures, they can be placed in boreholes at various depths (before filling the boreholes with a repair mortar or similar). It is very common to use thermocouples for temperature monitoring e.g. Pt/Rh types. A commercial device is for example Pt-1000 sensor. In Norway, thermocouples of type T, copper-constantan are recommended (Eri et al., 2022). The same publication gives detailed information on accuracy, and material and installation requirements in existing concrete structures.

The typical working principle of a thermocouple is shown below where temperature is converted into an electrical voltage output signal. The measured voltage is proportional to the temperature. Two different metals with different thermoelectric properties are joint together at the "Hot junction". Temperature change at the hot junction will create a potential change at the "cold junction" that is read out with a multimeter.

There are also optical fibre temperature sensors, however with little practical experience yet.

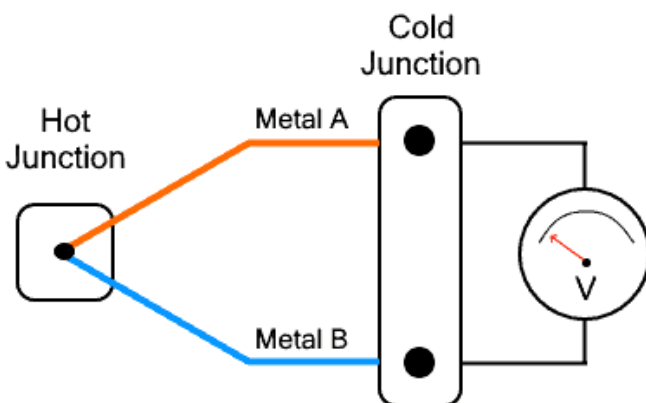


**Figure 72: Working principle of temperature measurement with a thermocouple converting temperature to voltage measurement (www.electricaltechnology.org)**

### 6.2.2 Relative humidity (RH)

As for the temperature sensors, several producers offer equipment for measuring the internal relative humidity (RH) in concrete. Most of these sensors also have temperature sensors integrated. The RH sensors can either be cast in during production of the concrete structures, or alternatively, for existing structures, they can be placed in boreholes at various depths (normally inside plastic tubes that are put into the boreholes before being sealed).

As part of the COIN project (<https://www.sintef.no/en/projects/2007/coin/coinp/>) De Weerd and Geiker summed up the presentations at the COIN workshop “Moisture in concrete” organized by SINTEF and NTNU 6<sup>th</sup> and 7<sup>th</sup> of February 2012 in Trondheim (De Weerd and Geiker, 2016). A brief extract from this report, in which chapter 2 presents and compares a range of RH sensors, is given (partly re-written) in the following. The report also discusses various ways of measuring RH and the corresponding sources of possible errors. The relative humidity of field exposed concrete which is relevant for durability studies is in the range 70-100% RH. The accuracy of most RH sensors is in general poorest in the upper limit of this interval (95-100% RH).

There are different types of RH sensors:

- Capacitive polymer RH sensors
- Resistive polymer RH sensors
- Electrolytic RH sensors
- Dew point RH sensors / chilled mirror sensors

A capacitive humidity sensor consists of a hygroscopic dielectric material placed between a pair of electrodes, which form a small capacitor. The capacitance in the sensor depends on its moisture content and hence on the RH of the air it is in contact with. Most of the RH sensors referred to in the COIN report are capacitive sensors, e.g., the *Vaisala HM44 Concrete Humidity Measurement System* (Figure 73, right). Another example is the *Rotronic probe (HC2)* that measures humidity with a *ROTRONIC Hygromer® IN1* and temperature with a *Pt100 RTD* (Figure 73, left) (Ref: Rotronic AG, HygroClip 2 (HC2) - Humidity temperature probes: user guide, 2018). In Norway, the Rotronic sensor is sold as part of a monitoring system for concrete structures called *CAMUR* distributed by Protector (CAMUR II Hygro Temp, Technical datasheet, 2022: <https://www.protector.no/en/support/support/camur/datasheets/technical/sensors/hygrotemp.html>). SINTEF and the NPRA are currently testing this system remotely at SINTEF’s field exposure site in Trondheim. The system installed by Protector transfer the data via 4G.

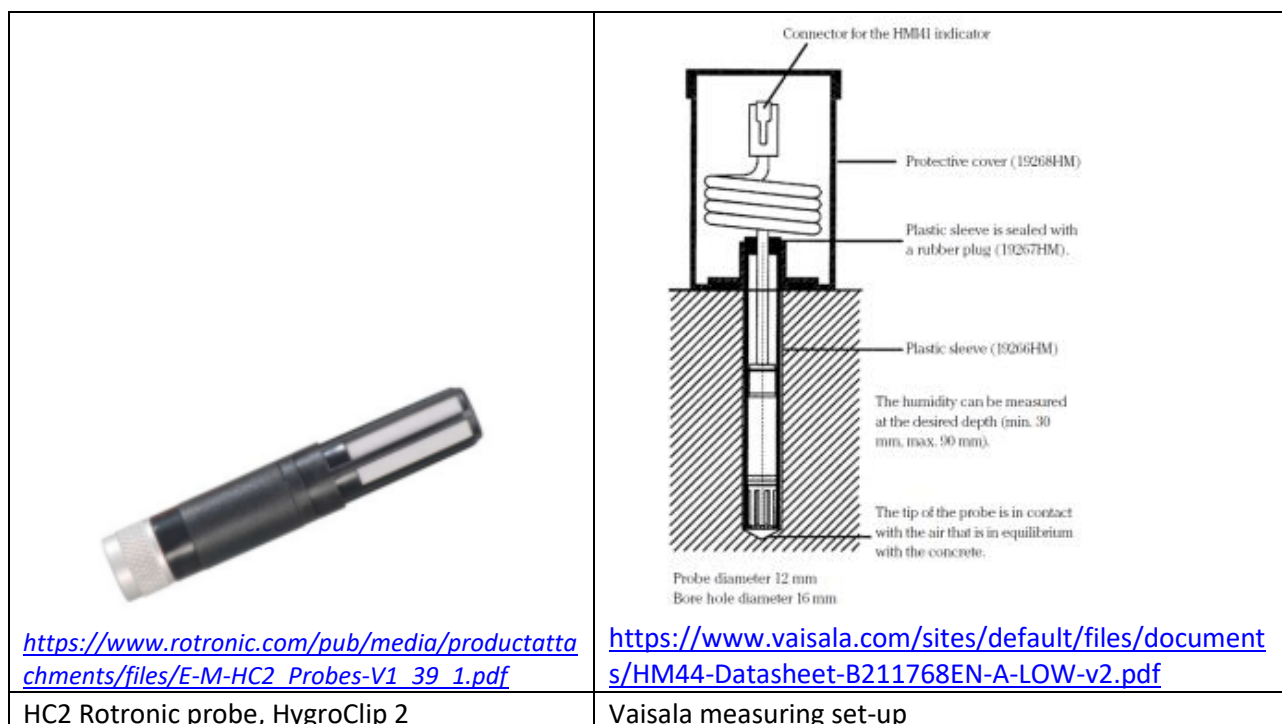


**Figure 73: Rotronic HC2 (left) and Vaisala HM44 (right) RH sensor**

Similarly, a resistive humidity sensor contains hygroscopic material, e.g., a polymer or wood, of which the resistivity changes with the RH.

The electrolytic humidity sensor contains an electrolyte of which the electric conductance changes with the RH.

The chilled mirror sensors measure the dew - or frost point temperature directly by controlling a reflective surface to an equilibrium temperature between dew - / frost formation and evaporation. Due to its accuracy SINTEF Community uses the chilled mirror sensor for calibrating other RH sensors, e.g., the Vaisala sensors.

In general, measuring RH in field is notorious uncertain due to many possible sources of errors. The COIN report sums up the most relevant of these. The sources of errors can be split between “inherent error” (i.e., sources or errors connected to the RH sensors used) and “user errors” (i.e., errors connected to execution of the RH measurements). One of the most frequent sources of error is temperature differences between the RH sensor and the surrounding concrete, leading to very significant errors (e.g., a temperature difference of 1°C between the RH sensor and the surrounding concrete can result in an error of ± 5% RH). Experiences from several years of RH measurements in field exposed concrete at a field station in Trondheim will be summed up in a separate report.

Measurement of RH in concrete was also the topic for a second workshop arranged by SINTEF in 2018 (Skjølsvold and Lindgård, 2018). Relevant topics for the workshop were:

- Requirements and experience from use of different RH measuring devices/sensors and procedures for in-situ measurements
- Experience from relative humidity measurements in the laboratory and in-situ for research purposes (incl. various sources of errors).

As summed up in the workshop proceeding; In most Nordic countries, the main technique for measuring RH in concrete floors (that traditionally has been the most frequent reason for measuring RH in-situ in concrete) is to drill holes before installing plastic tubes. Subsequently, calibrated RH sensors can be placed at the aimed depth. The RH is normally measured manually over time, i.e., remote RH measurements has not been frequently used. However, the title of one of the interesting presentations (by Stefan Nordmark, Electro-tech) at the Nordic workshop was “The challenge of developing a moisture sensor that is cast into concrete” (i.e., wireless measuring of RH in concrete). In the system they had developed, the RH data are transmitted to an external access point in the vicinity of the concrete structure. The external access point is connected to internet via GPRS, and the information is sent to a database.

**Table 15: Strengths and limitations of different RH sensor types (Schumacher et al., 2021)**

RH sensor type	Strengths	Limitations
Resistive, capacitive	Easy to deploy Long-term stability inexpensive	Measurement errors due to natural weathering and thermal cycling Upper RH limit Lon-term exposure might cause response shift Each sensor requires own wiring
Fiber-optic	Multiple measurement points Wiring at each sensor not required	Expensive in comparison

Due to all the possible sources of errors connected to in-situ measurements of RH in concrete (De Weerd and Geiker, 2016), SINTEF Community and University of Lund in Sweden prefer performing controlled RH measurements in the laboratory (with a stable temperature and environment) on smaller samples split from concrete cores carefully extracted from the concrete structures enabling maintaining the in-situ moisture state.

### 6.2.3 Corrosion sensors

In general, there are two different electrochemical approaches for assessing the risk of corrosion, and one distinguishes between sensors measuring the likelihood of ongoing corrosion and sensors measuring the actual kinetics, i.e. the corrosion rate.

#### *Likelihood of ongoing corrosion*

Measuring the electrochemical potential of the steel is a useful and probably the most used tool to obtain information on the corrosion state of the reinforcement (passive state or actively corroding). A typical set-up is to electrically connect a reference electrode to the steel reinforcement via a voltmeter for measuring the voltage difference.

The most common reference electrode for measuring the corrosion potential at concrete surfaces is the copper-copper sulphate (Cu-CuSO<sub>4</sub>) electrode, whereas there are several types of reference electrodes designed to be embedded/immersed in the concrete (Myrdal, 2007). Surface potential mapping is illustrated in Figure 74, and one type of an embeddable reference electrode for concrete is shown in Figure 75. As soon as the reinforcement starts to corrode, the measured voltage will drop towards more negative values. Reference electrode technology for concrete applications is very mature and tested under field conditions on several occasions in Norway.

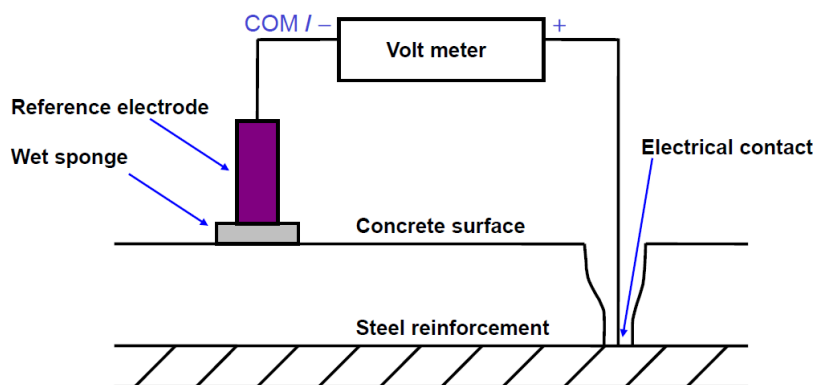


**Figure 74: Measurement of corrosion potential at a concrete surface.**





**Figure 75: ERE 20 reference electrode from Force Technology ([www.forcetechnology.com](http://www.forcetechnology.com))**

#### *Corrosion rate of steel reinforcement*

When the corrosion rate (current density) is of interest, an electrochemical method which allows to determine the polarization resistance of the reinforcement should be used. The current density represents the rate at which a metal corrodes in an electrolytic solution (e.g. pore solution in concrete). Polarization resistance refers to the resistance of a steel reinforcement to oxidise.

In order to determine the polarization resistance ( $R_p$ ) of the reinforcement a counter electrode is needed in the vicinity of the steel bar to be measured. An electric wire is then connected to the steel reinforcement and to the counter electrode (on the concrete surface or embedded in the concrete) via an electronic hardware/instrument (i.e. potentiostat). The corrosion potential is measured and registered, and an impress electric signal (voltage or current) is sent to the steel from the counter electrode. The response to this 'shock' is then used to calculate the  $R_p$ .

The polarization resistance can be measured with different techniques like linear polarization resistance (LPR), electrochemical impedance spectroscopy (EIS), galvanostatic pulse polarization (GP), or macro-cell current.

With the linear polarization resistance (LPR) technique, the polarization resistance ( $R_p$ ) is determined by polarizing the reinforcement potentiostatically in both anodic and cathodic directions. That means imposing a difference in potential between the steel and the reference electrode, and then measuring the current response. The slope of the relationship between the potential and the current density is defined as the polarization resistance ( $R_p$ ).

Impedance spectroscopy determines the polarization resistance by polarizing the reinforcement applying an alternating potential signal at varying frequencies to the corroding system and measuring the resulting current density. The polarization resistance is determined by fitting an equivalent circuit to the recorded response.

Galvanostatic pulse determines the polarization resistance by polarizing the reinforcement galvanostatically. A constant electrical current pulse for a specific time, e.g. 10 s, is applied to the corroding system; between steel and reference electrode, and the difference in potential is measured. The polarization resistance is determined by fitting an equivalent circuit to the transient while the reinforcement goes back to the open circuit potential after the polarization.

In contrast to LPR, EIS and GP, macro-cell current sensors are passive, i.e. no disturbance of the corroding system by applying currents or potential is needed.

### Macro-cell current sensors

In macro-cell current sensors, electrical currents between artificial anodes and cathode are measured, not the steel reinforcement itself. The principle for measuring macro-cell current is to electrically connect two dissimilar metals (also referred to as galvanic currents). There are several commercial sensors available, e.g. anode ladders. Several anodes (e.g. steel) that are electrically connected with a cathode of a different metal are introduced at different cover depth in the concrete (Figure 76). When one of the anodes starts to corrode, electrical currents are measured between anode and cathode with an amperemeter in the sensor. Anode ladders however, rather provide information about corrosion initiation than corrosion rate.

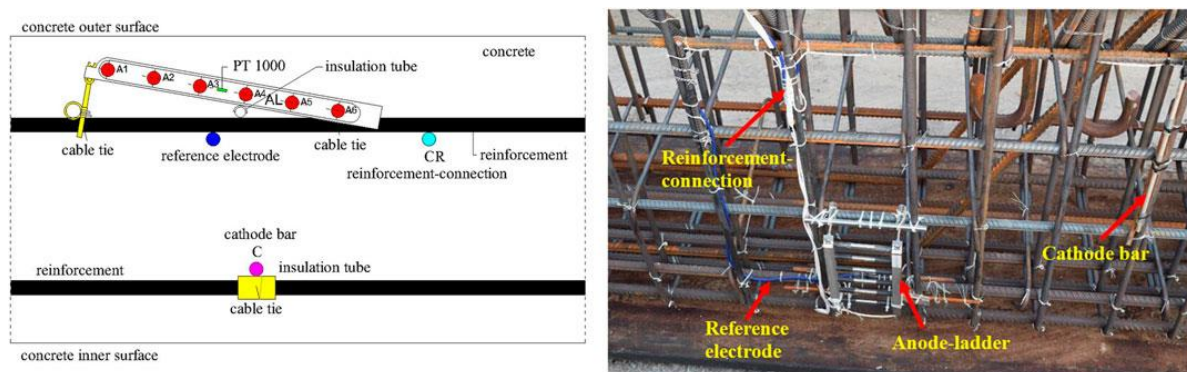


**Figure 76: An example of anode ladder sensor (Liu et al., 2021))**

It is an advantage to choose a sensor with an anode material that is similar to the reinforcement of interest. Most available sensors typically measure the corrosion of an internal working electrode and not the reinforcing steel of interest. Furthermore, recent research has revealed challenges with the reliability of too small sensors. Therefore, also a lot of hand-made solutions can be applied to measure macro-cell currents. In current Norwegian research projects with field exposed concrete, custom made sensors are applied consisting of larger reinforcement bars as anodes (80 cm length). In addition to the structural reinforcement of the concrete beams, additional reinforcement bars are cast into the concrete at different cover depth and in different exposure zones. The reinforcement bars are electrically connected either between different cover depths or different exposure zones. Originally similar, the condition of connecting two dissimilar metals is achieved as soon as one of the reinforcement bars have a different thermodynamical state, as it e.g. gets embedded in carbonated concrete or attacked by chloride contamination. As soon as one of the reinforcement anodes starts to get active, galvanic currents can be measured between the corroding rebar and the yet passive rebars to obtain information on the corrosion rate.

For all corrosion sensors it is best to be cast in the concrete during the building phase. Casting in corrosion sensors in existing structures, or establishing systems for corrosion monitoring, is challenging but can be achieved during major repair works.

### 6.2.4 Chloride and pH

There are different possibilities and developments ongoing for sensors that directly or indirectly measure the chloride content and pH in the concrete. There are no commercial embeddable sensors available today that directly measure pH or chloride concentration. However, sensor systems including such sensors are available, for instance from the company Duramon (<https://duramon.ch/>).

A typical electrical based embeddable chloride sensor for concrete is made of a silver wire coated with silver chloride. The electrochemical potential of such an electrode is sensitive to the chloride concentration in the pore water. The potential – measured with a reference electrode – is linearly dependent on the chloride concentration in the pore water, allowing for the determination of free chloride content.

Fibre optic sensors are often based on the principle that the light transmitted through the fibre is disturbed by changes on the surface of the fibre resulting in different degrees of reflection, adsorption or changes in refractive index. An example is a fibre coated with silver nitrate or silver chromate. In reaction with chloride ions, silver chloride will precipitate, and the change of colour is sensed. These sensors are non-reversible and the durability in alkaline environments is limited. There are also sensors under development incorporating sol-gel membranes at the tip of fibres that react with chlorides in the pore solution. FOS can also be used to detect changes in pH of the pore solution. A light absorbing species can be attached to the tip of an optical fibre, where changes in the light absorption can be correlated to changes in pH. So far fibre optic technology for chloride and pH sensing is very immature.

Another indirect method of sensing chloride ions are wireless passive radio frequency identification (RFID) sensors with wire-based triggers. Wires with similar chemistry of the reinforcing steel are used to measure the resistivity as sectional area changes due to corrosion. The size of the wires and its corrosion showed good correlation to the chloride concentration. These sensors are inexpensive, have shown good stability under robustness testing and are readily available for field application. Furthermore, no power supply is required.

**Table 16. Strengths and limitations of a selection of chloride sensor types (Schumacher et al., 2021)**

Sensor	Strengths	Limitations
Electric based	Effective for practical field application	Limited electrode longevity Temperature and pH sensitive Require fluid to allow flow of ions Local measurements
Fibre optic	Immune to electromagnetic interference Multiple measurement points along fiber	Non-reversible reactions in some type of sensors (e.g. sol.gel based) Long term stability to be proven
RFID	Inexpensive Wireless communication No need for power supply	

A typical embeddable pH sensor for concrete is made of an iridium wire coated with iridium oxide. The electrochemical potential of such an electrode is sensitive to the pH of the pore water. The electrode must be calibrated, preferable in the pH range 9.0 – 13.5, prior to installation in concrete. A reference electrode is used to measure the potential which is proportional to the pH at a given temperature. Ir/IrO<sub>2</sub> sensors show good long-term stability of several years and are stable over a wide pH range.

A separate note on chloride and pH sensors is being prepared within WP5.3 (by Roar Myrdal).

### 6.2.5 Water pressure in dams

Piezometers are commonly used to monitor the hydraulic pressure at various locations in dams especially uplift pressures at the base of the dam and foundation rocks, as well as pore water pressure in soil or rock of dam foundations and abutments. In field measuring systems it is commonly distinguished between open and closed systems. Furthermore, potential crack propagation can be monitored. In an open system, sensors

are lowered into accessible pipes when needed. In a closed system the sensors are embedded during installation and not accessible after that.

In the open system, water is allowed to enter the pipe. The height of the water in the pipe is then related to the hydrostatic pressure at the location of the water inlet.

Closed system piezometers often operate after the principle of vibrating wire sensors, strain gauges, pneumatic sensors or hydraulic twin tubes.

**Table 17: Strengths and limitations of different piezometer types (Schumacher et al., 2021)**

Sensor	Strengths	Limitations
Open system	Inexpensive installation and operation Long-term reliability	Slow response time Nearly vertical installed pipes required Insensitive to pore pressure change Average readings Freezing and clogging problems Costly drilling for repair
Vibrating wire	Fast response time Positive and negative pore pressure readings Low operation and maintenance costs Potential automatic recordings	Sensitive to temperature and barometric changes Slight Risk of zero shift Inability to de-air the tip
Strain gauge	Same as vibrating wire	High risk of zero shift limiting long-term applications
Pneumatic	Continuous readings	De-airing required Skilled operator required Unreliable long-term performance
Hydraulic twin tube	Continuous readings	Freezing and corrosion problems De-airing required Complex flushing procedure High initial costs

## 6.3 Norwegian case studies on existing infrastructure

### 6.3.1 Bridge monitoring

(Myrland Jensen, 2012) gave an overview over the market potential for monitoring systems in Norway. In the report an overview over known existing bridges was given where sensors were installed after some years. Until 2012, 98 bridges with a span larger than 400 m were identified of which 21 were monitored during some time.

**Table 18: Overview of identified bridges with monitoring in 2012 according to (Myrland Jensen, 2012)**

No.	Bridge name	Ref.	Year of completion	Bridge type	Length [m]	Main span [m]	Monitoring			
							Year	Constr. phase	Completed structure	Type of monitoring <sup>(1)</sup>
14	Bergsøysund Bridge		1992	Floating bridge	931	106	2002-2009	?	X	L1, L3, R2, R3
82	Gjemmessundet bridge		1992	Suspension bridge	1257	623	1997-1999	-	X	L1, L2, R1, R3
97	Helgelands Bridge		1991	Cable stayed bridge	1065	425	1989-1995	X	X	L1, L2, R1, R2, R3
107	Hundvåkøy Bridge		2007	Cantilever bridge	460	233	?	X	X	L2, R2
108 / 327	Hølandalen Bridge (Raylway)		1996	Cantilever bridge	416	128	1994-1998	X	X	L2, R1, R2, R3
137	Kråkerøy Bridge		1957	Beam bridge	180	48	2009-2010	-	X	?
152	Lodalen Bridge		?	?	?	?	1986	?	?	R1
180	Norddalsfjord Bridge	[5.1]	1987	Cantilever bridge	401	231	1985-1986 1989-2001	X -	- X	R2 R1, R2
181	Nordhordland Bridge		1994	Cable stayed / floating bridge	1614	172	?	X	X	L1, L3, R2, R3
184	Nordsundet Bridge (Namsos)		?	Steel bridge	?	?	1996-1997	-	X	L1, L2, R2, R3
190	New Svinesund Bridge		2005	Arch bridge	704	247	2003-2008	X	X	L1, R1, R2, R3
207	Raftsundet Bridge		1998	Cantilever bridge (LWAC/NDC)	711	298	?	X	-	L1, R3
215	Rolvøysund Bridge		?	?	?	?	2007	?	?	?
220	Rugsundet Bridge		2002	Cantilever bridge (LWAC/NDC)	302	190	1999-2000	X	-	R2
227	Sandesund Bridge		2008	Cantilever bridge	1528	139	2006-2008	X	?	?
232	Skarnsundet Bridge		1991	Cable stayed bridge	1010	530	1990-1995	X	X	L1, L2, R1, R2, R3
254	Stolma Bridge	[5.1]	1998	Cantilever bridge (LWAC/NDC)	467	301	1999-2001	-	X	R1, R2
264	Straumsbrua Bridge		2004	Arch bridge (steel)	290	?	2001-2002	X	-	L1
271	Støvset Bridge	[5.1]	1993	Cantilever bridge (LWAC/NDC)	420	220	1992-1994 1996-2001	X	X	L1, L2, R1, R2, R3

<sup>(1)</sup> L1 = Wind, L2 = Temperature, L3 = Stream/waves, R1 = Displacement, R2 = Strain, R3 = Acceleration



The monitoring of bridges covers mostly structural parameters like displacement, strain (e.g. vibrating wire dynamometers) and accelerations in addition to weather data like wind and temperature. The focus of most monitoring systems is currently on the dynamic behaviour due to different loads, e.g. Hardanger Bridge (wind loads (Fenerci et al., 2021)), Bergsøysund (wind, wave action (Kvåle et al., 2023)).

A more recent example of intensive continues monitoring is Stavåbru. The bridge monitoring system was installed in 2019 and a digital twin was constructed. Stavåbru is a critical infrastructure object on the E6 between Trondheim and Oppdal and closure of the bridge has considerable consequences on traffic.



**Figure 77: Bird perspective of Stavåbru**

Based on information in notes provided from the Norwegian Public Roads Administration (NPRA), 29 sensors and a data cabinet with antenna were installed. Sensors were placed at the longitudinal support beam, columns, arches and along cracks and at abutments. Changes in crack width were measured with mechanical sensors, similar as changes in distance between different parts of the bridge (e.g. columns and support beam). Accelerometers were installed at abutments, support beam, columns, foundations, and the arches. All sensors were placed on the concrete surface. All sensors had to be placed with free view between the antenna of the sensors and the antenna of the receiver.



**Figure 78: Installed sensors, Foto: NPRA**

With the installed sensors information could be gathered on global displacements and strain as well as local development of specific cracks. The system was continuously monitored and sending warning messages when measurements are outside certain defined ranges for e.g. movements.



**Figure 79: Accelerometers with battery package from the monitoring (left and middle) and distance measuring device (right); ([www. Lisab.se/product/eds-series/](http://www.Lisab.se/product/eds-series/))**

Herøysund bridge in Northern Norway is an example of many bridges potentially affected by corrosion of post-tensioned ducts and tendons. The corrosion damage on Herøysund bridge is severe, so that it must be demolished for construction of a new bridge. Intensive investigations were started and the bridge is now used as case study for research on NDT methods and sensors for structural monitoring. In 2020, 6 strain sensors and 2 crack width sensors were installed. Later as part of the Herøy FoU project, 7 additional strain sensors have been installed to develop a Bridge Weigh-in-motion (BWIM) system. Furthermore, several accelerometers were installed with the goal of performing operational modal analysis, which will be the basis for developing and updating numerical models of the bridge. All strain gauges are glued on composite bands, which are glued underneath the bridge to the concrete, measuring in longitudinal direction. All strain gauges are temperature compensated to distinguish between expansion/contractions due to temperature variations and physical load. The sensor providers were HBK for strain and crack-widths and Wise technology (Italy) for accelerometers and analysis of data (personal communication with Daniel Cantero, 2023)

### 6.3.2 Dam monitoring

There are around 3000 concrete dams in Norway and dam owners are required to carry out monitoring of their facilities (Myrland Jensen, 2012). The typical external loads on a concrete dam and the possible responses (output) are illustrated in Figure 80. Typical monitoring of dams includes deformation measurements, water level, concrete, and water temperature. With regard to age deterioration the major durability problem in Norway affecting concrete dams is related to alkali-silica reactions. In case of ASR, expansion, potential resulting crack propagation can be monitored with e.g. sliding micrometers. Furthermore, pore pressure, leakages and settlements are important parameters for the integrity of concrete dams. Recent reviews on dam monitoring practices with a Norwegian perspective are available from Multiconsult (Lu et al., 2021) and Sweco (Sweco, 2018). The main parameters required to be monitored according to Norwegian dam safety law are water level, leakage, deformation, and pore pressure.

An example of displacement measurements on a concrete dam in Switzerland affected by ASR can be seen in Figure 81 (Droz et al., 2013). Displacement was monitored with automatic pendulum measurements for more than 50 years. Large seasonal changes in displacement are visible to temperature and water level changes. This highlights the importance of good calibration and long-term continuous monitoring to identify displacement trends over time due to concrete deterioration.

Another example of structural health monitoring of an ASR affected dam in Portugal is given in Figure 82. Radial, uniaxial and triaxial accelerometers were installed at different locations of the dam to monitor dynamic response under ambient and operational conditions. Variations in natural frequencies due to

variations in water level were identified with good precision. This makes it possible to identify potential structural changes over time due to concrete deterioration, through correlation with the temporal evolution of natural frequencies and mode shapes (Oliveira and Alegre, 2019).

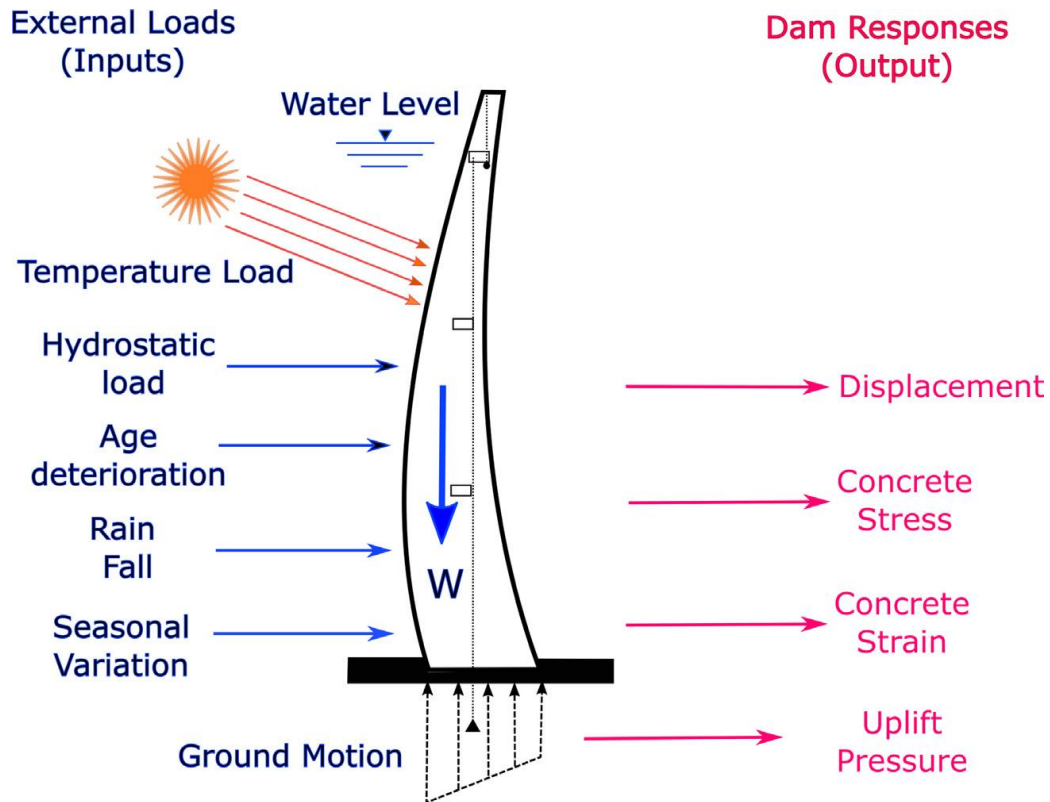


Figure 80: Illustration of external loads on a concrete dam and the structural and material response/output (Prakash et al., 2022)

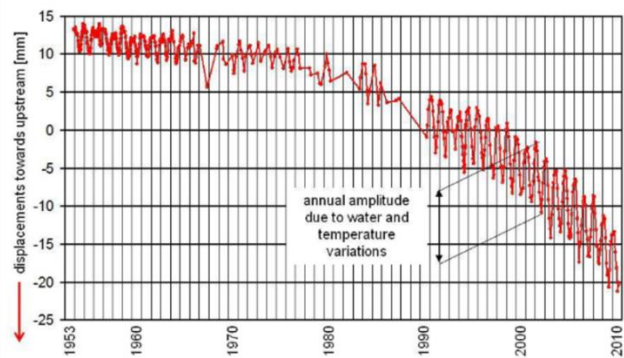


Fig. 2  
Pendulum displacement of block 13 versus time [4]

Figure 81: Displacement measurements at Salanfe Dam in Switzerland. (Droz et al., 2013)

In Norway, Votna Dam 1 and 2 have been extensively studied for many years and several rehabilitation works have been conducted due to alkali silica deterioration. Measuring bolts have been installed and yearly measurements have been performed to monitor displacement and deformation with time. Figure 83 shows FEM simulations of deformations due to temperature load and measured displacement with time caused by ASR (Larsen et al., 2008)



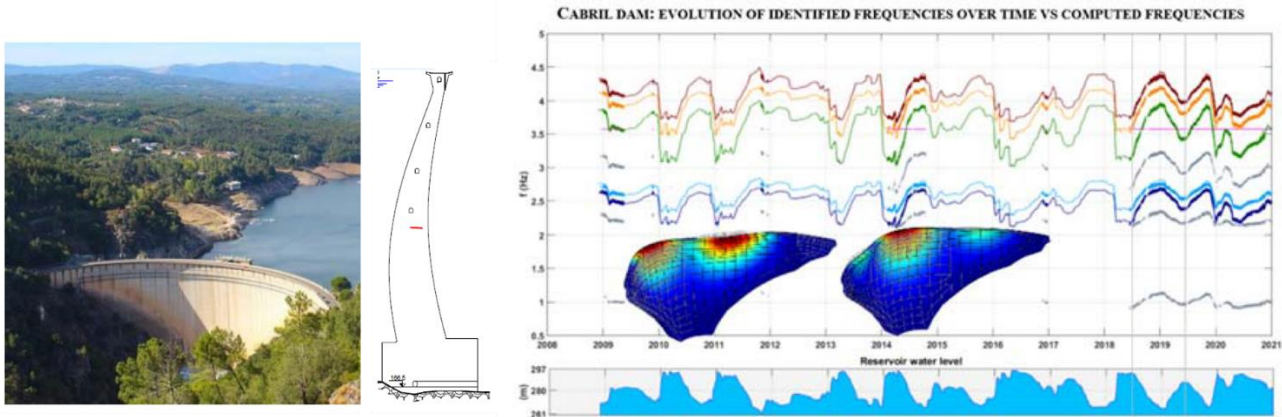


Figure 82: seismic and structural health monitoring (SSHM) installed in Cabril dam, Portugal (Oliveira and Alegre, 2019)

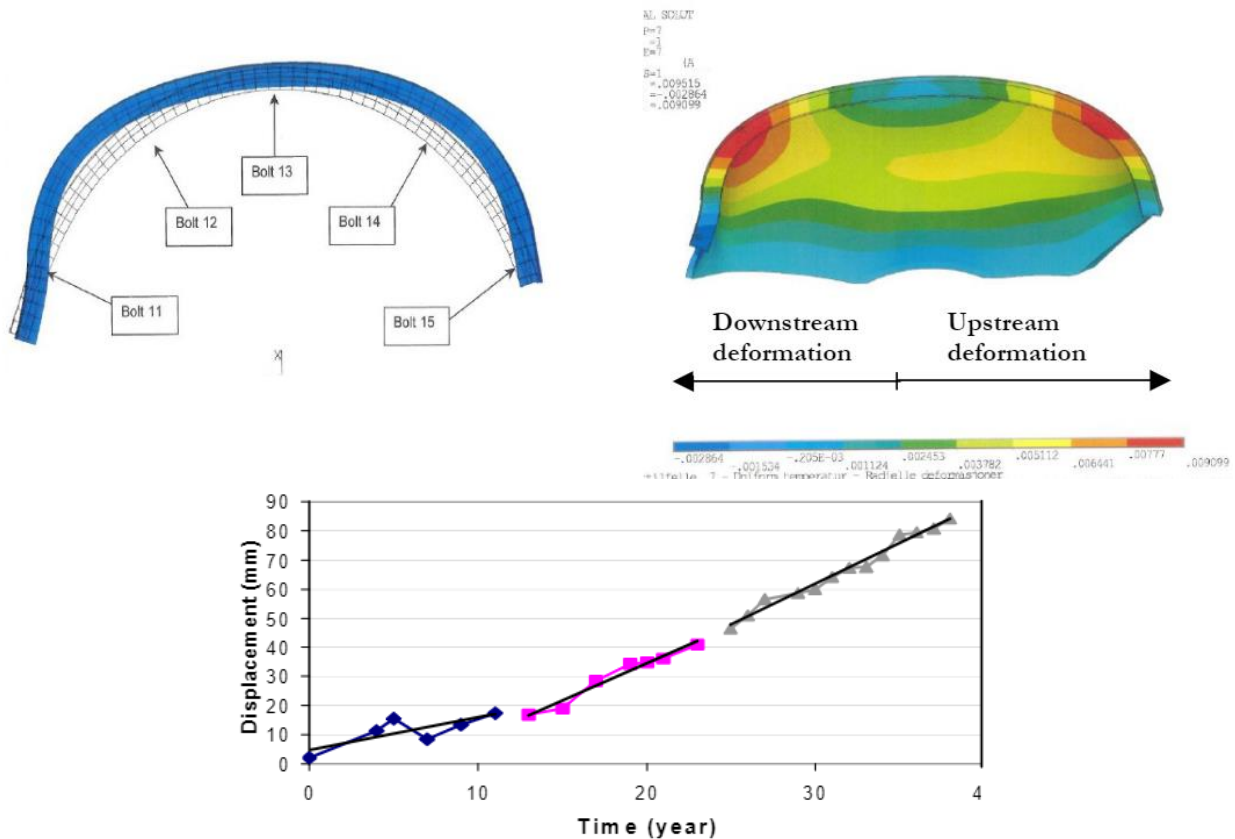


Figure 83: Simulated and measured deformations of Votna 2 dam in Norway affected by ASR. Top left: Location of measuring bolts and calculated horizontal deformations due to uniform temperature load; Top right: Calculated radial deformation due to uniform temperature load. Bottom: Yearly measured displacement of bolt 12 (in mm) between 1966-2004 (Larsen et al., 2008)

### 6.3.3 Field stations

According to the authors knowledge there are no case studies of direct continuous measurements of corrosion parameters. However, the Norwegian Public Road Administration (NPRA) owns several field stations for marine exposure of concrete beams (Hornbostel and Pedersen, 2019). Different set-ups and sensor designs are used, but the most common sensors installed (cast in) include resistivity and temperature

sensors as well as reference electrodes connected to reinforcement and custom-made macro-cell current sensors (working electrodes). This allows for measurements of electrochemical potential and corrosion currents (corrosion rate) after onset of reinforcement corrosion.



**Figure 84: Instrumented concrete beams exposed to tidal water at Austefjord Field Station, Bergen (Foto: Andres Belda Revert 2021)**



## 7 References

- Ahlborn, T.M., Brooks, C.N., Michigan Technological University, 2015. Evaluation of bridge decks using non-destructive evaluation (NDE) at near highway speeds for effective asset management. (No. RC-1617).
- Alani, A.M., Aboutalebi, M., Kilic, G., 2014. Integrated health assessment strategy using NDT for reinforced concrete bridges. *NDT & E International* 61, 80–94. <https://doi.org/10.1016/j.ndteint.2013.10.001>
- Al-Khateeb, H.T., Shenton, H.W., Chajes, M.J., Aloupis, C., 2019. Structural Health Monitoring of a Cable-Stayed Bridge Using Regularly Conducted Diagnostic Load Tests. *Frontiers in Built Environment* 5.
- Alonso Medina, P., León González, F.J., Todisco, L., 2022. Data-driven prediction of long-term deterioration of RC bridges. *Construction and Building Materials* 317, 125790. <https://doi.org/10.1016/j.conbuildmat.2021.125790>
- An, Y.-K., Kim, M.K., Sohn, H., 2014. 4 - Piezoelectric transducers for assessing and monitoring civil infrastructures, in: Wang, M.L., Lynch, J.P., Sohn, H. (Eds.), *Sensor Technologies for Civil Infrastructures*, Woodhead Publishing Series in Electronic and Optical Materials. Woodhead Publishing, pp. 86–120. <https://doi.org/10.1533/9780857099136.86>
- Baqersad, J., Poozesh, P., Niezrecki, C., Avitabile, P., 2016. Photogrammetry and optical methods in structural dynamics – A review. *Mechanical Systems and Signal Processing* 86. <https://doi.org/10.1016/j.ymssp.2016.02.011>
- Barros, F., Aguiar, S., Sousa, P.J., Cachaço, A., Tavares, P.J., Moreira, P.M.G.P., Ranzal, D., Cardoso, N., Fernandes, N., Fernandes, R., Henriques, R., Cruz, P.M., Cannizzaro, A., 2022. Displacement monitoring of a pedestrian bridge using 3D digital image correlation. *Procedia Structural Integrity* 37, 880–887. <https://doi.org/10.1016/j.prostr.2022.02.022>
- Bergmeister, K., Aktan, A.E., Bucher, C., Dorfmann, L., Fehling, E., Frey, R.P., Geier, R., Huth, O., Inaudi, D., Maier, J.E., Santa, U., Schwesinger, P., Slowik, V., Wenzel, H., Catbas, F.N., Cervenka, V., Cutts, J.M., Degriek, J., De Roeck, G., De Waele, W., Eichinger, E.M., Glisic, B., Grimmelsman, K.A., Jacobs, S., Kolleger, J., Matthys, S., Meerman, W., Novak, D., O'Connor, J.P., Olson, C.A., Pervizpour, M., Pukl, R., Raphael, B., Robert-Nicoud, Y., Smith, J.F.C., Strauss, A., Taerwe, L., Vurpillot, S., Yates, G.R., 2003. fib Bulletin 22. Monitoring and safety evaluation of existing concrete structures, fib Bulletins. fib. The International Federation for Structural Concrete. <https://doi.org/10.35789/fib.BULL.0022>
- Bertolini, L., Elsener, B., Pedefferri, P., Polder, R., 2003. Carbonation-Induced Corrosion, in: *Corrosion of Steel in Concrete*. John Wiley & Sons, Ltd, pp. 79–90. <https://doi.org/10.1002/3527603379.ch5>
- Bertolini, L., Elsener, B., Pedefferri, P., Redaelli, E., Polder, R.B., 2013. *Corrosion of Steel in Concrete: Prevention, Diagnosis, Repair*. Wiley.
- Bhandari, J., Khan, F., Abbassi, R., Garaniya, V., Ojeda, R., 2015. Modelling of Pitting Corrosion in Marine and Offshore Steel Structures - A Technical Review. *Journal of Loss Prevention in the Process Industries* 37. <https://doi.org/10.1016/j.jlp.2015.06.008>
- Blanksvärd, T., 2017. Icke-förstörande provning i samband med tillståndsbedömning. Luleå Tekniska Universitet.
- Candy, J., 2021. Accelerometer Modeling in the State-Space (No. LLNL-TR-819364, 1777338, 1030353). <https://doi.org/10.2172/1777338>
- CEB, 1992. CEB Bulletins : Durable Concrete Structures (PDF). fib. The International Federation for Structural Concrete.
- Chang, P.C., Flatau, A., Liu, S.C., 2003. Review Paper: Health Monitoring of Civil Infrastructure. *Structural Health Monitoring* 2, 257–267. <https://doi.org/10.1177/1475921703036169>
- Cultural heritage imaging [WWW Document], n.d. URL <https://culturalheritageimaging.org/Technologies/Photogrammetry/> (accessed 8.15.23).

- De Weerd, K., Geiker, M., 2016. Workshop on Moisture in Concrete, Trondheim, Norway 6–7 February 2012 SINTEF Bokhandel [WWW Document]. URL [https://www.sintefbok.no/book/index/1266/workshop\\_on\\_moisture\\_in\\_concrete\\_trondheim\\_norway\\_67\\_february\\_2012](https://www.sintefbok.no/book/index/1266/workshop_on_moisture_in_concrete_trondheim_norway_67_february_2012) (accessed 11.6.23).
- Dinh, K., Gucunski, N., Kim, J., Duong, T.H., 2016. Understanding depth-amplitude effects in assessment of GPR data from concrete bridge decks. *NDT & E International* 83, 48–58. <https://doi.org/10.1016/j.ndteint.2016.06.004>
- Droz, P., Menouillard, T., Vallotton, O., Leroy, R., 2013. Slot cutting an AAR-affected dam: case study of the Salanfe dam. *International Journal on Hydropower and Dams* 20, 102.
- Eri, J., Larsen, C.K., Østmoen, T., Myrdal, R., Stavem, P., Hornbostel, K., Belda Revert, A., 2022. Betongrehabilitering. Bestandighet av betongkonstruksjoner - instrumentert overvåkning (No. Publikasjon Nr. 2). Norsk Forening for betongrehabilitering, Oslo, Norway.
- Fagerlund, G., 1992. Betongkonstruksjoners beständighet : en översikt. Cementa, Lund Universitet.
- Fathi, H., Brilakis, I., 2011. Automated sparse 3D point cloud generation of infrastructure using its distinctive visual features. *Advanced Engineering Informatics, Special Section: Advances and Challenges in Computing in Civil and Building Engineering* 25, 760–770. <https://doi.org/10.1016/j.aei.2011.06.001>
- Fenerci, A., Andreas Kvåle, K., Wiig Petersen, Ø., Rønquist, A., Øiseth, O., 2021. Data Set from Long-Term Wind and Acceleration Monitoring of the Hardanger Bridge. *Journal of Structural Engineering* 147, 04721003. [https://doi.org/10.1061/\(ASCE\)ST.1943-541X.0002997](https://doi.org/10.1061/(ASCE)ST.1943-541X.0002997)
- Feng, Q., 2012. Practical Application of 3D Laser Scanning Techniques to Underground Projects, Phase 2-3: A Part of ISRM-Swedish National Task: “A Survey of 3D Laser Scanning Techniques for Applications to Rock Mechanics.” Stiftelsen Bergteknisk forskning.
- fib, 2023. Existing Concrete Structures Life Management, Testing and Structural Health Monitoring - State of the Art Report, Task Group 3.3 - preliminary draft (fib bulletin). fib. The International Federation for Structural Concrete.
- Gastineau, A., Johnson, T., Schultz, A., 2009. Bridge Health Monitoring and Inspections - A Survey of Methods (No. Mn/DOT 2009-29). Center for Transportation Studies.
- Germann Instruments, n.d. DOCTer - Technical data sheet.
- Glisic, B., 2019. Long-term Monitoring of Civil Structures and Infrastructure Using Long-Gauge Fiber Optic Sensors, in: 2019 IEEE SENSORS. Presented at the 2019 IEEE SENSORS, pp. 1–4. <https://doi.org/10.1109/SENSORS43011.2019.8956705>
- Glisic, B., Inaudi, D., 2007. Fibre Optic Methods for Structural Health Monitoring. John Wiley & Sons.
- Harries, K.A., Kasan, J., Miller, R., Brinkman, R., 2012. Updated Research for collision damage and repair of prestressed concrete beams (No. NCHRP20- 07(307)).
- Helmerich, R., Baessler, R., Buhr, B., Holm, G., Krüger, M., Niederleithinger, E., Tomor, A., Brühwiler, E., Bernardini, G., Phares, B., 2007. NDT-Toolbox. Background document SB3.16 (No. Deliverable 3.16), Sustainable Bridges – Assessment for Future Traffic Demands and Longer Lives.
- Hohmann, B.P., Bruck, P., Esselman, T., Yim, S., Schmidt, T., 2012. The Use of Digital Image Correlation as a Predictive Maintenance Tool for Long-term Operation of Nuclear Power Plants, in: 9th International Conference on NDE in Relation to Structural Integrity for Nuclear and Pressurized Components. Presented at the 9th International Conference on NDE in Relation to Structural Integrity for Nuclear and Pressurized Components, Seattle, Washington, USA (JRC-NDE 2012).
- Hornbostel, K., Pedersen, B., 2019. Betongelementer for langtidsprøving - Austefjorden feltstasjon - prøving av betong i marint miljø (Statens Vegvesen Rapport No. 494).
- Kaiser, H., Karbhari, V.M., 2004. Non-destructive testing techniques for FRP rehabilitated concrete. I: a critical review. *IJMPT* 21, 349. <https://doi.org/10.1504/IJMPT.2004.004996>
- Kakade, A., Limaye, H., 2019. Challenges in Nondestructive Testing of Post-tensioned Bridges. *Concrete Science*.

- Kashif Ur Rehman, S., Ibrahim, Z., Memon, S.A., Jameel, M., 2016. Nondestructive test methods for concrete bridges: A review. *Construction and Building Materials* 107, 58–86. <https://doi.org/10.1016/j.conbuildmat.2015.12.011>
- Kerdoncuff, H., Lin, W.-I., Wacker, L.J., 2017. Spectroscopic techniques for corrosion detection using drones.
- Kim, H., Kim, C., 2020. Deep-Learning-Based Classification of Point Clouds for Bridge Inspection. *Remote Sensing* 12, 3757. <https://doi.org/10.3390/rs12223757>
- Koltsida, I.S., Tomor, A.K., Booth, C.A., 2013. THE USE OF DIGITAL IMAGE CORRELATION TECHNIQUE FOR MONITORING MASONRY ARCH BRIDGES.
- Krüger, M., Grosse, C.U., 2007. Impact-Echo-techniques for Crack Depth Measurement : Sustainable Bridges Background document D3.7.
- Kvåle, K.A., Fenerci, A., Petersen, Ø.W., Rønquist, A., Øiseth, O., 2023. Data Set from Long-Term Wave, Wind, and Response Monitoring of the Bergsøysund Bridge. *Journal of Structural Engineering* 149, 04723002. <https://doi.org/10.1061/JSENDH.STENG-12095>
- Larsen, S., Lindgård, J., Thorenfeldt, E., Rodum, E., Haugen, M., 2008. EXPERIENCES FROM EXTENSIVE CONDITION SURVEY AND FEM ANALYSES OF TWO NORWEGIAN CONCRETE DAMS WITH ASR. Presented at the ICAAR.
- Lavezzi, G., Ciarcià, M., Won, K., Tazarv, M., 2024. A DIC-UAV based displacement measurement technique for bridge field testing. *Engineering Structures* 308, 117951. <https://doi.org/10.1016/j.engstruct.2024.117951>
- Lee, J.H., Lee, S.S., 2011. Electrolytic tilt sensor fabricated by using electroplating process. *Sensors and Actuators A: Physical* 167, 1–7. <https://doi.org/10.1016/j.sna.2011.01.011>
- Liu, Hongbiao, Zhang, B., Liu, Haicheng, Ji, Z., 2021. Analysis of Long-Term Durability Monitoring Data of High-Piled Wharf with Anode-Ladder Sensors Embedded in Concrete. *Frontiers in Materials* 8.
- López-Higuera, J.M., 2002. Handbook of optical fibre sensing technology. (No Title).
- Lu, H., Hoppe, S., Strokkenes, S.A., 2021. Review of dam monitoring and data management techniques (No. 10211223- RIEn- RAP- 001E).
- Mandić Ivanković, A., Thöns, S., Matos, J., 2018. Introduction: The Value of Health Monitoring in Structural Performance Assessment. *Structural Engineering International* 28, 243–243. <https://doi.org/10.1080/10168664.2018.1473964>
- Matt, P., 2000. Durability of Prestressed Concrete Bridges in Switzerland. Presented at the 16th Congress of IABSE.
- McCann, D.M., Forde, M.C., 2001. Review of NDT methods in the assessment of concrete and masonry structures. *NDT & E International* 34, 71–84. [https://doi.org/10.1016/S0963-8695\(00\)00032-3](https://doi.org/10.1016/S0963-8695(00)00032-3)
- Mihailov, S.J., 2012. Fiber Bragg Grating Sensors for Harsh Environments. *Sensors* 12, 1898–1918. <https://doi.org/10.3390/s120201898>
- Milovanović, B., Banjad Pečur, I., 2016. Review of Active IR Thermography for Detection and Characterization of Defects in Reinforced Concrete. *Journal of Imaging* 2, 11. <https://doi.org/10.3390/jimaging2020011>
- Monsberger, C.M., Lienhart, W., Hayden, M., 2020. Distributed fiber optic sensing along driven ductile piles: Design, sensor installation and monitoring benefits. *J Civil Struct Health Monit* 10, 627–637. <https://doi.org/10.1007/s13349-020-00406-3>
- Myrdal, R., 2007. 3 - Reference electrodes for concrete, in: Myrdal, R. (Ed.), *The Electrochemistry and Characteristics of Embeddable Reference Electrodes for Concrete*, European Federation of Corrosion (EFC) Series. Woodhead Publishing, pp. 13–23. <https://doi.org/10.1533/9781845692551.13>
- Myrland Jensen, T., 2012. Structural Monitoring - Preliminary market investigation in Norway (SINTEF report No. SBF 2012 F0245). SINTEF AS, Trondheim, Norway.
- Oliveira, S., Alegre, A., 2019. Seismic and Structural Health Monitoring of Dams in Portugal, in: Limongelli, M.P., Çelebi, M. (Eds.), *Seismic Structural Health Monitoring: From Theory to Successful*



- Applications, Springer Tracts in Civil Engineering. Springer International Publishing, Cham, pp. 87–113. [https://doi.org/10.1007/978-3-030-13976-6\\_4](https://doi.org/10.1007/978-3-030-13976-6_4)
- Phares Brent M., Washer Glenn A., Rolander Dennis D., Graybeal Benjamin A., Moore Mark, 2004. Routine Highway Bridge Inspection Condition Documentation Accuracy and Reliability. *Journal of Bridge Engineering* 9, 403–413. [https://doi.org/10.1061/\(ASCE\)1084-0702\(2004\)9:4\(403\)](https://doi.org/10.1061/(ASCE)1084-0702(2004)9:4(403))
- Pieraccini, M., 2013. Monitoring of Civil Infrastructures by Interferometric Radar: A Review. *TheScientificWorldJournal* 2013, 786961. <https://doi.org/10.1155/2013/786961>
- Pla-Rucki, G.F., Eberhard, M.O., 1995. Imaging of Reinforced Concrete: State-of-the-Art Review. *Journal of Infrastructure Systems* 1, 134–141. [https://doi.org/10.1061/\(ASCE\)1076-0342\(1995\)1:2\(134\)](https://doi.org/10.1061/(ASCE)1076-0342(1995)1:2(134))
- Polder, R., 1999. Cathodic Protection of Reinforced Concrete Structures in The Netherlands - Experience and Developments, in: *Corrosion of Reinforcement in Concrete (EFC 25)*. CRC Press.
- Popescu, C., Sas, G., Arntsen, B., 2019a. Structural health monitoring of a buttress dam using digital image correlation, in: *Sustainable and Safe Dams Around the World: Proceedings of the ICOLD 2019 Symposium*. Presented at the Sustainable and Safe Dams Around the World: Proceedings of the ICOLD 2019 Symposium, CRC Press, Ottawa, Canada.
- Popescu, C., Täljsten, B., Blanksvärd, T., Elfgrén, L., 2019b. 3D reconstruction of existing concrete bridges using optical methods. *Structure and Infrastructure Engineering* 15, 912–924. <https://doi.org/10.1080/15732479.2019.1594315>
- Prakash, G., Dugalam, R., Barbosh, M., Sadhu, A., 2022. Recent advancement of concrete dam health monitoring technology: A systematic literature review. *Structures* 44, 766–784. <https://doi.org/10.1016/j.istruc.2022.08.021>
- Ptacek, L., Strauss, A., Hinterstoisser, B., Zitek, A., 2021. Curing Assessment of Concrete with Hyperspectral Imaging. *Materials* 14, 3848. <https://doi.org/10.3390/ma14143848>
- Raoufi, K., Pour-Ghaz, M., Poursaee, A., Weiss, J., 2011. Restrained Shrinkage Cracking in Concrete Elements: Role of Substrate Bond on Crack Development. *Journal of Materials in Civil Engineering* 23, 895–902. [https://doi.org/10.1061/\(ASCE\)MT.1943-5533.0000247](https://doi.org/10.1061/(ASCE)MT.1943-5533.0000247)
- Ri, S., Wang, Q., Tsuda, H., Shirasaki, H., Kuribayashi, K., 2023. Deflection Measurement of Bridge Using Images Captured Under the Bridge by Sampling Moiré Method. *Exp Tech* 47, 1085–1095. <https://doi.org/10.1007/s40799-022-00616-y>
- Riveiro, B., Solla, M., 2006. *Non-Destructive Techniques for the Evaluation of Structures and Infrastructure*. CRC Press.
- Sajid, S., Chouinard, L., 2019. Impulse response test for condition assessment of concrete: A review. *Construction and Building Materials* 211, 317–328. <https://doi.org/10.1016/j.conbuildmat.2019.03.174>
- Salamon, J., Dressel, W., Liechty, D., 2021. Monitoring of Dams Suffering from ASR at the Bureau of Reclamation, in: Saouma, V.E. (Ed.), *Diagnosis & Prognosis of AAR Affected Structures: State-of-the-Art Report of the RILEM Technical Committee 259-ISR*, RILEM State-of-the-Art Reports. Springer International Publishing, Cham, pp. 95–116. [https://doi.org/10.1007/978-3-030-44014-5\\_4](https://doi.org/10.1007/978-3-030-44014-5_4)
- Sayyar-Roudsari, S., Hamoush, S.A., Szeto, T.M.V., Yi, S., 2020. Using a 3D Computer Vision System for Inspection of Reinforced Concrete Structures, in: Arai, K., Kapoor, S. (Eds.), *Advances in Computer Vision, Advances in Intelligent Systems and Computing*. Springer International Publishing, Cham, pp. 608–618. [https://doi.org/10.1007/978-3-030-17798-0\\_49](https://doi.org/10.1007/978-3-030-17798-0_49)
- Schumacher, T., ElBatanouny, M., Araiza, J.C., Basheer, M.P.A., Bittencourt, T.N., Brown, M.C., Forde, M.C., Glisic, B., Harris, D.K., Hedegaard, B.D., Heidbrink, F.D., Hertlein, B.H., Liu, M., Mahgoub, M.A., Malhas, F.A., Nassif, H.H., Okeil, A.M., Popovics, J.S., Pour-Ghaz, M., Suksawang, N., Vicente, M.A., Zatar, W.A., Ziehl, P.H., Scott, R.H., Smith, M.D., 2021. 444.2-21: Structural Health Monitoring Technologies for Concrete Structures—Report.

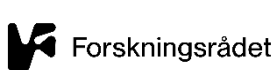


- Skjølsvold, O., Lindgård, J., 2018. Relative humidity (RH) in concrete - PROCEEDINGS FROM A NORDIC WORKSHOP. The Nordic Concrete Federation, Trondheim, Norway.
- Sweco, 2018. Damhistorikk og instrumentering - Evaluering og dokumentering av eksisterende dammers sikkerhet.
- Taillade, F., Quiertant, M., Benzarti, K., Dumoulin, J., Aubagnac, C., Taillade, F., Quiertant, M., Benzarti, K., Dumoulin, J., Aubagnac, C., 2012. Nondestructive Evaluation of FRP Strengthening Systems Bonded on RC Structures Using Pulsed Stimulated Infrared Thermography, in: Infrared Thermography. IntechOpen. <https://doi.org/10.5772/27488>
- Täljsten, B., Hedlund, H., Blanksvärd, T., n.d. Oförstörande provning, OFP, av betongkonstruktionser.
- Trafikverket, 2015. Trafikverket. Bro och tunnel management - Handbok för inspektion av byggnadsverk. Ängelholm:
- Trafikverket, n.d. BaTMan Ett system för förvaltning av Byggnadsverk [WWW Document]. URL <https://bransch.trafikverket.se/tjanster/system-och-verktyg/forvaltning-och-underhall/BaTMan/> (accessed 9.11.24).
- Tuutti, K., 1982. Corrosion of steel in concrete (Doctoral Thesis (monograph)). Swedish Cement and Concrete Research Institute, Stockholm.
- Valença, Jónatas, Dias-da-Costa, D., Gonçalves, L., Júlio, E., 2013. Processamento de Imagens Multi-Espectrais para Monitorização de Danos em Estruturas de Betão.
- Valença, J., Gonçalves, L.M.S., Júlio, E., 2013. Damage assessment on concrete surfaces using multi-spectral image analysis. Construction and Building Materials, Special Section on Recycling Wastes for Use as Construction Materials 40, 971–981. <https://doi.org/10.1016/j.conbuildmat.2012.11.061>
- Woodward, R., 2001. Durability of Post-Tensioned Tendons on Road Bridges in the UK. Presented at the Workshop on Durability of Post-Tensioning Tendons, fib.
- Wu, T., Liu, G., Fu, S., Xing, F., 2020. Recent Progress of Fiber-Optic Sensors for the Structural Health Monitoring of Civil Infrastructure. Sensors 20, 4517. <https://doi.org/10.3390/s20164517>
- Xia, Y., Lei, X., Wang, P., Sun, L., 2022. A data-driven approach for regional bridge condition assessment using inspection reports. Structural Control and Health Monitoring 29, e2915. <https://doi.org/10.1002/stc.2915>
- Xu, G., Azhari, F., 2022. Data-driven optimization of repair schemes and inspection intervals for highway bridges. Reliability Engineering & System Safety 228, 108779. <https://doi.org/10.1016/j.res.2022.108779>
- Yang, R., He, Y., Zhang, H., 2016. Progress and trends in nondestructive testing and evaluation for wind turbine composite blade. Renewable and Sustainable Energy Reviews 60, 1225–1250. <https://doi.org/10.1016/j.rser.2016.02.026>



# EXCON

<https://www.sintef.no/prosjekter/2023/excon-gronn-forvaltning-av-konstruksjoner-for-infrastruktur/>



Prosjektet er finansiert av Grønn Plattform ordningen som er et samarbeid mellom Forskningsrådet, Innovasjon Norge, Siva og Enova, og følgende deltagere:

